Turun yliopisto
University of Turku

ALTERNATIVE ELECTRON TRANSFER ROUTES INVOLVED IN PHOTOPROTECTION OF CYANOBACTERIA

Luca Bersanini

TURUN YLIOPISTON JULKAISUJA – ANNALES UNIVERSITATIS TURKUENSIS
Sarja - ser. AI osa - tom. 534 | Astronomica - Chemica - Physica - Mathematica | Turku 2016

University of Turku

Faculty of Mathematics and Natural Sciences
Department of Biochemistry
Laboratory of Molecular Plant Biology

Supervised by

Prof. Eva-Mari Aro
Laboratory of Molecular Plant Biology
Department of Biochemistry
University of Turku
FI-20014 Turku, Finland

Dr. Yagut Allahverdiyeva
Laboratory of Molecular Plant Biology
Department of Biochemistry
University of Turku
FI-20014 Turku, Finland

Dr. Natalia Battchikova
Laboratory of Molecular Plant Biology
Department of Biochemistry
University of Turku
FI-20014 Turku, Finland

Reviewed by

Dr. Marc Nowaczyk
Laboratory of Cyanobacterial Membrane Protein Complexes
Plant Biochemistry Department
Ruhr-University of Bochum
Germany

Prof. Ondřej Prášil
Laboratory of Photosynthesis
Institute of Microbiology
The Czech Academy of Science
Czech Republic

Opponent

Prof. Hans C. P. Matthijs
Aquatic Microbiology
Institute for Biodiversity and Ecosystem Dynamics
University of Amsterdam
The Netherlands.

Front cover Luca Bersanini/Volha Chukhutsina

The originality of this thesis has been checked in accordance with the University of Turku quality assurance system using the Turnitin OriginalityCheck service.

ISBN 978-951-29-6393-5 (PRINT)
ISBN 978-951-29-6394-2 (PDF)
ISSN 0082-7002
Painosalama Oy - Turku, Finland 2016

LIST OF ORIGINAL PUBLICATIONS

This thesis is built on the following scientific articles, referred in the text by their Roman numerals.

I. Battchikova N, Wei L, Du L, Bersanini L, Aro EM, Ma W (2011) Identification of novel Ssl0352 protein (NdhS), essential for efficient operation of cyclic electron transport around photosystem I, in NADPH:plastoquinone oxidoreductase (NDH-1) complexes of *Synechocystis* sp. PCC 6803. Journal of Biological Chemistry 286 (42): 36992–37001.

II. Bersanini L, Battchikova N, Jokel M, Rehman A, Vass I, Allahverdiyeva Y, Aro EM (2013) Flavodiiron protein Flv2/Flv4-related photoprotective mechanism dissipates excitation pressure of photosystem II in cooperation with phycobilisomes in cyanobacteria. Plant Physiology 164: 805–818.

III. Chukhutsina V*, Bersanini L*, Aro EM, van Amerongen H (2015) Cyanobacterial *flv4-2* operon-encoded proteins optimize light-harvesting and charge separation in photosystem II. Molecular Plant 8: 747–761. *equal contribution to first authorship.

IV. Bersanini L, Battchikova N, Heinz S, Lespinasse M, Ruohisto E, Mustila H, Deak Z, Nickelsen J, Vass I, Aro EM (2015) Dissecting the photoprotective mechanism encoded by the *flv4-2* operon: a distinct contribution of Sll0218 in photosystem II repair. Manuscript.

Other publications related to the topic:

- Allahverdiyeva Y, Mustila H, Ermakova M, Bersanini L, Richaud P, Ajlani G, Battchikova N, Cournac L, Aro EM (2013) Flavodiiron proteins Flv1 and Flv3 enable cyanobacterial growth and photosynthesis under fluctuating light. Proceedings of National Academy of Sciences USA 110: 4111-4116.
- Chukhutsina V, Bersanini L, Aro EM, van Amerongen H (2015) Cyanobacterial light-harvesting phycobilisomes uncouple from photosystem I during dark-to-light transitions. Scientific Reports 5: 14193.
- Ermakova M, Huokko T, Richaud P, Bersanini L, Howe CJ, Lea-Smith DJ, Peltier G, Allahverdiyeva Y (2015) Characterizing the function of terminal oxidases and flavodiiron as electron sinks for photosynthesis in the cyanobacterium *Synechocystis* sp. PCC 6803. Manuscript submitted.

TABLE OF CONTENTS

ABBREVIATIONS

$^1O_2$	singlet oxygen
AET	alternative electron transfer
APC	allophycocyanin
ATP	adenosine triphosphate
BG11	growth medium for cyanobacteria with/without combined N
BN-PAGE	blue native polyacrylamide gel electrophoresis
CBB	Calvin-Benson-Bassham cycle
CCM	carbon concentrating mechanism
cDNA	complementary DNA
CET	cyclic electron transfer
Chl	chlorophyll *a*
C_i	inorganic carbon
Cm^R	chloramphenicol resistance cassette
Cox	cytochrome *c* oxidase
CP47-RC	PSII core complex lacking CP43
Cyd	quinol oxidase
Cyt	cytochrome
DAS	decay associated spectrum
DBMIB	2,5-dibromo-3-methyl-6-isopropyl-*p*-benzoquinone
DCBQ	2,6-dichloro-*p*-benzoquinone
DCMU	3-(3,4-dichlorophenyl)-1,1-dimethylurea
DMBQ	2,6-dimethyl-*p*-benzoquinone
DNA	deoxyribonucleic acid
EET	excitation energy transfer
F_0	the minimal level of fluorescence in the dark
F_{mD}	the maximum fluorescence in the dark
F_m'	the maximum level of fluorescence under the light
F_q	$(F_m' - F_s)$
F_s	the level of steady-state fluorescence under the light
F_v	variable fluorescence, $(F_m - F_0)$

FAD	flavin adenine dinucleotide
Fd	ferredoxin
FDP, Flv	flavodiiron protein
Fdx	flavodoxin
FMN	flavin mononucleotide
$FNR_{(S/L)}$	ferredoxin:$NADP^+$ oxidoreductase (short/long form)
HC	high CO_2 conditions (3% CO_2)
HEPES	4-(2-hydroxyethyl)-1-piperazineethanesulfonic acid
Hg^R	hygromycin resistance cassette
HL	high light conditions
Hlip	high-light inducible protien
Km^R	kanamycin resistance cassette
LET	linear electron transfer
LC	low CO_2 conditions, air level CO_2
LL	low light
mRNA	messenger ribonucleic acid
MS/MS	tandem mass spectrometry
NADH	nicotinamide adenine dinucleotide (reduced)
NADPH	nicotinamide adenine dinucleotide phosphate (reduced)
$NADP^+$	nicotinamide adenine dinucleotide phosphate (oxidized)
NDH-1	NAD(P)H dehydrogenase complex
NPQ	non-photochemical quenching
OCP	orange carotenoid protein
OD_{750}	optical density at 750 nm
$P680/P680^+$	red/ox primary electron donor of Photosystem II
$P700/P700^+$	red/ox primary electron donor of Photosystem I
PDM	Prat-A defined membranes
PM	plasma/cytoplasmic membrane
PBS	phycobilisomes
Pc	plastocyanin
PC	phycocyanin

PCC	Pasteur Culture Collection
PCR	polymerase chain reaction
pH	negative logarithm of the proton concentration
Pheo	pheophytin
PS	photosystem
PQH_2/PQ	plastoquinol/plastoquinon
Q_A	the primary electron-accepting plastoquinone of PSII
Q_B	the secondary electron-accepting plastoquinone of PSII
RC	reaction center complex
RNA	ribonucleic acid
ROS	reactive oxygen species
RTO	respiratory terminal oxidase
RT-PCR	real-time quantitative reverse transcription PCR
Rubisco	ribulose bisphosphate carboxylase/oxygenase
SDH	succinate dehydrogenase
SDS	sodium dodecyl sulfate
SH3	Src (sarcoma) homology 3 domain
sp.	species
Sp^R	spectinomycin resistance cassette
TL	thermoluminescence
TM	thylakoid membrane
WT	wild type
Y(II)	the yield of Photosystem II
YFP	yellow fluorescent protein
TCSPC	time-correlated single photon counting
TyrZ	tyrosine residue of the D1 protein of Photosystem II

ABSTRACT

In oxygenic photosynthesis, the highly oxidizing reactions of water splitting produce reactive oxygen species (ROS) and other radicals that could damage the photosynthetic apparatus and affect cell viability. Under particular environmental conditions, more electrons are produced in water oxidation than can be harmlessly used by photochemical processes for the reduction of metabolic electron sinks. In these circumstances, the excess of electrons can be delivered, for instance, to O_2, resulting in the production of ROS. To prevent detrimental reactions, a diversified assortment of photoprotection mechanisms has evolved in oxygenic photosynthetic organisms. In this thesis, I focus on the role of alternative electron transfer routes in photoprotection of the cyanobacterium *Synechocystis* sp. PCC 6803. Firstly, I discovered a novel subunit of the NDH-1 complex, NdhS, which is necessary for cyclic electron transfer around Photosystem I, and provides tolerance to high light intensities. Cyclic electron transfer is important in modulating the ATP/NADPH ratio under stressful environmental conditions. The NdhS subunit is conserved in many oxygenic phototrophs, such as cyanobacteria and higher plants. NdhS has been shown to link linear electron transfer to cyclic electron transfer by forming a bridge for electrons accumulating in the Ferredoxin pool to reach the NDH-1 complexes.

Secondly, I thoroughly investigated the role of the entire *flv4-2* operon in the photoprotection of Photosystem II under air level CO_2 conditions and varying light intensities. The operon encodes three proteins: two flavodiiron proteins Flv2 and Flv4 and a small Sll0218 protein. Flv2 and Flv4 are involved in a novel electron transport pathway diverting electrons from the Q_B pocket of Photosystem II to electron acceptors, which still remain unknown. In my work, it is shown that the *flv4-2* operon-encoded proteins safeguard Photosystem II activity by sequestering electrons and maintaining the oxidized state of the PQ pool. Further, Flv2/Flv4 was shown to boost Photosystem II activity by accelerating forward electron flow, triggered by an increased redox potential of Q_B. The Sll0218 protein was shown to be differentially regulated as compared to Flv2 and Flv4. Sll0218 appeared to be essential for Photosystem II accumulation and was assigned a stabilizing role for Photosystem II assembly/repair. It was also shown to be responsible for optimized light-harvesting. Thus, Sll0218 and Flv2/Flv4 cooperate to protect and enhance Photosystem II activity. Sll0218 ensures an increased number of active Photosystem II centers that efficiently capture light energy from antennae, whilst the Flv2/Flv4 heterodimer provides a higher electron sink availability, in turn, promoting a safer and enhanced activity of Photosystem II. This intertwined function was shown to result in lowered singlet oxygen production. The *flv4-2* operon-encoded photoprotective mechanism disperses excess excitation pressure in a complimentary manner with the Orange Carotenoid Protein-mediated non-photochemical quenching.

Bioinformatics analyses provided evidence for the loss of the *flv4-2* operon in the genomes of cyanobacteria that have developed a stress inducible D1 form. However, the occurrence of various mechanisms, which dissipate excitation pressure at the acceptor side of Photosystem II was revealed in evolutionarily distant clades of organisms, i.e. cyanobacteria, algae and plants.

TIIVISTELMÄ

Veden käyttö elektronien lähteenä oli suuri harppaus fotosynteesin evoluutiossa ja sen myötä tuotettu happi on mahdollistanut nykyisenkaltaisen elämän kehityksen maapallolla. Veden hajotus auringon valoenergian avulla on luonnosta löytyvistä reaktioista hapettavin ja voi johtaa reaktiivisten happiradikaalien muodostumiseen. Nämä puolestaan voivat vahingoittaa fotosynteettistä koneistoa ja vaikuttaa solujen elinkykyyn. Joissakin ympäristöoloissa fotosynteettinen veden hajotus tuottaa enemmän virittyneitä elektroneja kuin solu pystyy turvallisesti hyödyntämään aineenvaihdunnassaan. Nämä elektronit voidaan luovuttaa hapelle, jolloin seurauksena on reaktiivisten happiyhdisteiden muodostuminen. Estääkseen vahingolliset reaktiot, happea vapauttavat fotosynteettiset eliöt ovat kehittäneet moninaisia mekanismeja, joilla suojautua happiradikaalien muodostumiselta. Väitöskirjassani keskityin *Synechocystis* sp. PCC 6803 -syanobakteerin vaihtoehtoisiin elektroninsiirtoreitteihin, jotka suojaavat fotosynteesikoneistoa happiradikaaleilta. Löysin tutkimuksissani NDH-1 -kompleksiin kuuluvan uuden alayksikön, NdhS, jolla on ratkaiseva merkitys kompleksin toiminnan ymmärtämisessä. NDH-1 on oleellinen valosysteemi I:n kautta tapahtuvan syklisen elektroninsiirron toiminnalle ja siten vähentää elektronien siirtymistä hapelle. Syklinen elektroninsiirto on avainasemassa fotosynteettisen ATP/NADPH -tuottosuhteen säätelyssä stressiolosuhteissa. NdhS-alayksikkö on konservoitunut happea vapauttavissa yhteyttävissä organismeissa, syanobakteereista putkilokasveihin.

Tutkimukseni toisena kohteena olivat valosysteemi II:n suojausmekanismit hapekkaassa ympäristössä, varsinkin *flv4-2* -operonin toiminta. Operoni koodaa kolmea proteiinia: kahta flavodi-ironproteiinia, Flv2 ja Flv4, sekä pientä Sll0218-proteiinia. Flv2 ja Flv4 ovat osa uutta elektroninsiirtoreittiä, joka ohjaa elektroneja suoraan valosysteemi II:n Q_B -taskusta vielä tuntemattomalle vastaanottajalle, joka ei kuitenkaan ole happi. Työssäni osoitin, että *flv4-2* -operonin koodaamat proteiinit suojaavat ja jopa kiihdyttävät valosysteemi II:n aktiivisuutta toimien tehokkaina elektronien sieppaajina ja siten samanaikaisesti pitäen plastokinonivarannon hapettuneena. Osoitin myös, että Sll0218-proteiinin tuotto samasta operonista on säädelty toisin kuin Flv2- ja Flv4-proteiinien. Sll0218-proteiini osoittautui olennaisen tärkeäksi proteiiniksi valosysteemi II:n kokoamisessa toiminnalliseksi, yli 20 erilaista proteiinialayksikköä käsittäväksi pigmentti-proteiinikompleksiksi. Sll0218- ja Flv2-/Flv4-proteiinit toimivat siis yhteistyössä suojellen ja tehostaen valosysteemi II:n aktiivisuutta. Tämä kolmen proteiinin yhteistoiminta osoittautui tärkeäksi suojamekanismiksi, joka estää singlettihapen tuottoa valosysteemi II:ssa.

Marina Abramović and Ulay from the performance “The artist is present” by Marina Abramović, 2010, MoMA-New York.

(Screenshot from Youtube)

1. INTRODUCTION

1.1 Cyanobacteria

Cyanobacteria, also known as blue-green algae, represent the largest, most varied, and most widely distributed group of photosynthetic prokaryotes. They differ from the two other major groups of photosynthetic bacteria, purple and green bacteria, both by characteristics of their photosynthetic pigment apparatus (presence of chlorophyll *a* - Chl *a*- and phycobilins) and by their ability to perform oxygenic photosynthesis (Stanier and Cohen-Bazire, 1977).

Cyanobacteria are abundant and widespread. An estimate of their global biomass is $3X10^{14}$ g C or 10^{15} g of wet biomass (Garcia-Pichel et al., 2003). Morphologically diverse species exhibit a versatile physiology and high ecological flexibility that support their success over a broad array of environments, from Antarctic glaciers all the way to the Sahara desert (Rippka 1988).

The existence of photosynthetic microbial mats and colonies has been demonstrated in fossils estimated to be 2.5 to 3.5 billion years old (Tyler and Barghoorn 1954; Schopf 1996; Westall 2005, Lopez-García et al., 2006). The ability of cyanobacteria to release O_2 as a product of photosynthesis significantly shaped the characteristics of the atmosphere and life on the planet Earth. An ozone layer developed as a consequence of O_2 accumulation, sheltering Earth against UV radiation and providing protection to its many life forms. Further, these events favored the evolution of complex heterotrophic life forms able to obtain energy using O_2 as a strong terminal acceptor of electrons (Blankenship 1992).

Primordial autotrophs are considered to be the ancestors of chloroplasts (Cavalier-Smith 2000; Rodriguez-Ezpeleta et al., 2005). The primary endosymbiosis event involving the engulfment of an ancient cyanobacterium in a primitive eukaryotic cell took place about 1.5 billion years ago (Hedges et al., 2004, Yoon et al., 2004), giving rise to three main lineages of chloroplasts in the glaucophytes, chlorophyta (green algae and plants), and rhodophyta (red algae).

1.1.1 Significance and features

Cyanobacteria are considered the most successful group of microorganisms on Earth. They are vital to maintaining the balanced ecology of natural waters by being the main primary producers in the oceans and thus providing for more than one third of the net primary production on Earth (Field et al., 1998; Bryant 2003). Some cyanobacteria are capable of fixing atmospheric nitrogen, thus making a major contribution to the nitrogen cycle occurring in the world's oceans (Montoya et al., 2004). A few

cyanobacteria are endosymbionts in lichens, plants, protists, or sponges and provide biologically available fixed carbon and nitrogen for the host.

Cyanobacteria comprise various morphological groups including solitary and colonial unicellular and filamentous species (Knoll 2008). Furthermore, cells with specialized purposes, such as heterocysts (N_2-fixing cells, Flores and Herrero 2010), hormogonia (motile multicell filaments) or akinetes (dormant stress-resistant cells, Singh and Montgomery 2011), can differentiate from vegetative cells (Rippka et al., 1979). The cyanobacterial metabolism is also versatile, with photoautotrophy, photoheterotrophy (Stanier et al., 1971; Rippka 1972) and even heterotrophy in a light-activated manner (Anderson and McIntosh 1991; Kurian et al., 2005), being performed by various species of the clade.

Based on characteristics of cell wall composition and organization, cyanobacteria are generally classified as Gram-negative prokaryotes. The cell is delimited by an outer membrane, a peptidoglycan layer and a selectively permeable plasma membrane (PM) (see review by Liberton and Pakrasi 2008). A layer of polysaccharides, the glycocalyx, contributes to protect cells from desiccation. Interior to the PM is the thylakoid membrane (TM) system, i.e. the site of photosynthetic and respiratory electron transfer reactions which are coupled to ATP and NADPH production.
Cyanobacterial TMs are loosely arranged into a network and layers of sheets instead of the stacked grana found in plant chloroplasts (Nevo et al., 2007). A special feature of the cyanobacterial photosynthetic apparatus is the extra-thylakoidal location of the light-harvesting antenna, i.e. the phycobilisomes. Other structural components of a cyanobacterial cell are pili, icosahedral carboxysomes (the sites of carbon fixation), ribosomes, gas vesicles and various storage granules made of cyanophycin, glycogen, polyphosphate or lipids (Nevo et al., 2007; Liberton and Pakrasi 2008; Kerfeld et al., 2010).

Since cyanobacteria perform oxygenic photosynthesis similarly to plants, they have been utilized as model organisms to investigate biological issues that are more challenging to solve in eukaryotes. Numerous cyanobacterial strains are competent for DNA-mediated natural transformation and detailed genetic information is available. Therefore photosynthetic light reactions, carbon fixation and circadian gene expression, as well as cell differentiation and acclimation to environmental stress are easier to investigate with the help of the molecular manipulation of cyanobacteria (Cohen and Gurevitz 2006). Additionally, recent research has shown the high potential of employing cyanobacteria for the production of renewable energy and high-value compounds by utilizing sunlight and CO_2 (see reviews by Quintana et al., 2011; Nozzi et al., 2013; McCormick et al., 2015). These photosynthetic prokaryotes might therefore

represent a promising future alternative to fossil fuels, by consuming CO_2 and eliminating pollution issues; and to plant-derived biofuels, by considerably reducing arable land and water requirements and by producing less waste (reviewed in Branco dos Santos et al., 2014).

1.1.2 *Synechocystis* sp. PCC6803

The most popular model organism among cyanobacteria is *Synechocystis* sp. PCC 6803 (hereafter *Synechocystis*). Its 3.6 Mbp genome with more than 3000 open reading frames was the first one to be sequenced among photosynthetic organisms and the third amongst prokaryotes (Kaneko et al., 1996). *Synechocystis* is a unicellular, non-toxic and non-diazotrophic freshwater cyanobacterium which was originally isolated from a Californian freshwater lake in 1968 (Stanier et al., 1971; Ikeuchi and Tabata 2001). The isolated strain was then deposited in the Pasteur Culture Collection (PCC) (Rippka et al., 1979) and since then, has been used consistently in research. Many laboratories use a glucose-tolerant strain because it is able to grow photoheterotrophically (Williams 1988). *Synechocystis* belongs to the group of β-cyanobacteria which possess β-carboxysomes and Form-1B Rubisco and are ecologically widespread. Conversely, α-cyanobacteria contain α-carboxysomes and Form-1A Rubisco (Badger et al., 2002; Badger and Price 2003) and are marine species mostly found in open waters. These groups are also characterized by different metabolic features related to inorganic carbon (C_i) and iron assimilation (Badger and Price 2003). Importantly, *Synechocystis* is naturally competent for transformation with exogenous DNA (Grigorieva and Shestakov 1982; Williams 1988; Eaton-Rye 2004). Other popular model species are the unicellular *Synechococcus elongatus* sp. PCC 7942, the filamentous and nitrogen fixing *Anabaena* sp. PCC 7120, the thermophilic *Thermosynechococcus elongatus* BP-1 (*T. elongatus*) and the marine *Prochlorococcus marinus* MED4.

1.2 Cyanobacterial Photosynthesis

Oxygenic photosynthesis is a process utilized by cyanobacteria, algae and plants to convert the physical energy of sunlight into chemical energy to obtain carbohydrates that can be later consumed to sustain the organisms' activities. Thus, photosynthesis maintains atmospheric O_2 concentrations and supplies all of the organic molecules and most of the energy essential for life on Earth (Bryant et al., 2006).

Components of the photosynthetic light reactions are localized in the TM, or in its proximity, and include the membrane-associated protein complexes: photosystem I (PSI), cytochrome b_6f (Cyt b_6f), photosystem II (PSII) and ATP synthase. The light-harvesting phycobilisomes (PBS) are stromal complexes which associate to the TM.

Mobile components are also present and include: plastoquinones (PQ), plastocyanins (Pc), cytochrome c_6 (Cyt c_6), ferredoxins (Fd) and ferredoxin:NADPH oxidoreductase (FNR) (see reviews by Nelson and Yocum 2006, DeRuyter and Fromme 2008).

In cyanobacteria (similarly to algae and plants), sugars are generated by a chain of light-independent reactions known as the Calvin-Benson-Bassham (CBB) cycle, which takes place in the cytoplasm. The Ribulose-1,5-bisphosphate carboxylase/oxygenase enzyme (Rubisco) catalyzes the fixation of CO_2 into ribulose 1,5-bisphosphate. In cyanobacteria, Rubisco is packed into proteic icosahedral shells, known as carboxysomes. The primary product of the CBB cycle is glyceraldehyde-3-phosphate, that is used to produce more complex sugars (see review by Raines 2003). In addition to carboxylation, the Rubisco enzyme can perform an energetically "wasteful" oxygenation reaction, photorespiration, which also produces toxic intermediates (see review by Raines 2003). The availability of C_i is often limiting for photosynthetic carbon fixation and enhances photorespiration. Cyanobacteria have developed carbon-concentrating mechanisms (CCMs, reviewed by Badger and Price 2003) to increase the CO_2 concentration near Rubisco to prevent photorespiration. Five active uptake mechanisms for C_i have been identified in cyanobacteria, although not all are conserved in all species (see reviews by Price et al., 2008; Burnap et al., 2015). BCT1, SbtA and BicA transporters take up bicarbonate (Price et al., 2008), and there are two systems for CO_2 uptake: the low-CO_2 inducible NDH-1MS and the constitutively functioning NDH-1MS' (see "Cyanobacterial NDH-1 complexes" section).

1.2.1 Light-harvesting antenna: the phycobilisomes

Most of the visible light spectrum can be utilized by cyanobacteria. They have numerous pigments with defined absorption features. The Chl *a* pigment has absorption maxima at the wavelengths 430–440 and 670 nm. Carotenoid pigments contribute to light-harvesting by absorbing predominantly at 420–480 nm (Mimuro and Katoh 1991, DeRuyter and Fromme 2008). Phycobiliproteins absorb sunlight wavelengths mostly between 500 and 650 nm (Glazer 1984) and they make up the major light-harvesting complexes in cyanobacteria, known as phycobilisomes (PBSs). The PBSs are big assemblies (3-10 MDa, diameter: 32–70 nm) and are associated with the cytoplasmic surface of the TM. The PBS complex is composed of colored stacks of phycobiliproteins, and colorless linker polypeptides (Grossman et al., 1993). Each phycobiliprotein has a defined absorption and fluorescence emission maximum in visible light. Their particular arrangement allows the PBSs to behave as an energy funnel, with unidirectional absorption and transfer of light energy to Chl *a* of PSII and PSI. In this way, the cells take advantage of the available wavelengths of light,

especially deeper in the water column where the 500-650 nm range of light is enriched and would otherwise be inaccessible to Chl (Fig. 1).

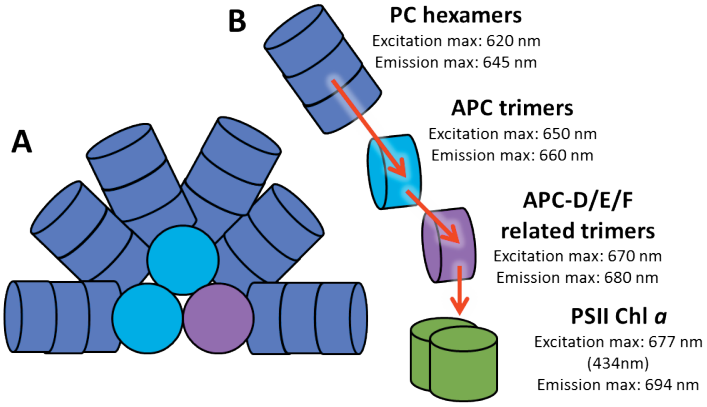

Figure 1. A schematic representation of the PBS structure (**A**) and the antenna energy funneling system from PBS components to PSII (**B**). The excitation and emission maxima for PBS components are reviewed in Kirilovsky et al. (2014). PSII Chl *a* excitation and emission maxima are found respectively in Tomo et al. (2008) and Kashino et al. (2002).

The structure of a *Synechocystis* hemidiscoidal PBSs is formed by a set of rods (composed of three stacked hexameric phycocyanin (PC) discs) radiating from the central core composed of three cylinders of allophycocyanin (APC) (four APC trimers per cylinder) (Fig. 1). The core and the multiple rods are connected via linker proteins (L_{RC}, or CpcG), encoded by two independent genes (CpcG1 and CpcG2). PBSs are associated with the cytoplasmic side of the TM (Gantt and Conti 1966) via the large, chromophorylated, core membrane linker protein ApcE (Redlinger and Gantt 1982), which functions as terminal energy emitter. Two more terminal emitters, ApcD, ApcF, are also responsible for excitation energy transfer (EET) from PBSs towards the PSs (Mullineaux 1992; Ashby and Mullineaux 1999). The PBSs associate mainly with PSII, but can also associate with PSI (see review by Mullineaux 2008).

1.2.2 LET-Linear Electron Transfer and Major Protein Complexes

The "Z-scheme" (Hill and Bendall 1960) describes linear electron transfer (LET) from water to $NADP^+$ by the two photosystems (Fig. 2). The photons absorbed by antennae excite the reaction center Chls, P680 in PSII and P700 in PSI. In a few picoseconds, the excited state of P680 (P680*) reduces a pheophytin *a* molecule (Pheo) to form the radical pair $P680^+Pheo^-$. Within a few hundred picoseconds, $Pheo^-$ reduces a tightly bound plastoquinone molecule Q_A to form $P680^+PheoQ_A^-$. $P680^+$ has a very high redox potential (>1 V) and, on a nanosecond time scale, it oxidizes a tyrosine residue TyrZ to generate $Tyr_Z^+P680PheoQ_A^-$. $TyrZ^+$ is deprotonated to form a neutral radical, TyrZ•. In the millisecond time frame, Tyr• removes an electron from a cluster of four Mn atoms

that bind two substrate water molecules and, at the same time Q_A^- reduces a second plastoquinone Q_B to form Tyr•P680Pheo$Q_AQ_B^-$. Next, Q_B^- is reduced to Q_B^{2-}, and protonated to PQH_2 and finally released from the Q_B pocket of PSII to the PQ pool. The oxidized $P680^+$ is then reduced with electrons coming from the water-splitting reaction. The oxidation of PQH_2 takes place at the Q_o site of the Cyt b_6f complex, coupled with the release of two H^+ into the thylakoid lumen. One electron is transferred back to the PQ pool; the other electron is transferred to the lumen-soluble Cyt c_6 or Pc. These carriers deliver the electron to PSI, reducing oxidized $P700^+$ which was formed upon charge separation. In PSI, an electron released from P700* is transferred to the soluble electron carrier ferredoxin (Fd) or flavodoxin (Fdx) at the cytoplasmic side of the TM. Finally, through ferredoxin-$NADP^+$ oxidoreductase (FNR), the electron reduces $NADP^+$ to NADPH. Together, the water-splitting reaction and oxidization of PQH_2 generate a proton gradient across the TM which is used by ATP synthase to produce ATP (Fig. 2). The ATP synthase complex requires $12H^+$ to obtain one complete rotation. Each complete rotation yields 3 ATP molecules. In total, it takes $4H^+$ to synthesize one ATP. Thus, 2.667 photons per ATP are required and normally the ATP:NADPH ratio is 3:2 (Behrenfeld et al., 2008).

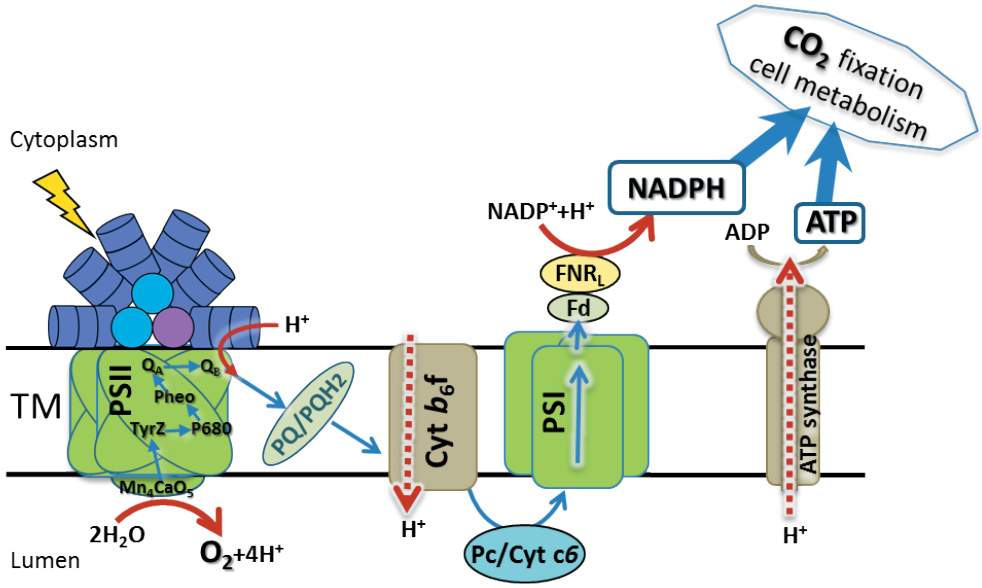

Figure 2. Schematic view of Linear Electron Transfer (LET) in the TM of *Synechocystis*. Blue arrows indicate electron transport. Red arrows indicate reactions consuming or releasing protons. Dotted red arrows indicate proton translocation across the membrane. Figure modified from Allahverdiyeva et al. (2015a).

1.2.2.1 Photosystem II

PSII uses sunlight to drive the thermodynamically and chemically demanding reaction of water splitting. In doing so, it provided biology with an unlimited source of electrons and protons required to convert CO_2 into the organic compounds of life (Barber 2012).

PSII is a multisubunit protein complex of approximately 350 kDa, located in the TM (Barber 2003). The PSII core comprises at least 20 protein subunits, 35 Chls, 2 pheophytins, 11 β-carotenes, 2 PQ, 2 hemes (in cyanobacteria), 1 non-heme iron, and the Mn_4CaO_5 cluster that catalyzes the water splitting reaction and the production of O_2 (Umena et al. 2011; Shen 2015). The structure of cyanobacterial PSII has recently been solved at close to atomic resolution (Fig. 3, Umena et al., 2011; Shen 2015).

The PSII core (pRC) is the heart of the PSII complex, where photons are converted to electrochemical energy and where the water-splitting reaction takes place. The pRC is composed of two homologous proteins, D1 and D2, and two other related Chl-binding proteins, CP43 and CP47. The core is surrounded by low molecular mass subunits: in particular PsbE and PsbF attach to the high potential heme of cytochrome b_{559} (Cyt b_{559}). The oxidation of Cyt b_{559}, a β-carotene molecule, and a Chl *a* molecule probably provide a safety valve against the harmful reactions induced by the very high redox potential of the P680 radical cation when the rate of water oxidation becomes limited (Stewart and Brudvig 1998).

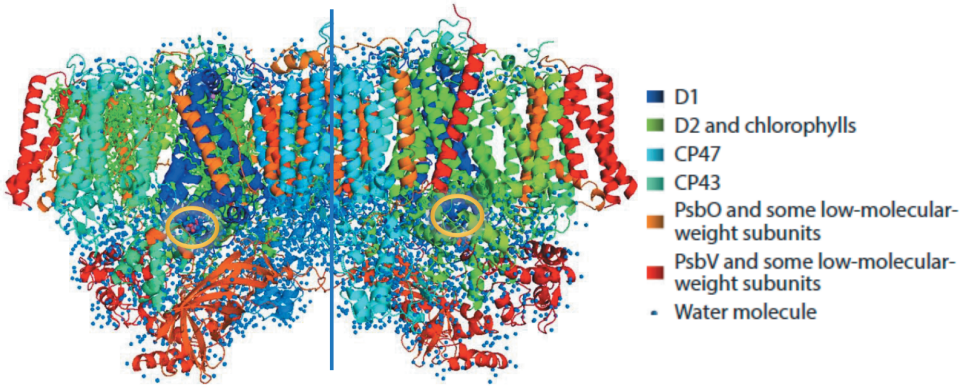

Figure 3. The structure of a PSII dimer (1.9-Å resolution). The vertical blue line divides the two monomers, and the two yellow circles designate the binding regions of the Mn_4CaO_5 cluster. Modified from Shen (2015).

Finally, the PSII complex contains extrinsic proteins bound to its luminal surface that form a protein shield over the catalytic site of water-splitting, the Mn_4CaO_5 cluster. Other extrinsic subunits are transitorily attached during the life cycle of PSII. The PSII complex usually functions as a dimer and the monomers might be an intermediate step in the assembly/repair cycle (Barbato et al., 1992, Hankamer et al., 1997). In

Synechocystis, the isolated PSII dimer is more active than the monomer (Nowaczyk et al., 2006). The dimeric complex is serviced by the PBS.

1.2.2.1a PSII Biogenesis and Assembly

Many factors are involved in the assembly of a functional PSII multiprotein complex in *Synechocystis* (see reviews by Nixon et al., 2010; Nickelsen and Rengstl 2013). It is a highly ordered process, which is schematically represented in Fig. 4. The first transient, intermediate subcomplexes of PSII are the D2-Cyt b_{559} aggregate (Komenda et al., 2004) and a dimer containing the D1 precursor (pD1) and PsbI. The pD1-PsbI complex is then incorporated in the D2-Cyt b_{559} complex (Dobakova et al., 2007) forming the Reaction Centre (RC) complex. While the RC complex is forming, pD1 is processed in two steps at its C terminus by CtpA (C-terminal processing protease), generating an intermediate D1 form (iD1), and finally a mature D1 (Anbudurai et al., 1994; Komenda et al., 2007). In addition, general insertases belonging to the Alb3/Oxa1/YidC family sustain the integration, folding, and/or assembly of pD1 (Ossenbühl et al., 2004, 2006).

Following the insertion of pD1 into the membrane, the soluble PratA protein binds to an α-helix of the D1 C-terminus, in proximity to the amino acids implicated in the formation of the Mn_4CaO_5 cluster (Schottkowski et al., 2009a; Umena et al., 2011). Further, PratA binds Mn^{2+} with high affinity, suggesting that PratA is responsible for Mn^{2+} preloading of PSII sub-complexes (Stengel et al., 2012). YCF48 optimizes RC complex formation by successively stabilizing the synthesized pD1, and its following interaction with the D2-Cyt b_{559} complex, and finally associates to RC forming RCa and RC* complexes (Komenda et al., 2008). YCF48 also contributes to the replacement of damaged D1 during PSII repair (Komenda et al., 2008). The *Synechocystis* Sll0933 protein (PAM68 in plants) interacts with several PSII core proteins and YCF48/HCF136 (Armbruster et al., 2010, Rensgstl et al., 2013) and might connect RC- and PSII monomer formation. The RC complex is then converted into a CP47-RC complex, which comprises the inner-antenna protein CP47, but not CP43 (Fig. 4).

The relocation of PSII precomplexes from the PM to the TM system is required for the transition from RC to CP47-RC complexes (Zak et al., 2001). Schottkowski et al. (2009a) identified a membrane sub-fraction presenting a mixture of PM and TM properties, which was represented by the accumulation of the PratA protein and therefore named as the PratA-defined membrane (PDM) fraction. PratA-dependent circular structures in the periphery of the cell at TM convergence sites have been identified using microscopy (Stengel et al., 2012), whereby the structures were partially surrounding areas called thylakoid centers (Kunkel 1982). Both PratA and pD1 particularly localize to these areas at TM convergence sites (Stengel et al., 2012). In those sub-

compartments, other specific proteins, such as YCF48, Slr1471 (Oxa1 homologue, Ossenbühl et al., 2006), POR (Chl biosynthesis enzyme, He and Vermaas 1998) and Pitt (a membrane-bound TPR protein that binds and stabilizes POR, Schottkowski et al., 2009b) also accumulate. The presence of these proteins indicates that the PDMs are subcellular biogenesis centers where the early steps of PSII assembly, involving D1 preloading with Mn^{2+} and perhaps Chl insertion (Stengel et al., 2012), take place. The biogenesis centers which are composed of a central thylakoid rod (van de Meene et al., 2006) and the surrounding PDMs, host the RC complex formation. The complex can then be relocated into the evolving thylakoid lamellae (for a review Nickelsen and Rengstl 2013).

CP47 is incorporated into the TM separately, developing as a subcomplex with numerous low-molecular-mass PSII subunits. Once integrated with the RC complex (CP47-RC) it subsequently combines with another preformed complex that includes CP43 (Fig. 4). The Psb27 protein binds to the CP43 pre-complex and CP47-RC, and stabilizes the assembly of the Mn_4CaO_5 cluster (Nowaczyk et al., 2006; Komenda et al., 2012). Monomeric PSII possesses all of the amino acid residues essential for the light-driven association of the Mn_4CaO_5 cluster, a process known as photoactivation (Dasgupta et al., 2008). At the lumenal side of cyanobacterial PSII, the extrinsic subunits PsbO, PsbP, PsbQ, PsbU, and PsbV are bound to stabilize the Mn_4CaO_5 cluster. Active PSII located in the TMs forms dimers (Folea et al., 2008; Kouril et al., 2012) with the help of other low-molecular-mass subunits (Shi et al., 2012).

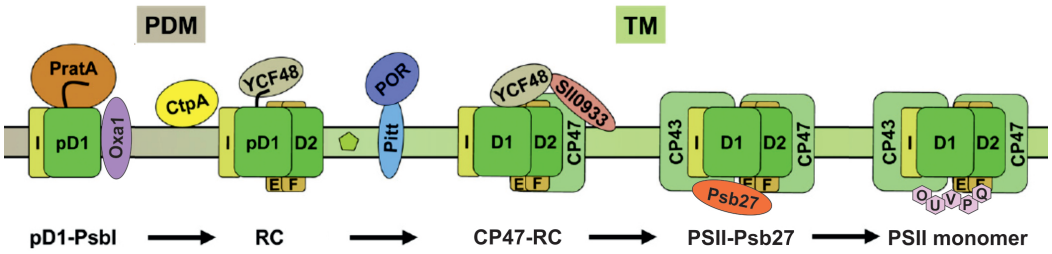

Figure 4. Schematic model for PSII assembly in *Synechocystis*. PSII biogenesis starts in PDMs with the interaction of PratA-bound pD1 protein with PsbI, forming the pD1-PsbI complex. Oxa1 (Slr1471) facilitates integration/folding of pD1 in the membrane. After the addition of D2-Cyt b_{559} to pD1-PsbI, RC complexes are obtained. Insertion of Chl *a* (green pentagon) is possibly mediated by Pitt-POR, while YCF48 and Sll0933 optimize the formation of RC and CP47-RC complexes. The resulting CP47-RC is relocated to the TM, where CP43 is attached with the help of Psb27 to form PSII-Psb27 complex. The attachment of PsbU, -O, -V, -P, and -Q on the lumenal side completes the formation of active PSII dimers. Figure modified from Rengstl et al. (2011).

1.2.2.1b PSII photoinhibition and repair

Photoinhibition is commonly defined as the light-induced decline of photosynthetic activity, resulting from an imbalance between photodamage and repair processes, in favor of the former (for reviews see Vass 2011; 2012). The major site of photodamage is represented by PSII, resulting in inhibition of electron transport and damage to its protein structure (Prasil et al., 1992; Aro et al., 1993). Traditionally, photoinhibition is assumed to happen when an excess of electrons is accumulated in the photosynthetic chain due to the unavailability of terminal acceptors. An excess of excitation energy is accumulated, modifying the activity of the Q_B (Kyle et al., 1984) and Q_A quinones (Vass et al., 1992a). Under excess excitation, mechanisms of light-induced photodamage involve: i) charge recombination of $P680^+Pheo^-$, producing highly reactive Chl triplets (Vass et al., 1992a; Vass and Cser 2009); ii) stable charge separated states produced by oxidized intermediates of the Mn_4CaO_5 cluster and reduced quinones ($S_2Q_A^{-\bullet}$, $S_2Q_B^{-\bullet}$ and $S_3Q_B^{-\bullet}$) under flashing or low light (Keren et al., 1997, Szilárd et al., 2005); and iii) damage of the catalytic Mn cluster (Hakala et al., 2005, Ohnishi et al., 2005, Tyystjärvi 2008). Due to the variety of photodamage targets, a mechanism that could be generalized to different conditions cannot yet be ascribed (Vass 2011).

An important effect of light absorption and the following reactions in PSII, is the development of the triplet excited state of Chls. These Chls easily react with O_2, leading to the production of singlet oxygen, $^1O_2$ (Krieger-Liszkay 2005; Vass 2011; Rehman et al., 2013). Singlet oxygen, the most dangerous ROS for photosynthetic cells (Krieger-Liszkay et al., 2008, Triantaphylides et al., 2008, Triantaphylides and Havaux 2009) is produced under photoinhibitory conditions. The role of $^1O_2$ in photoinhibition has been corroborated by: i) the presence of $^1O_2$-specific lipid peroxidation (Triantaphylides et al., 2008); and ii) photoprotection performed by $^1O_2$-quenching compounds, such as α-tocopherol (Trebst et al., 2002; Inoue et al., 2011), PQ (Kruk and Trebst 2008; Yadav et al., 2010) and the orange carotenoid-binding protein (Sedoud et al., 2014).

D1 protein is the primary target of photodamage during photoinhibition *in vivo* (reviewed by Edelman and Mattoo 2008). The rapid synthesis and degradation of D1 reveals the action of a PSII repair cycle, replacing damaged D1 subunits by newly synthesized copies (Ohad et al., 1984; Aro et al., 1993). The PSII repair cycle involves monomerization and partial disassembly of PSII, degradation of damaged D1, integration of a newly synthesized D1 into a subcomplex and reassembly of the holoenzyme (discussed in Aro et al., 2005). PSII repair occurs at all light intensities, but is enhanced in higher light, thus constituting a photoprotective mechanism in photosynthetic organisms (Edelman and Mattoo 2008). The PSII repair cycle is also

affected by environmental stress, resulting in an aggravation of the sensitivity of PSII to photoinhibition (Takahashi and Murata 2008). In *Synechocystis*, a specific role for the FtsH2 protease was demonstrated in D1 degradation, the PSII repair cycle and protein quality control in the TM (Silva et al., 2003; Komenda et al., 2006, 2010). Recently, Sacharz et al. (2015) demonstrated the existence of separated repair areas away from active PSII, suggesting that they could help to reduce the harmful effects of ROS on PSII repair.

Some cyanobacterial species utilize distinct D1 forms under low and high light (HL) conditions (see review by Mulo et al., 2009). The light-dependent substitution of D1 protein forms is associated with photoprotection (Sippola and Aro 2000; Sicora et al., 2006). The tuning of non-radiative charge recombination via modification of the redox potential of Pheo through the substitution of Gln with Glu residues at the 130th amino acid position (Q130E) in the D1:2 form protein plays a central role in this process (Tichý et al., 2003; Cser and Vass 2007; Kós et al., 2008; Sugiura et al., 2010). The exchange of D1 protein forms, whereby there is a preference for D1:2 in HL, is responsible for an increased phototolerance (Krupa et al., 1991; Clarke et al., 1993; Soitamo et al., 1996), that is related to accelerated non radiative charge recombination with a subsequent decreased production of $^1O_2$ (Tichý et al., 2003; Cser and Vass 2007; Sander et al., 2010).

1.2.2.2 Cytochrome b_6f

The Cyt b_6f complex oxidizes PQH_2 and constitutes the electron transport link between PSII and PSI, to which H^+ pumping is coupled, thus contributing to the transmembrane ΔpH. Electrons are transported to PSI via Pc or cytc_6 (Fig. 2).

The Cyt b_6f complex is a 220 kDa dimer and contains 8 firmly bound subunits per monomer. There are 7 prosthetic groups (4 hemes, 1 [2Fe-2S] cluster, 1 Chl *a* and 1 β-carotene) in the cyanobacterium *Mastigocladus laminosus*, and 9 in plant chloroplasts (Whitelegge et al., 2002). The two-electron oxidation of PQH_2 occurs via a split route where one electron is provided to the high potential Rieske-type subunit, which is the electron donor to cyt f, and the other one to the pair of lower potential cyt b_6 hemes.

Pc is a water-soluble electron carrier localized in the thylakoid lumen. It encloses a single Cu atom coordinated to two His residues and a Cys residue in a distorted tetrahedron. This mobile electron carrier transfers electrons from Cyt b_6f to PSI.

1.2.2.3 Photosystem I

The final step of the light reactions is performed by PSI (Fig. 2). In cyanobacteria, the PSI complex typically functions as a light-driven Pc/Cyt c_6: Fd/Fdx oxidoreductase (see review Nelson and Yocum 2006). The malleability of cyanobacterial metabolism to

fluctuations of nutrient availability allows Pc to be substituted by Cyt c_6 when Cu is limiting, and Fd to be exchanged with Fdx when iron is limiting. PSI incorporates a group of 11 polypeptides to provide ligands to the photoactive machinery, approximately 110 antenna Chl *a* molecules supply a broad optical cross-section to incoming photons, inorganic and organic cofactors to perform charge separation and charge stabilization (Jordan et al., 2001). A PsaA and PsaB (hetero)dimer contains a Chl dimer (the primary electron donor, P700), Chl monomers (the primary electron acceptor, A_0), two quinones (the intermediate electron acceptors, phylloquinones A_1) and the inter-polypeptide iron-sulfur cluster, F_X. Two other iron-sulfur clusters, F_B and F_A, located on PsaC, divert electrons from the membrane to the stromal phase, reducing Fd with high quantum efficiency. The other PSI subunits provide auxiliary roles in: stabilizing PsaC and docking Fd or Fdx (PsaD), or Pc (PsaF); in improving Fd reduction and allowing for cyclic electron transfer (PsaE); and in PSI trimeric complex formation (PsaL, peculiar function in cyanobacteria). Although this transformation of photon energy into chemical free energy goes against a steep thermodynamic gradient, the photoconversion process is remarkably efficient (Nelson 2009; Croce and Amerongen 2011).

Fd-$NADP^+$ reductase (FNR long isoform in *Synechocystis*, FNR_L) performs the electron transfer from reduced Fd to $NADP^+$ and associates with PBSs (van Thor et al., 1999). This reaction occurs on the cytoplasmic side of the TM and the uptake of a proton by $NADP^+$ further increase the ΔpH across the TM.

1.3 Mechanisms of balanced energy distribution and dissipation: the regulation of light-harvesting

Changes in light regimes, often rapid and extreme in the natural environment, are a major challenge to photosynthetic organisms. To cope with short-term fluctuating irradiances, photoprotective mechanisms which are different from photoacclimation have evolved (Niyogi 2000), involving transient and reversible reorganization and modification of existing photosynthetic units. The regulation of light-harvesting efficiency, which has been studied in plants, algae and cyanobateria is, perhaps, the most characterized of this type of photoprotective processes (Horton et al., 1996; Finazzi et al., 2006).

1.3.1 Non-Photochemical Quenching: The role of Orange Carotenoid binding Protein (OCP) and Hlips

When irradiance is excessive, the harvested energy that is utilized to drive PSII activity decreases as a consequence of non-radiative losses (Horton and Ruban 2005), thus

avoiding an over accumulation of excited Chls. This process ensures the minimization of dangerous ROS generation, whereby excited Chls might otherwise decay to triplet Chls, able to interact with O_2 to generate $^1O_2$ (Müller et al., 2001; Krieger-Liszkay 2005).

The non-radiative dissipation of absorbed light energy competes with fluorescence to decay excited Chls to their ground state. The quenching of Chl fluorescence is driven by photochemistry and by processes that cannot be attributed to photochemistry, collectively referred to as Non-Photochemical Quenching (NPQ, see review by Bailey and Grossman 2008).

In many cyanobacteria, it has been established that the orange carotenoid protein (OCP), a soluble protein binding a ketocarotenoid, is essential for the triggering of NPQ (Wilson et al., 2006, 2007; Boulay et al., 2008). The OCP-dependent NPQ mechanism requires only PBSs, OCP, and the Fluorescence Recovery Protein (FRP) (see review by Kirilovsky 2014). OCP is activated by changes in the ketocarotenoid induced by blue-green light. Active OCP binds to an APC trimer, inducing fluorescence and energy quenching. FRP induces detachment of OCP from the PBS and thus the recovery of fluorescence in darkness or low light (Gwidzala et al., 2011; reviewed in Kirilovsky 2014). Photoinhibition and state transitions are minor NPQ components.

Cyanobacteria can express a family of high-light-inducible proteins (Hlips) that are considered ancestors of the LHC superfamily in algae and plants (Dolganov et al., 1995; Engelken et al., 2010). Hlips have a photoprotective role, being involved in the synthesis of Chl-binding proteins (Chidgey et al., 2014), Chl recycling (Vavilin et al., 2007) and PSII assembly (Yao et al., 2007; Knoppova et al., 2014). In particular, two Hli proteins named HliC and HliD form a subcomplex with the Ycf39 protein, called Ycf39-Hlip, which associates to the RCa complex to form RC* (Knoppova et al., 2014). The β-car and Chls bound to Ycf39-Hlip safely dissipate excess excitation energy in the RC* complex through NPQ, thus protecting the RC complex from photodamage (Knoppova et al., 2014; Staleva et al., 2015).

1.3.2 State transitions and PBS detachment

One of the processes regulating the allocation of absorbed light energy between PSI and PSII is the mechanism of state transitions (Bonaventura and Myers 1969; Murata 1969). State transitions are fast dynamic processes that poise the relative activities of PSI and PSII by adjusting the supply of excitation energy to PSI and PSII in response to an imbalanced light regime, which is induced by specific illuminations of PSI or PSII (for general reviews on state transitions see Minagawa and Takahashi 2004; Mullineaux and Emlyn-Jones 2005; Kirilovsky et al., 2013, 2014). Such specific illumination creates an imbalance in the electron transfer chain altering, in particular, the redox state of the

PQ pool, which acts as a trigger for state transitions (Mullineaux and Allen 1990; Mao et al., 2002).

A first state transitions model based on fluorescence data proposed that PBS movement is essential for state transitions. According to this model, under PSII light (or darkness) PBSs migrate from PSII to PSI (State II) while PSI light provokes the opposite (State I, Joshua and Mullineaux 2004; Li et al., 2004, 2006). However, Chukhutsina et al. (2015) have suggested that in natural white light conditions, the light state is based on PBS uncoupling from PSI and not on PBS migration between the PSs.

The second "spillover" model of state transitions involves rearrangements of PSs in the TM (Olive et al., 1986, 1997). In State I, PSII complexes form rows from which PSI (more abundant as a monomer) is excluded. In State II, a lower amount of rows of PSII is observed and more abundant PSI trimers interact with PSII (Olive et al., 1986; 1997; Folea et al., 2008). The row organization of PSII probably prevents energy spillover from PSII to PSI. Nowadays, it is largely accepted that fluorescence changes observed in state transitions could result from a combination of both mechanisms (Emlyn-Jones et al., 1999; McConnell et al., 2002). This hypothesis was recently supported by the isolation and characterization of a functional cyanobacterial megacomplex, composed of PBS, PSI and PSII (Liu et al., 2013).

Decoupling of PBSs from PSs is another regulation mechanism of cyanobacteria to modulate the excitation energy arriving at the PSs, in particular under stressful conditions (see review by Kirilovsky 2014). For example, the exposure of *Synechocystis* cells to strong light leads to an energetic uncoupling and detachment of PBSs from RCs, at least from those of PSII (Stoitchkova et al. 2007; Kaňa et al., 2009; Tamary et al., 2012). A similar effect has been observed in mutants with a destabilized PSII structure (Sakurai et al., 2007). The PBS detachment mechanism is advantageous under continuous stress conditions, when the photoprotective responses have been exhausted and the maintenance of efficient light harvesting and energy transfer would be both unnecessary and harmful (Tamary et al., 2012).

1.4 Dissipation of excess electrons and regulation of NADPH/ATP ratio: Alternative Electron Transfer (AET) pathways in the TM

In fluctuating environmental conditions, photosynthesis requires an optimization of light energy conversion by PSs in relation to its use by metabolic reactions or dissipative mechanisms. A particularly important parameter which needs to be fine-tuned is the balance between phosphorylating (ATP) and reducing (NADPH) power

supplies. In addition to the main route of electrons, LET, which operates during oxygenic photosynthesis, auxiliary routes of electron transfer (AET) have also been described (Fig. 5, see review by Peltier 2010).

AET reactions of the TM including: i) electron input from stromal reductant/respiration; ii) electron output from the PQ pool or Fd pool to terminal acceptors like O_2; and iii) cyclic electron transfer around PSI (CET) contribute to the regulation of photosynthesis by preventing over-reduction of electron carriers and tuning the NADPH/ATP ratio according to metabolic demand. Further, electron transport pathways can be controlled by the stoichiometry, interactions or proximity of a number of electron transfer complexes in and around the TM.

Since the PQ pool plays a central role between the two PSs, its redox state has been identified as an essential factor that acts as a sensor of environmental modifications and which can signal photosynthetic imbalances (Mullineaux and Allen 1990; Ma et al., 2010; Allen et al., 2011). The oxidation of PQH_2 by the Cyt b_6f complex is considered to be the rate-limiting stage in photosynthetic electron transfer, because it depends on the rate of diffusion of PQ/PQH_2 through the TM (Blankenship 2002). In cyanobacteria, it appears that the capability to homeostatically regulate the redox state of the PQ pool is more relevant than maintaining maximum amounts of free energy in the forms of NADPH and ATP (Schuurmans et al., 2014). Since cyanobacteria grow in open water columns, where mixing can rapidly expose them to HL and/or to nutrient fluctuation, this type of regulation may be an important survival strategy (Schuurmans et al., 2014).

Importantly, the PQ pool is shared by both photosynthetic and respiratory electron transport in cyanobacteria (Aoki and Katoh 1983; Matthijs et al., 1984; Scherer 1990). Respiratory electron transport allows cells to form ATP in the dark, but this is not restricted to darkness. Apart from PSII activity, the electron transport into the PQ pool is the consequence of the joint action of respiratory dehydrogenases (NAD(P)H:PQ oxidoreductase, NDH-1; succinate dehydrogenase, SDH), and cyclic electron transfer around PSI mediated by NDH-1 and the PGR5-like protein (Mi et al., 1995; Cooley et al., 2000; Yeremenko et al., 2005). In turn, the oxidation of PQH_2 is catalyzed by Cyt b_6f, and respiratory terminal oxidases (RTOs) (Nicholls et al., 1992; Pils and Schmetterer 2001; Berry et al., 2002; Peltier et al., 2010), and might be influenced by the activity of hydrogenases and flavodiiron proteins (Fig. 5).

1.4.1 Electron inputs into LET

Stromal reducing equivalents can reduce the PQ pool through a non-photochemical electron pathway (reviewed in Peltier and Cournac 2002). The chloroplast and cyanobacterial NAD(P)H dehydrogenase-like complex (NDH-1) is involved in this

process. NDH-1 is structurally related to the multi-subunit type I NADH dehydrogenase present in bacteria and mitochondria (Complex I). NDH-1 complexes transfer electrons from an electron donor (it is unclear whether this is NADPH (Mi et al., 1995; Ma et al., 2006), or Fd (Yamamoto et al., 2011)) to PQ with a concomitant generation of ΔpH used for ATP synthesis (Berger et al., 1991). This specific function of NDH-1 complexes sustains respiration in cyanobacteria, allowing growth in photoheterotrophic conditions (Ohkawa et al., 2000; see "Cyanobacteral NDH-1 complexes" section).

In *Chlamydomonas reinhardtii*, NADH-dependent PQ reduction is also mediated by a single-subunit-type enzyme (NDH-2), but this reaction is not coupled with proton transfer (Melo et al., 2004). In *Synechocystis*, there are three NDH-2 homologues; however they are thought to play a regulatory role responding to the redox state of PQ rather than PQ reduction (Howitt et al., 1999). Recently, a more specific role in the biosynthesis of Vitamin K_1 has been revealed for the cyanobacterial NdbB isoform of NDH-2 (Fatihi et al., 2015).

In darkness, a large contribution of electrons to the PQ pool is mediated by succinate dehydrogenase (SDH), a homologue of eukaryotic Complex II (Cooley et al., 2000). According to Cooley et al. (2001), the contribution of NDH-1 and NDH-2 to PQ reduction is minimal compared to that of SDH activity, but no further reports have confirmed this hypothesis.

1.4.2 Electron outputs from LET

Mechanisms that remove electrons from LET are also called "electron valves", or AET, which prevent hazardous over-reduction of the electron transfer chain. The flavodiiron proteins Flv1-4 are examples of cyanobacterial AET that sequester electrons from LET and divert them to alternative acceptors (see "Flavodiiron proteins" section).

Under aerobic conditions, Flv1/3 proteins and the thylakoid respiratory terminal oxidases RTOs (cytochrome bd-quinol oxidase, Cyd, and cytochrome c oxidase, Cox) are important electron valves. Deletion mutants of Flv1/3 and RTOs are disadvantaged under fluctuating light and 12 h dark/high-light transitions respectively (Allahverdiyeva et al., 2013; Lea-Smith et al., 2013). Flv1/3 acts at the PSI acceptor side, likely receiving electrons from NADPH (Vicente et al., 2002; Helman et al., 2003; see "Flavodiiron protein" section); Cyd is reduced by PQH_2 (Berry et al., 2002); and Cox receives electrons from Pc/Cyt c_6 (Howitt and Vermaas 1998). All reactions result in O_2 reduction to H_2O (Fig. 5, also defined as water-water cycle in Branco dos Santos et al., 2014). Cox can potentially couple the electron transport to O_2 with the translocation of protons across the membrane (Iwata et al., 1995; Brändén et al., 2006). In algae, plants

and a few cyanobacterial species, other than *Synechocystis*, a plastid terminal oxidase (PTOX) is also involved in PQ pool reoxidation (McDonald et al., 2011).

Under anaerobic conditions, other cyanobacterial electron valves are relevant. Bidirectional hydrogenase (Hox), which is inhibited by O_2, can sequester electrons from the acceptor side of PSI and use them to reduce protons to produce H_2 (Appel et al., 2000; Gutekunst et al., 2014). Hox consumes protons in the cytoplasm, thus it could contribute to increase the proton gradient across the TM (as do Flv1/Flv3 and RTOs, which reduce O_2 to H_2O). Therefore, some electron valves might influence ATP/NADPH ratios. Hox could be involved in a rapid electron transfer mechanism (Appel et al., 2000), with H_2 evolution terminating with the rise in O_2 concentration due to PSII activity (Cournac et al., 2004).

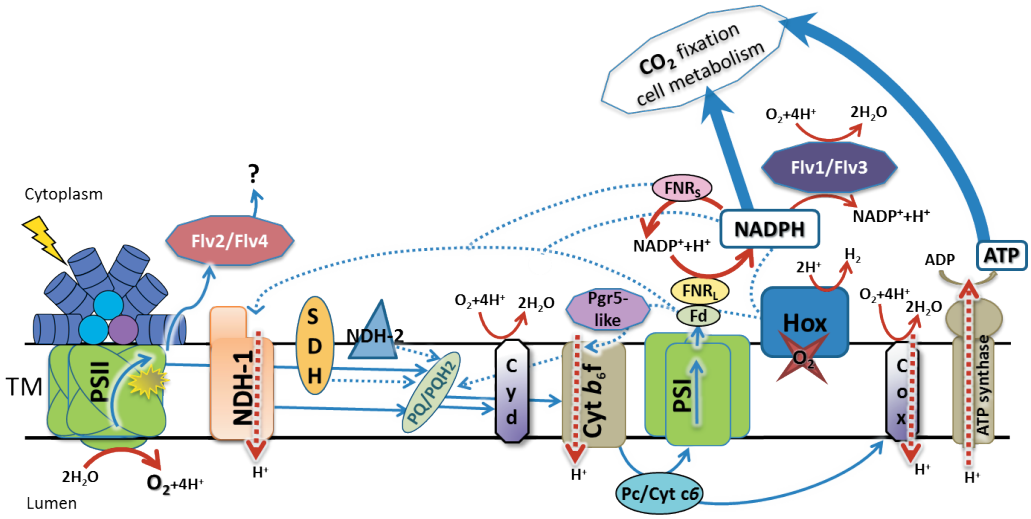

Figure 5. Schematic diagram of electron transport routes in the TM of *Synechocystis*. Blue arrows indicate electron transport. Dotted blue arrows indicate possible or unverified electron transport pathways. Red arrows indicate reactions consuming or releasing protons. Dotted red arrows indicate proton translocation across the membrane. The reactions of PQ reduction involve the uptake of two protons from the cytoplasmic side of the membrane. The red spark on the Hox complex indicates inhibition by O_2. For clarification, the FNR_L isoform can associate with PC (van Thor et al., 1999). Modified from Allahverdiyeva et al. (2015a).

In autotrophic cultures, bidirectional hydrogenase is constitutively expressed, suggesting that Hox is also important under prolonged constant conditions and especially during adaptation to higher light intensity (Appel et al., 2000). Further, the bidirectional NiFe-hydrogenase in *Synechocystis* can be reduced by Fdx and Fd and is important under mixotrophic, nitrate-limiting conditions (Gutekunst et al., 2014).

In the review of Lea-Smith et al. (2015), Fd is described as the electron donor to metabolic pathways involving reduction of sulfite (Kaneko et al., 1996), nitrate and nitrite (Flores et al., 2005), glutamate (Navarro et al., 2000), biliverdin (Frankenberg et al., 2001) and thioredoxin (Hishiya et al., 2008). Of these, only nitrate and nitrite reduction have been demonstrated to be a significant electron sink (Flores et al., 2005; Klotz et al., 2015). In diazotrophic cyanobacteria, the reducing power of NADPH and reduced Fd can be utilized as a substrate for nitrogen fixation and H_2 evolution by another O_2-sensitive enzyme, nitrogenase (see review by Böthe et al., 2010).

1.4.3 CET vs LET: poising the ATP/NADPH ratio

CET plays an important physiological role and is essential for photosynthesis when cells are exposed to stressul environmental conditions and require elevated ATP levels (reviewed in Nixon and Mullineaux 2001; Rumeau et al., 2007). The control of CET vs. LET is critical for the redox poise of the cell. In cyanobacteria and plant chloroplasts, CET functions to increase the ATP/NADPH ratio produced by LET. CET facilitates ATP synthesis: 4 photons absorbed by PSI result in 8 H^+ released into the lumen by Cyt b_6f, driving the synthesis of 2 ATP molecules. Therefore, 2 photons per ATP are required, while LET necessitates 2.667 photons per ATP.

Cyanobacteria have multiple routes for CET (see review by Mullineaux 2014). The major pathway of CET involves electron transport from NADPH/Fd to PQ via NDH-1 (Mi et al., 1995), while another route might involve electron transport from Fd to PQ via the cytoplasmic PGR5-like protein (Fig. 3, Yeremenko et al., 2005). FNR_L is required for salt stress-inducible CET (van Thor et al., 2000). A route via FNR short isoform (FNR_S), NADPH, and NDH-1 is also plausible (Fig.3, Thomas et al., 2006; Korn 2010), with electron donation to the intersystem chain via NDH-1 being enhanced in HL (Mi et al., 2001). Control over the extent of CET vs. LET could be obtained through changes in the expression of NDH-1, PGR5, FNR_L and FNR_S. FNR_L can associate with PBSs while FNR_S is stromal and this different localization could affect electron transfer routes (Thomas et al., 2006; Korn 2010). Interestingly, the distribution of a number of electron transfer complexes in the TM is under physiological control and plays a relevant role in regulating the pathway of electron flow (Liu et al., 2012; Burroughs et al., 2014). For example, a larger-scale distribution of NDH-1 in the TM is regulated in response to changes in the redox state of the PQ pool (Liu et al., 2012), thus changing the probability that electrons from respiratory complexes are transferred to PSI rather than to a RTO (Liu et al., 2012). On shorter timescales, post-translational mechanisms could be important in the shift between CET and LET.

1.5 Cyanobacterial NDH-1 complexes

1.5.1 NDH-1 and Complex I: comparison of subunits and function

The type 1 NADPH dehydrogenase (NDH-1) complex is an NAD(P)H:quinone oxidoreductase, also known as complex I. The complex is identified in a multitude of organisms, from bacteria to mammals (Friedrich et al., 1995; Friedrich and Scheide 2000; Brandt et al., 2003). In general, the complex functions in transferring electrons from an electron donor to a quinone (Yagi et al., 1998), developing a transmembrane proton motive force used for ATP synthesis (Berger et al., 1991).

Complex I in eubacteria consists of three main structural modules or sub-complexes: an activity module responsible for NADH-binding and oxidation (input of electrons); a linking amphipathic segment with Fe-S clusters; and a hydrophobic fragment embedded in the membrane which performs proton translocation and binding the quinone molecule (Friedrich et al., 1995; Sazanov 2007). The size of Complex I differs substantially, the "minimal" Complex I in bacteria is about 500 KDa with 13-15 subunits (reviewed in Sazanov 2007), while bovine Complex I has 45 subunits and reaches almost 1MDa (Carroll et al., 2006).

Cyanobacterial and plastidial NDH-1 complexes form a subclass of the complex I family (Battchikova et al., 2011). This group is characterized by a few common features: the absence of three subunits of the activity module homologous to NuoE, NuoF, and NuoG of the *Escherichia coli* complex, the presence of 11 subunits, NdhA-NdhK, conserved within the complex I family (Friedrich and Scheide 2000), and the occurrence of several subunits specific for complexes of oxygenic phototrophs (NdhL, NdhM, NdhN, NdhO, NdhP, and NdhQ, Birungi et al., 2010; Nowaczyk et al., 2011; Schwarz et al., 2013; Wulfhorst et al., 2014).

In *Escherichia coli*, Complex I genes are found in one *nuo* cluster (Weidner et al., 1993), whereas cyanobacterial *ndh* genes are dispersed in the genome, sometimes as small operons. Interestingly, genes encoding NdhD and NdhF are found in most of cyanobacterial genomes in several copies. *Synechocystis* has six *ndhD* genes (*ndhD1-D6*) and three *ndhF* genes (*ndhF1*, *ndhF3* and *ndhF4*) in its genome (Kaneko et al., 1996). The *ndhD3-D6*, *ndhF3* and *ndhF4* genes are specific to cyanobacteria, as well as *cupA* (*chpY*), *cupB* (*chpX*) and *cupS* genes (Ogawa and Mi 2007).

Mitochondrial and bacterial complex I is an NADH-dependent oxidoreductase (Friedrich et al., 1995; Yagi et al., 1998; Brandt 2006), but cyanobacterial NDH-1 was suggested to be an NADPH-dependent enzyme (Matsuo et al., 1998; Deng et al., 2003a-b; Ma et al., 2006). However, the active subunits have not been assigned yet, thus the

electron donor is still under debate. FNR_S may provide electrons from NADPH to the NDH-1 complex (Thomas et al., 2006; Korn 2010) but Fd could also be the electron donor to the NDH-1 complex in oxygenic phototrophs. In *Arabidopsis thaliana*, the CRR31 protein functions as a Fd-binding Ndh subunit in the chloroplast NDH-1-like complex (Yamamoto et al., 2011). A recent purification of NDH-1 complexes from *T. elongatus* contained Fd and FNR together with the NDH-1 complex, suggesting an electron donation from NADPH to NDH-1 via interaction with FNR and Fd (Hu et al., 2013). In mammalian Complex I, NADH is the electron donor, giving two electrons to the quinone molecule, via FMN and the sequence of Fe-S clusters. While two electrons are transferred in the complex, the translocation of four protons through the membrane occurs (Efremov et al., 2010; Hunte et al., 2010).

1.5.2 Cyanobacterial NDH-1 variants and physiological roles

Complex I of mitochondria and eubacteria plays a solitary role in respiration, whereas cyanobacterial NDH-1 complexes are involved in respiration, CET and CO_2 acquisition. Importantly, for applied research, deletion of NDH-1 in *Synechocystis* provoked an accumulation of reducing equivalents in the light which prolonged the activity of the Hox hydrogenase, resulting in enhanced H_2 photoevolution (Cournac et al., 2004).

The different functions assigned to cyanobacterial NDH-1 complexes are based on the diversity of the NdhD and NdhF subunits that results in an occurrence of diverse NDH-1 complexes within a cyanobacterial cell (reviewed in Battchikova et al., 2011; Peltier et al., 2015). The diversity of cyanobacterial NDH-1 complexes predicted by reverse genetic studies is illustrated in Fig. 6.

1.5.2.1 NDH-1M complex

NDH-1M complex is an assembly intermediate for both the NDH-1L and NDH-1MS complexes (Fig. 6). The NDH-1M complex consists of 14 subunits (NdhA-C, NdhE, NdhG-O). NdhI, J, K and H form a soluble domain and the NdhA-C, NdhE, NdhG and NdhL-O are supposed to be the components of the hydrophobic membrane arm (see review by Battchikova et al., 2011). The NdhO subunit was recently shown to strongly interact with NdhI and NdhK subunits in the hydrophilic domain, thereby destabilizing the NDH-1M complex and repressing NDH-CET activity (Zhao et al., 2014). A small transmembrane NdhQ subunit (Nowaczyk et al., 2011), is also assigned to the NDH-1M complex according to Wulfhorst et al. (2014). The assembly of the NDH-1M complex is fairly obscure, with only one maturation factor, Slr1097, being identified in *Synechocystis* (Dai et al., 2013).

1.5.2.2 NDH-1L complex(es)

NDH-1L is a 450 kDa protein complex, localized in the TM of all cyanobacteria. NDH-1L contains the subunits present in the NDH-1M complex with the addition of the NdhD1 and NdhF1 in the membrane domain, giving the typical L-shape to the complex (Fig. 6, for a review see Battchikova et al., 2011). Recently, it was shown that the NDH-1L complex has another specific subunit, NdhP, which is localized to the membrane arm and is essential for stabilization and optimal activity of the NDH-1L complex (Schwarz et al., 2013; Wulfhorst et al., 2014).

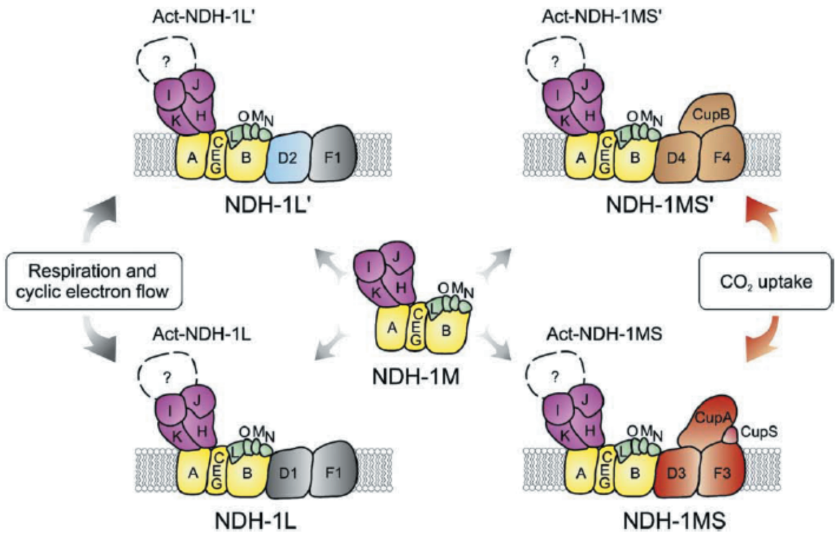

Figure 6. The functional and structural multiplicity of cyanobacterial NDH-1 complexes. The unknown activity domain (Act-NDH) is indicated by a question mark. Figure from Battchikova et al. (2011).

The canonical "dark" respiration and CET functions are assigned to the NDH-1L complex (see review Battchikova et al., 2011). The malfunction of the NDH-1L complex induces the glucose-sensitive phenotype under photoheterotrophic conditions (Ohkawa et al., 2000). The NDH-1L complex is the main contributor to cyanobacterial CET and thus plays a crucial physiological role, particularly when cyanobacteria are exposed to environmental stresses and require additional ATP to maintain their growth and development (Ohkawa et al., 2000).

A hypothetical NDH-1L' complex, harboring the NdhD2 subunit instead of the NdhD1 subunit, is likely to be expressed in particular environmental conditions, although the complex and NdhD2 has never been found at protein level (Fig. 6). Indeed, the *ndhD1* gene is rather constitutively expressed but *ndhD2* has been shown to be highly expressed upon CO_2 limitation and HL (Hihara et al., 2001; Wang et al., 2004) and poorly expressed upon iron depletion (Hernández-Prieto et al., 2012). This might indicate a

different function for the NDH-1L' complex as compared to the ordinary NDH-1L complex.

1.5.2.3 NDH-1MS complexes

The NDH-1MS complex includes NDH-1M plus the specific subunits NdhD3 and NdhF3 in the membrane arm and two extra proteins, CupA and CupS, bound to the NdhD3 and NdhF3 proteins (NDH-1S, Fig. 6). The NDH-1MS complexes, first isolated from *T. elongatus* (Zhang et al., 2005), easily dissociate into the NDH-1M complex and two small NDH-1S subcomplexes in native gels (Fig. 6, Herranen et al., 2004; Zhang et al., 2004). The NDH-1MS' complex has only recently been evidenced at the protein level, with the identification of specific subunits NdhD4, NdhF4 and CupB, which form NDH-1S' (Wulfhorst et al., 2014, Fig. 6). Despite, the constitutively expressed NDH-1MS' complex demonstrating a low expression level, NDH-1MS'-mediated CET has been established (Bernat et al., 2011).

Both NDH-1MS and NDH-1MS' have been shown to function in cyanobacteria as part of the CCM (Ogawa 1991, Ohkawa et al., 2000; Price et al., 2008; Burnap et al., 2015). In CCM, CO_2 enters cyanobacterial cells by diffusion and the NDH-1MSs complexes situated in the TM catalyze its hydration to HCO_3^-, which accumulates in the cytosol and is transported into the carboxysome. In the carboxysome, carbonic anhydrase converts HCO_3^- to CO_2 in close proximity to Rubisco (for a review, see for example, Price et al., 2008).

Typically, the NDH-1MS complex is missing from cyanobacteria growing in HC (1-5 %) but appears rapidly upon CO_2 stepdown to LC conditions (Battchikova et al., 2010). CupA and CupS subunits are likely essential for CO_2 hydration to HCO_3^-, whereas the rest of the complex is likely to energize the CO_2 pumping mechanism by performing CET (Bernat et al., 2011) to produce ATP.

1.6 Flavodiiron proteins

1.6.1 A conserved family of modular enzymes

Flavodiiron proteins (FDPs) form a conserved family of enzymes which are present in prokaryotes (Wasserfallen et al., 1998), some eukaryotes including algae and lower plants (Zhang et al., 2009; Allahverdiyeva et al., 2015b), and anaerobic protozoa (*Trichomonas*, *Giardia* and *Entamoeba* spp., Saraiva et al., 2004; Di Matteo et al., 2008). FDPs reduce nitric oxide (NO) to nitrous oxide (N_2O) and/or reduce O_2 to H_2O (Saraiva et al., 2004; Vicente et al, 2008a-b). These proteins protect cells from nitrosative stress (Rodrigues et al., 2006) and, in case of anaerobic organisms, from harmful O_2 accumulation (Hillman et al., 2009). FDPs show a shared structural and functional

pattern. The prototype core includes a β-lactamase-like domain containing a non-heme diiron center, and a flavodoxin-like domain with an FMN binding site. The presence of extra structural domains fused at the prototype C-terminus has led to the establishment of four FDP subfamilies (Classes A-D, see Fig. 7). In many organisms, the prototype FDP (Class A) acts as terminal oxidase of a 3-component system where rubredoxin (Rd) is the intermediate carrier, thus involving the presence of an NADH:Rd oxidoreductase. This enables the coupling of NADH oxidation to O_2 reduction, as observed in the Rd:oxygen oxidoreductase, ROO, from *Desulfovibrio Gigas* (Chen et al., 1993).

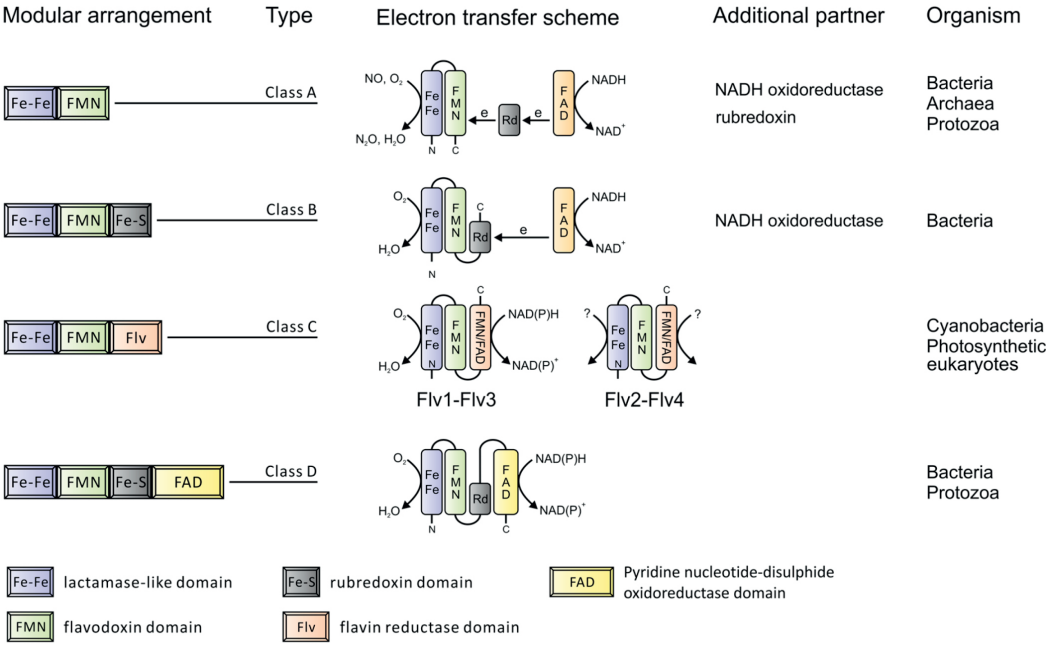

Figure 7. Modular organization of the flavodiiron protein family and occurrence in different organisms. Figure from Allahverdiyeva et al. (2015b).

Class B FDPs are called flavorubredoxins (FlRd) since at the C-terminus they contain a Rd-like domain. This type of enzyme is restricted to enterobacteria (*Escherichia* and *Salmonella* spp.). FlRds accept electrons directly from NADH:FlRd reductase, forming a 2-component electron transport module (Gomes et al., 2002; Vicente et al., 2007).

Class C FDPs are typically present in cyanobacteria. They have an NADPH flavin reductase domain at the C-terminus (Wasserfallen et al., 1998; Vicente et al., 2002; Saraiva et al., 2004). Importantly, in a single protein, these FDPs condense the whole electron transport reaction that couples NADPH oxidation to O_2 and/or NO reduction.

Class D FDPs result from the fusion of a Class B FDP with the respective NADH:FlRd reductase. The resulting 4-domain protein is likely to perform O_2 or NO reduction

concomitantly with NADPH oxidation in the anaerobic protozoan *Trichomonas vaginalis* and the anaerobic bacterial pathogen *Clostridium perfringens* (Shimizu et al., 2002).

Some FDPs might reduce both O_2 and NO; however, in other cases substrate selection is strict (Vicente et al., 2007, Seedorf et al., 2007). It has been postulated that common structural features might define O_2-specificity (Vicente et al., 2009; Goncalves et al., 2014).

1.6.2 FDPs in *Synechocystis* and oxygenic phototrophs: structural features and biochemical properties

The genome sequences of cyanobacteria and other oxygenic photosynthetic organisms (algae, mosses, lycophytes and even the gymnosperm *Picea sitchensis*) contain genes encoding FDPs, which form a distinct clade from the other classes of FDPs (Peltier et al., 2010; Allahverdiyeva et al., 2015b). All cyanobacterial FDPs and those from oxygenic phototrophs are part of Class C (Fig. 7), the only exception being *Picea sitchensis* FDP, which lacks the flavin reductase domain (Goncalves et al., 2012; Allahverdiyeva et al., 2015b). Each sequenced cyanobacterium has at least two FDP encoding genes. Among FDP producing organisms, cyanobacteria have high numbers of FDP homologues in a single genome, with up to 6 FDP homologues found in most filamentous heterocystous cyanobacteria (Allahverdiyeva et al., 2015b). Several copies of FDP genes are detected in paralog pairs in cyanobacterial genomes and are often genetically clustered. Examples of this are the *flv1-flv3* and *flv2-flv4* pairs (Zhang et al., 2009). The genome of *Synechocystis* comprises four FDP genes: *flv1* (*sll1521*) and *flv3* (*sll0550*); and *flv2* (*sll0219*) and *flv4* (*sll0217*). The latter pair is organized in an operon with the *sll0218* gene, coding for a protein with unclear function. The FDPs of cyanobacteria form two distinct clusters, A and B. FDPs with conserved residues matching the canonical ones known to be involved in iron coordination are part of cluster B (Flv3 and Flv4), while cluster A FDPs (Flv1 and Flv2) have a significant variation in these residues (Zhang et al., 2009; Allahverdiyeva et al., 2015b), with the absence of canonical ligands in the Fe-Fe center (Goncalvez et al., 2011; 2012). Importantly, of the minimum two FDP genes per genome, one codes for a cluster A FDP and the second for a cluster B enzyme. In contrast to FDPs from anaerobes forming homodimers or homotetramers (Seedorf et al., 2007; Petoukhov et al., 2008), cyanobacterial FDPs were suggested to be arranged in heterodimers, so that two proteins from different clusters form an active unit (Zhang et al., 2009; 2012). Numerous FDP structures are now available, revealing a conservation of a "head to tail" arrangement (the diiron site of one monomer is almost in Van Der Waals contact with the FMN from the other

monomer), as well as of the diiron ligand sphere (Silaghi-Dumitrescu et al., 2005, Seedorf et al., 2007; Di Matteo et al., 2008, Goncalvez et al., 2011; Zhang et al., 2012).

Biochemical and *in vivo* biophysical analysis have shown that *Synechocystis* Flv3 is an NAD(P)H:oxygen oxidoreductase capable of reducing O_2 to H_2O *in vitro* (see Fig. 7, Vicente et al., 2002; Helman et al. 2003). Further, *in vivo* studies have demonstrated that Flv1 and Flv3 proteins function in photoreduction of O_2. This function is also referred to as the "Mehler-like" reaction (Allahverdiyeva et al., 2013), because unlike the plant-type "true" Mehler reaction, it is a four-electron transfer which does not produce ROS (Vicente et al., 2002). In cyanobacteria, there is no clear evidence of the "true" Mehler reaction, which results in H_2O_2 accumulation and thus requires effective H_2O_2 scavenging systems. In fact, it has been demonstrated that cyanobacterial blooms could be fought by the addition of H_2O_2 directly into lakes (Matthijs et al., 2012), implying no sufficient activity of peroxidases and thus for the function of the "true" Mehler reaction in cyanobacteria. Recently, the indispensable role of Flv1 and Flv3 proteins under fluctuating light conditions has been revealed in *Synechocystis* (Allahverdiyeva et al., 2013), whereby a lack of Flv1 or Flv3 proteins arrested cell growth under fluctuating light. Importantly, exposure to fluctuating light resulted in strong damage of, and malfunction in, the PSI complex (Allahverdiyeva et al., 2013). Flv1 and Flv3 form a heterodimer that sequesters electrons from the acceptor side of PSI and utilizes them to reduce O_2 (Allahverdiyeva et al., 2011; 2013). In *Anabaena* sp. PCC7120, an additional copy of Flv3, called Flv3B, is localized in heterocysts and protects nitrogenase from oxidative stress (Ermakova et al., 2014). Flv1 and Flv3 homologues in *Chlamydomonas reinhardtii* (FlvA and FlvB) facilitate acclimation to anoxia during sulfur deprivation, indicating a role in the water-water cycle (Jokel et al., 2015). Interestingly, Flv1 and Flv3 in *Synechocystis* and FLVB in *Chlamydomonas reinhardtii* were found to be possible Fd interactors (Hanke et al., 2011; Peden et al., 2013). Flv3, in particular, might interact with Fd9, one of the minor Fd of *Synechocystis* (Cassier-Chauvat and Chauvat 2014), suggesting that Fd could act as a direct electron donor for these cyanobacterial and algal FDPs.

1.6.3 The *flv4-2* operon

The *flv2* (*sll0219*) and *flv4* (*sll0217*) gene pair is organized in the *flv4-2* operon with the *sll0218* gene (Fig. 8). The *flv4-2* operon is conserved in the genome of many β-cyanobacteria (Zhang et al., 2012). Sll0218 is a hypothetical protein with a PsiE (Phosphate Starvation-Inducible E) superfamily domain (http://www.ncbi.nlm.nih.gov/cdd), however its function is yet to be determined. Sll0218 orthologues are found in many sequenced cyanobacteria, bacteria, and

archaea and form three phylogenetic clades. A first clade of Sll0218 orthologues is comprised of those encoded by the *flv4-2* operon; a second clade groups other bacteria and archaea sequences; and the third clade, which is more closely related to the second clade, consists of Sll0218 found outside the *flv4-2* operon in filamentous cyanobacteria. Interestingly, some filamentous cyanobacteria possess two to three copies of Sll0218 (Zhang et al., 2012);

The *flv4-2* operon-encoded proteins are important for the protection of PSII centers against photoinhibition (Zhang et al., 2009; Hakkila et al., 2013). However, the biological mechanism behind this remains unclear. Expression of the *flv4-2* operon is strongly induced in LC at both the transcript and protein levels (Zhang et al., 2009, Battchikova et al., 2010; Eisenhut et al., 2012; Hackenberg et al., 2012). The most rapid induction occurs at combined LC and HL conditions (Zhang et al., 2009). Microarray data revealed strong expression of the operon under HL (Hihara et al., 2001) and low O_2 concentration (Summerfield et al., 2011), while a strong downregulation is observed under high CO_2 concentration (HC, Hackenberg et al., 2012), darkness (Kucho et al., 2005; Lehmann et al., 2013) and Fe depletion (Hernandez-Prieto et al., 2012). Importantly, a strong downregulation of the Flv4 protein is observed in the absence of the Flv2 proteins (Zhang et al. 2012). The existence of the Flv2/Flv4 heterodimer was revealed by biochemical and biophysical experiments (Zhang et al. 2012).

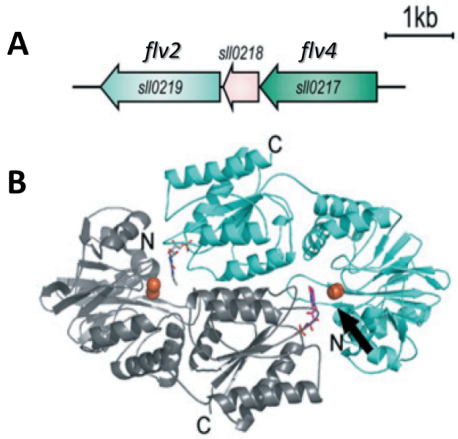

Figure 8. Schematic organization of the *flv4-2* operon in *Synechocystis* (**A**). Homology structural model of the Flv2/Flv4 heterodimer (**B**). The arrow indicates the functional reactive site with FMN (magenta) from the Flv2 monomer (gray) and diiron site from the Flv4 monomer (cyan). Orange spheres represent iron. Figures modified from Zhang et al. (2012).

The Flv2/Flv4 heterodimer has a high affinity for the membrane fraction in the presence of divalent cations. According to homology structural models (Zhang et al., 2012), the Flv2/Flv4 heterodimer shows a head-to-tail organization: the iron binding site in the Flv2 monomer faces the FMN binding site in the Flv4 monomer and *vice versa* (Fig. 8). The Flv2/Flv4 heterodimer possesses two reactive sites with different properties. The site shaped by the FMN binding site of the Flv2 monomer and the iron

binding site of the Flv4 monomer is conserved and, therefore, clearly functional. The iron binding sites in the Flv2 homodimer are not conserved whereas the FMN binding site of the Flv4 homodimer does not have all of the conserved residues. Consequently, the functional binding site of the Flv2/Flv4 heterodimer is structurally more conserved than either of the Flv homodimers (Zhang et al., 2012).

Sll0218 is associated with the TM. However, after fractionation in the original two-phase partitioning buffer system, it was undetectable in the TM or in the PM. This observation, together with its sensitivity to proteolysis by lysin and thermolysin (Zhang et al., 2012), suggests a heterogeneous distribution of Sll0218 in the TM. In its native form, Sll0218 is also found to be associated with a large complex (~500 kDa, Zhang et al., 2012).

Biophysical experiments performed with deletion mutants have provided evidence for a novel electron transport route from PSII to the Flv2/Flv4 heterodimer and subsequently to an unknown acceptor (Zhang et al., 2012) and have indicated a role for Sll0218 in the stabilization of PSII dimers (Zhang et al., 2012). Recent *in vitro* tests have shown that recombinant Flv4 is able to oxidize NADH and reduce O_2 to H_2O (Shimakawa et al., 2015).

The expression of the *flv4-2* operon is tightly regulated by four small RNAs (Eisenhut et al., 2012). One of them, the antisense RNA As1_flv4 avoids premature synthesis of Flv4 and Flv2 proteins after a shift from HC to LC (Eisenhut et al., 2012). As1_flv4 is negatively regulated by the AbrB-like transcription regulator Sll0822, whereas the *flv4-2* operon is positively regulated by the transcription factor NdhR (Eisenhut et al., 2012).

2. AIMS OF THE STUDY

Cyanobacteria are exposed to different environmental stresses in their natural habitats. Low concentrations of C_i and rapidly changing light intensities may induce harmful consequences to these photosynthetic organisms through an over accumulation of reducing power. When this reducing power cannot be efficiently consumed by the CBB cycle, it results in oxidative stress. Specific acclimation mechanisms have been developed by cyanobacteria to cope with such challenges. In this thesis, I have focused on the characterization of AET routes which sequester or redirect excess electrons away from LET. It is important to elucidate how such acclimation takes place, particularly when considering the application of cyanobacteria for biotechnology purposes, where direction of a maximum amount of electrons could be used to enhance the production of biofuels and other desired end-products. Both the NDH-1 complexes and the flavodiiron proteins Flv2/Flv4 (together with the small Sll0218 protein) are involved in the stress responses of cyanobacteria to challenging environmental conditions. In attempting to elucidate acclimation mechanisms of importance, I have investigated the physiological functions and localisation of these proteins and complexes, and explored their interplay with other photoprotective mechanisms.

In particular, the aspects focused on in this work are:

1) The identification and characterization of Ssl0352, a novel subunit of the NDH-1 complexes
2) The elucidation of the role of the entire *flv4-2* operon in the photoprotection of PSII and its cross talk with other photoprotective mechanisms and light-harvesting
3) The designation of the specific roles of the Flv2/Flv4 heterodimer and Sll0218 protein in photoprotection and PSII assembly/repair

3. MATERIAL AND METHODS

3.1 Cyanobacterial strains and growth conditions

Strain	Deleted genes	Reintroduced/ modified genes	Paper	Ref.
WT			I-II-III-IV	(1)
Δ*ndhS*	*ssl0352*::Km^R		I	I
M55	*ndhB*::Km^R		I	(2)
NdhS-YFP-His_6		*ssl0352*::YFP-His_6	I	I
NdhM-YFP-His_6		*slr1623*::YFP-His_6	I	(3)
Δ*flv2*	*sll0219*::Sp^R		IV	(4)
Δ*sll0218-flv2*	*sll0218-0219*::Hg^R		IV	(5)
Δ*sll0218*	*sll0218-0219*::Hg^R, *psbA2*::Sp^R	*flag-sll0217*::Km^R, *sll0219*::Sp^R	IV	IV
Δ*flv4*	*sll0217*::Km^R		II-III-IV	(4)
OE (WT::*flv4-2*)	*psbA2(slr1311)*::Sp^R	*sll0217-0218-0219*::Sp^R	II-III-IV	II
Δ*flv4::flv4-2*	*sll0217*::Km^R, *psbA2*::Sp^R	*sll0217-0218-0219*::Sp^R	III	III
Δ*psbA2*	*psbA2*::Sp^R		II	(4)
Sll0218-YFP		*sll0218*::YFP-His_6	IV	IV
PAL	*apcAB(slr2067-slr1986)*::Cm^R, *apcE(slr0335)*::Sp^R		II	(6)
CK	*cpcBAC1C2(sll1577-sll1580)*::Km^R		II	(7)
Δ*ApcDF*	*sll0928*::Cm^R, *slr1459*::Sp^R		II	(8)
ΔOCP	*slr1963*::Sp^R		II	(9)
Δ*ycf48*	*slr2034*::Cm^R		IV	(10)
Δ*sll0933*	*sll0933*::Km^R		IV	(11)
Δ*ycf48/sll0933*	*sll0933*::Km^R, *slr2034*::Cm^R		IV	(12)

Table 1. Cyanobacterial strains used in this research. Description of the mutants can be found in the references. Ref.: (1) Williams 1988; (2) Ogawa 1991; (3) Birungi et al., 2010; (4) Zhang et al., 2012; (5) Helman et al., 2003; (6) Ajlani and Vernotte 1998; (7) mutant constructed by Ughy and Ajlani and described in Thomas et al., 2006; (8) Jallet et al., 2012; (9) Wilson et al., 2006; (10) Komenda et al., 2008; (11) Armbruster et al., 2010; (12) Rengstl et al., 2013.

The *Synechocystis* sp. PCC 6803 WT (Williams, 1988) and mutant strains (Table 1) were grown at 30°C in BG-11 medium (Allen, 1968) supplemented with 20 mM HEPES-NaOH (pH 7.5). Illumination was provided by white fluorescent light (L 30W/865 Osram) with an intensity of ~50 µmol photons m^{-2} s^{-1} (Growth Light: GL). Higher light intensities were used for some experiments (500, 1500 µmol photons m^{-2} s^{-1}, respectively 500-HL (or simply HL) and 1500-HL). Cultures were grown in Erlenmeyer flasks with shaking at

120 rpm. In HC conditions, air was enriched with 3% CO_2. In LC conditions, normal air was used and Na_2CO_3 was omitted from the growth media. For physiological experiments, cells were harvested at the logarithmic phase (OD_{750} between 0.6 and 1.1). Before biophysical experiments, the cells were resuspended in fresh BG-11 medium, and adjusted to the same Chl concentration (5 to 10 mg mL^{-1}, depending on the experiment). Chl was extracted with 90% methanol and its concentration was estimated by absorbance measurement at 665 nm and determined with an extinction coefficient of 78.74 L g^{-1} cm^{-1} (Meeks and Castenholz 1971).

3.2 Biophysical methods

3.2.1 Oxygraphic analysis using a Clark-type electrode

Steady state O_2 evolution was determined using a Clark-type O_2 electrode (DW1, Hansatech) at 30°C under a saturating white light intensity of ~1000 µmol photons m^{-2} s^{-1}. The PSII electron transport rates were defined in the presence of an artificial electron acceptor, either 0.5 mM 2,6-dichloro-*p*-benzoquinone (DCBQ) or 2 mM 2,6-dimethyl-*p*-benzoquinone (DMBQ). In Paper II, these measurements were also performed in the presence of 10 mM $NaHCO_3$. Oxygen evolution measurements were also performed in the presence of 2 µM 2,5-dibromo-3-methyl-6-isopropyl-*p*-benzoquinone (DBMIB) to assess PSII electron transfer rates when the PQ pool was over-reduced.

3.2.2 Singlet oxygen detection

Quantification of $^1O_2$ production was based on His-mediated oxygen uptake measurements. This methodology, which was initially applied for isolated PSII complexes (Telfer et al., 1994), has recently been extended for intact cyanobacterial cells and was performed as described in Rehman et al. (2013).

3.2.3 Flash Fluorescence analysis

A fluorometer, FL 3500 (PSI Instruments), was used to determine the single flash-induced rise and subsequent decay of Chl fluorescence yield, according to the methodology of Vass et al. (1999). The cells were dark adapted for 5 min before the application of a single 10 µs saturating flash in the absence and presence of 20 µM DBMIB.

3.2.4 PAM fluorometry: chlorophyll fluorescence and P700 analysis

A pulse amplitude modulated fluorometer, Dual-PAM-100 (Walz, Effeltrich, Germany), was utilized to examine Chl fluorescence *in vivo*. Red (620 nm) or blue (460 nm) actinic lights were applied (depending on the experiment) and cells were stirred in 1cm x 1cm

cuvettes at 30°C during the measurements. Saturating pulses (red light, 5,000 µmol photons m^{-2} s^{-1}, 300 ms) were used to transiently close all PSII centers to measure F_{mD} and F_m'. The maximal photochemical efficiency of PSII (F_v/F_m) was measured in the presence of 3-(3,4-dichlorophenyl)-1,1-dimethylurea (DCMU). The yield of PSII, Y(II)= (F_m'-F_s)/ F_m', was measured in cells with an actinic light of 120 µmol photons m^{-2} s^{-1} for 2 min. The F_0 rise was monitored as described in Ma and Mi (2005). Variations in $P700^+$ levels, monitored with absorbance at 820 nm, were measured with Dual-PAM-100 as described in Paper I.

3.2.5 Steady-state fluorescence emission/excitation spectroscopy

Fluorescence emission spectra of intact cells at 77K were determined with a USB4000-FL-450 (Ocean Optics) spectrofluorometer (Paper II and IV) and a Fluorolog FL3-22 spectrofluorimeter (Horiba Jobin Yvon, Edison, NJ) and adjusted for wavelength-dependent sensitivity of the detection and for fluctuations in lamp output (Paper III). A 3 mm optical path length flow cuvette was used for measurements at RT (Paper III); samples were pumped from a chamber of 5 mL with a speed of ~2.5 mL s^{-1}. Fluorescence emission spectra were recorded by excitation with 580 nm or 440 nm light.

3.2.6 Time-resolved fluorescence spectroscopy: streak camera measurements

Time-resolved fluorescence emission spectra were obtained using a synchroscan streak-camera system as described in van Stokkum et al. (2006) and van Oort et al. (2009). Measurements were performed at RT and 77 K (excitation wavelength of 580 nm) and using a cuvette with 1 mm optical path. The laser power was 60 µW, the spot size 100 µm, and the repetition rate 250 kHz. An average of 100 images, all measured for 10 s, were recorded. Before proceeding with detailed analysis, the images were adjusted for the background signal and detector sensitivity and sliced into traces of 5 nm (RT) or 2 nm (77 K).

For RT measurements, the samples were pumped into a flow cuvette from a 5 mL chamber at a speed of ~2.5 mL s^{-1}. For 77 K measurements, cells were sampled in glass Pasteur pipettes with ~1 mm diameter and then frozen with liquid N_2. Streak-camera fluorescence images were examined using the TIMP package for R language (Mullen and van Stokkum, 2007) and Glotaran (Snellenburg et al., 2012). Details about the estimation of short and long components and fitting are found in Paper III.

3.2.7 Time-resolved fluorescence spectroscopy: TCSPC measurements

Time-correlated single-photon counting (TCSPC) measurements were performed as described previously (Somsen et al., 2005). Excitation was obtained with ~0.2 ps

vertically polarized pulses (440 nm) at a repetition rate of 3.8 MHz. The sample was kept in a flow cuvette and pumped from a reservoir (5 mL). The optical path length of the cuvette was 3 mm and the excitation spot was 2 mm in size. The measurements were performed on cells in two different states. The first condition was a minimal excitation pressure of PSII (low excitation pressure, LEP) where the RCs are mostly open. To obtain this, the samples were pumped from a reservoir to the cuvette and back, with a speed of ~2.5 mL s^{-1} and laser powers were low (~7 µW). Multiple excitations of PSII complexes by laser pulses were thus avoided, with an estimated probability of <5% that a PSII complex would be excited. The second condition was that of high excitation pressure (HEP): the flow speed was decreased to 0.2 mL s^{-1} and the laser power was brought to 50 µW. Here, a large increase of closed RCs (RCs with reduced Q_A) was obtained. Here, the probability of exciting a PSII complex with at least 1 photon from the laser beam rose to 95%. Detection of fluorescence traces was obtained with the following interference filters: 679, 693, and 724 nm (15 nm bandwidth) (Balzers, Liechtenstein model B40). Data analysis was performed as described in Paper III.

3.2.7 Thermoluminescence

TL was detected with a home-made apparatus, as in Tyystjärvi et al. (2009) in Paper III and as in Vass et al. (1992b) in Paper IV. The setup of the experiments is described in Paper III and IV.

3.3 Transcript analysis

Total RNA was isolated using TRIsure (Bioline) at 65°C, then purified with phenol:chloroform:isoamylalcohol (25:24:1) and precipitated by isopropanol. Any remaining DNA was degraded using 1 unit of DNase (Ambion Turbo DNase kit). Reverse transcription was achieved using1 µg of purified RNA, random hexamer primers and SuperScript III Reverse Transcriptase (Invitrogen). Synthesized cDNA was diluted 5-fold and used as a template for quantitative RT-PCR. Primers were designed with Primer3 Plus software (http://www.bioinformatics.nl/cgi-bin/primer3plus/primer3plus.cgi) to generate a similar length of amplicons for gene transcript analysis (primer sequences are listed in Paper II). The real-time quantitative RT-PCR reaction was a mix of cDNA, iQ SYBR Green Supermix (BioRad) and specific primers and amplification products were detected using an iQ5 system (Bio-Rad). Expression levels were estimated by averaging the results from three replicates. Relative changes in gene expression were examined using the qbaseplus (Biogazelle) software and, for all genes, expression levels were normalized to the reference gene *rnpB*.

3.4 Protein analysis and identification

3.5.1 Protein isolation, SDS-PAGE, BN/CN-PAGE and immunodetection

Total cell extracts, and soluble and membrane fractions of *Synechocystis* cells were isolated as described in Zhang et al. (2009, 2012). PDM fractions were obtained according to the protocol of Schottkowski et al. (2009a). Proteins were separated by 12% (w/v) SDS/PAGE containing 6 M urea. Protein complexes in the membrane extracts were studied by Blue Native (BN)-PAGE, which was performed as described by Zhang et al. (2012). Gradient polyacrylamide gels (4.5%-12%) were used. For electrophoresis in the second dimension (2D), a strip of the BN gel was incubated in the Laemmli SDS sample buffer containing 5% β-mercaptoethanol and 6 M urea for 1 h at 25 °C. The strip was then placed onto a 1-mm-thick 12% SDS polyacrylamide gel with 6 M urea (Laemmli 1970). After electrophoresis, the proteins were visualized by silver staining (Blum et al., 1987) or transferred to a PVDF membrane (Immobilon-P; Millipore) and examined with protein-specific antibodies. Clear native (CN)-PAGE was run with the addition of 0.02% *n*-dodecyl β-D-maltoside and 0.05% deoxycholate to the cathode buffer (Wittig et al., 2007). In investigations of YFP fluorescence, excitation was induced with 500 nm light obtained with the low pass filter LS500 (Corion, Newport Corp., Franklin, MA), and the emission was detected in the range of 550-600 nm (SyberGold filter, Geliance 1000 Imaging System, PerkinElmer Life Sciences).

3.5.3 Affinity Chromatography

A nickel-nitrilotriacetic acid-agarose resin (Qiagen, Hilden, Germany) or His SpinTrap columns (GE Healthcare) were utilized to purify proteins containing a His_6 tag. Chromatography was performed using buffers containing 25 mM Bis-Tris, pH 7.0, 20% glycerol (w/v), 20 mM NaCl, and 0.015% *n*-dodecyl β-D-maltoside, supplemented with 5, 10, and 200 mM of imidazole for binding, washing, and elution of the proteins, respectively. The eluted material was concentrated using Microcon YM-100 (Millipore) centrifuge filters prior to electrophoresis.

3.5.4 MS/MS analysis

CN-PAGE gels were stained with silver. The detected protein bands were excised and digested with Trypsin Gold (Promega). Peptides were extracted as described in Shevchenko et al. (1996) and dissolved in 2% formic acid. Positively charged precursor ions were analyzed using a Linear trap quadrupole Orbitrap Velos mass spectrometer (Thermo Fisher Scientific, Inc.) connected in line with an Easy-nLC II HPLC system (Thermo Fisher Scientific, Inc.). Data-dependent acquisition included MS/MS of the top 10 ions in each duty cycle. Database inquiries were submitted to the Protein Discoverer

program (Thermo Fisher Scientific, Inc.) with in-house Mascot server (version 2.2; Matrix Science) against a database of *Synechocystis* proteins supplemented with sequences of common contaminants (the ABSciex_ContaminantDB FASTA file suggested by Applied Biosystems, MDS-Sciex) and with a reverse decoy database.

3.5 Confocal microscopy

Fluorescence micrographs were recorded using an LSM 510 Meta confocal microscope (Carl Zeiss, Jena, Germany) with a 100x/1.4 plan apochromat oil immersion objective and an 80-µm confocal pinhole. The excitation of enhanced YFP and Chl autofluorescence were achieved with the argon ion laser (514 nm) and the helium laser (543 nm) respectively. Enhanced YFP fluorescence emission was collected with a 515-nm dichroic mirror and a band pass filter of 535–590 nm. Chl autofluorescence was obtained through a 545-nm dichroic mirror and a long pass filter of 560 nm. ImageJ software was used for image analysis. The radial profile plot plugin (Paul Baggethun) was used for the determination of cell radial fluorescence profiles using Chl autofluorescence to describe cell geometry. A circular area was selected manually for each cell. The radial distribution was determined by summing the fluorescence values at each given distance from the center, according to Sacharz et al. (2015) and distributions were normalized to the cell radius.

3.6 Bioinformatics

BLAST searches were performed using the *Synechococcus elongatus* PCC 7942 *psbA3* and *Synechocystis ssl0352* gene sequences against genome databases of cyanobacteria and other photosynthetic organisms listed in the National Center for Biotechnology Information database, Cyanobase and TAIR. The presence of a conserved 130E residue was used to discriminate the D1:2 form among other D1 protein sequences. Amino acid sequences were aligned with the ClustalW 1.83 program (Thompson et al., 1994), while domain analysis was performed using pfam software (http://pfam.sanger.ac.uk/).

4. RESULTS

4.1 A novel subunit of the NDH-1 complexes is strongly expressed under low CO_2

The uncertainties about the requirement for catalytic subunits in cyanobacterial NDH-1 complexes led to the investigation of a candidate protein, the small Ssl0352 protein. This protein has shown a coordinated increase in expression level along with known Ndh subunits in dynamic proteomic studies performed with cells shifted to LC conditions (Battchikova et al., 2010). A deletion mutant of Ssl0352 showed sensitivity to HL, whereas in moderate light conditions it demonstrated a phenotype similar to the WT. In Paper I, studies on deletion mutants and a YFP fusion to the Ssl0352 protein revealed that it is indeed a novel subunit of NDH-1 complexes, and was thus designated as the NdhS subunit.

4.1.1 NdhS localizes into the TM and associates with NDH1-M and NDH-1L complexes

NDH-1 complexes in thylakoid extracts were resolved by BN-PAGE and then subjected to SDS-PAGE in the second dimension. After electroblotting and analysis using specific antibodies against NdhH, NdhK, and Ssl0352, the Ssl0352 protein was found in NDH-1L and NDH-1M complexes but not in the NDH-1S complex (Paper I, Fig. 3). For validation of the interaction of the NdhS subunit with NDH-1 complexes, the Ssl0352 protein was fused with YFP and a His_6 tag. NdhM-YFP-His_6 was used as a control mutant.

Thylakoid extracts of Ssl0352-YFP-His_6 and NdhM-YFP-His_6 mutants were analyzed by affinity chromatography on a Ni^{2+} resin and the retained proteins were separated by CN-PAGE. The complexes identified by YFP fluorescence were analyzed by mass spectrometry. The MS/MS analysis of the fluorescent bands I, II, and III in the CN-PAGE confirmed the association of Ssl0352 (6.5 kDa) with the NDH-1M, the NDH-1I (Arteni et al., 2006), and NDH-1L complexes (Paper I, Fig. 4). The results confirmed that Ssl0352 is a novel subunit of NDH-1L and NDH-1M complexes and its binding to NDH-1 complexes was shown to become destabilized in BN-PAGE. However, the accumulation and assembly of NDH-1 complexes in Δ*ssl0352* and WT was comparable.

It has previously been established that the NDH-1L, NDH-1M, and NDH-1S complexes localize in the TM of *Synechocystis* (Ohkawa et al., 2001, 2002; Zhang et al., 2004; Xu et al., 2008). In agreement with this, the localization of the Ssl0352 protein to the TM was corroborated by two-phase partitioning (Paper I, Fig. 6) and by confocal microscopy of YFP fluorescence of Ssl0352-YFP-containing mutants (Paper I, Supplemental Fig. 4).

The relative abundance of the Ssl0352 protein further validated the role of this protein as a novel NDH-1 subunit.

4.1.2 NdhS is conserved in phototrophs and is required for efficient CET around PSI

Ssl0352 is composed of 58 amino acids and does not contain transmembrane helices. Homologues of the *ssl0352* gene encoding NdhS were found in genomes of all cyanobacteria and higher plants sequenced thus far (Paper I, Fig. 7). The conserved region of Ssl0352 constitutes an SH3-like domain which typically attaches to proline-rich sequences and is involved in protein-protein interactions that modulate enzymatic activity (De Mendez et al., 1994; Sumimoto et al., 1994; Kishan and Agrawal 2005). The Ssl0352 homologues in higher plants are larger than their cyanobacterial counterparts. An N-terminal extension with several proline-rich regions is typical for plant sequences. Furthermore, some proteins contain a block of positively charged lysine residues at the C-termini, which might be important for protein-protein interactions.

To study NDH-CET, the post-illumination rise in Chl fluorescence (F_0 rise), which reflects the redox state of inter-PS electron carriers (Mi et al., 1995; Holland et al., 2014), was measured in the Δ*ssl0352* mutant. The extent of NDH-CET in Δ*ssl0352* was reduced in comparison with the WT, yet it remained rather high compared with the M55 mutant, which is deficient the accumulation of NDH-1 complexes (Paper I, Fig. 2E). In line with these results, faster oxidation of P700 and slower re-reduction of $P700^+$ was observed in Δ*ssl0352* as compared to the WT (Paper I, Fig. 2F-5), demonstrating decreased CET in the mutant. Thus, the deletion of *ssl0352* was shown to impair the activity of NDH-CET.

4.2 The *flv4-2* operon-encoded proteins dissipate excitation pressure of Photosystem II in low CO_2, and boost its activity

In order to gain insights into the function of the *flv4-2* operon, different mutants were constructed and characterized (Paper II, III, and IV). The Δ*flv2* mutant expressed Sll0218 at WT levels, but Flv4 was observed at a very low level. The Δ*sll0218-flv2* mutant lacked Sll0218 and Flv2 and had very low levels of Flv4. The latter strain showed the same characteristics of the Δ*flv4* mutant, which lacks all of the proteins expressed by the operon (Paper IV, Zhang et al., 2012). The Δ*sll0218* strain was obtained by reintroducing Flv2 and Flv4 in Δ*sll0218-flv2*. The OE mutant overexpressed Flv4, Sll0218 and Flv2. Details about the content of Flv4, Sll0218 and Flv2 in the mutants are found in Table 2 and Fig. 1A, Paper IV.

A number of different biochemical and biophysical studies were performed with the *flv4-2* operon mutants grown in LC conditions at ~50 µmol photons m^{-2} s^{-1} (GL) or HL (~500 µmol photons m^{-2} s^{-1}). Importantly, an overexpression mutant of the entire *flv4-2* operon showed improved growth performance in HL conditions compared to control strains (Paper II).

		Proteins encoded by the *flv4-2* operon		
		Flv4 content	Sll0218 content	Flv2 content
Strains	Δ*flv2*	<	=	/
	Δ*sll0218-flv2*	<	/	/
	Δ*flv4*	/	/	/
	Δ*sll0218*	>	/	≥
	OE	>>	>>	>>

Table 2. Representation of the *flv4-2* operon-encoded proteins contents in the mutants used in this research, in comparison to WT (=, similar content; <, strongly decreased content; /, undetectable content; ≥, slightly increased content; >, increased content; >>, very increased content, compared to WT). For a deeper understanding, check Fig.1A in Paper IV.

4.2.1 Flv2/Flv4 mediates an electron transfer route at the Q_B site of PSII

The photochemistry of PSII was investigated in different *flv4-2* operon mutants by measuring the maximum photochemical efficiency of PSII (Fv/Fm, in the presence of DCMU) and effective quantum yield of PSII [Y(II)] (Paper II and IV). Improved Fv/Fm and Y(II) values were observed when the *flv4-2* operon was overexpressed (OE strain). The Δ*flv4* mutant demonstrated lowest values (Paper II, Supplemental Table S1). Similar results were observed for the Δ*flv2* and Δ*sll0218-flv2* mutants (Paper IV, Fig. 2B). The Y(II) values of cells grown in HL conditions were, for the most part, similar to those of cells grown in GL conditions. However, the differences between strains were larger. PSII activity was also measured in terms of O_2 evolution rates in the presence of the artificial electron acceptor DMBQ. In comparison to the WT, O_2 evolution activity was about 25% lower in Δ*flv2* and of about 40% lower in Δ*flv4* and Δ*sll0218-flv2*, while it was 10% less in Δ*sll0218*. Contrary to this, oxygen evolution activity was about 20% higher in the OE strain (Paper IV, Fig. 2B). Thus the Flv2/Flv4 heterodimer was shown to have a prominent role in preserving PSII activity in LC conditions, as well as in HL.

The OE mutant exhibited higher variable fluorescence (Fv) in the dark-adapted state as well as a higher Fq value (Fm' - Fs) in the light-adapted state (Paper II, Fig. 6), reflecting an increased amount of open PSII centers as compared to all other strains. This is in line with the Y(II) values. These experiments indicated that OE cells demonstrated less reduced Q_A than the other strains. The Δ*flv4* mutant had elevated F_0 and Fs levels, whereas the Fq level was decreased compared to the WT (Paper II, Supplemental Fig. S4). These results indicate that in the absence of the *flv4-2* operon-encoded proteins,

the open fraction of PSII centers is consistently reduced during illumination compared with control cells. Because of a disturbed energy transfer from PBSs to PSII RCs (Zhang et al., 2012), a strong contribution of PBSs fluorescence to the F_0 value (Acuña et al., 2015; Schuurmans et al., 2015) cannot be excluded in the Δ*flv4* mutant. The F_0 rise was less prominent in OE and stronger in Δ*flv4* compared with control strains (Paper II, Supplemental Fig. S3), implying that in the presence of the *flv4-2* operon-encoded proteins, there is a more oxidized PQ pool in darkness. Although the OE strain demonstrated an oxidized state of the PQ pool after the termination of illumination and in the light, its state transition kinetics were not modified (Paper II, Supplemental Fig. S2).

The flash-induced increase in fluorescence yield and its subsequent decay in darkness were measured for the different *flv* mutants grown in LC conditions. Experiments were performed in the presence of DBMIB, which blocks the Q_0 site of the Cyt b_6f complex, and thus also the main reoxidation route of PQH_2 (Trebst, 1980). The results showed that Flv2 and Flv4 facilitate Q_A^- reoxidation (Paper II, Fig. 9; Paper IV, Supplemental Fig. S1).

To further investigate the effect of the *flv4-2* operon-encoded proteins on PSII excitation energy transfer (EET) and charge separation processes, the fluorescence decay kinetics of WT, OE, and Δ*flv4* were determined using a time-correlated single-photon counting setup (TCSPC) at 440 nm excitation. Two conditions were studied: low excitation pressure (LEP) where the contribution of photochemistry is almost negligible and thus changes in PSII fluorescence lifetimes are mostly represented by energy trapping and primary/secondary charge separation rates (van Oort et al., 2010); and high excitation pressure (HEP) which induces photochemistry resulting in the lengthening of PSII lifetimes as a consequence of changes in charge separation as well as the Q_A and PQ redox state (Tian et al., 2013). OE fluorescence decay was faster than in the WT, both at LEP and HEP, while the Δ*flv4* fluorescence decay was slower than in WT (Paper III).

Fitting a multiexponential decay function and global analysis (Paper III, Table 2) described the data with four decay components. Significant changes were observed only in the second and third components. The second component (140–170 ps for WT/OE), is influenced by excitation trapping within PSII and primary charge separation kinetics (van Oort et al., 2010); the third component (360–400 ps for WT/OE) was attributed mostly to electron transfer to Q_A (secondary charge separation) in open RCs. Under LEP the OE strain already demonstrated a shorter lifetime of the third component compared to the WT. This shorter lifetime represents an increase of

secondary charge separation with a parallel decrease of back charge recombination (Schatz et al., 1988; Szczepaniak et al., 2009; Tian et al., 2013). In general, the amount of closed RCs was higher for the WT than for the OE strain in both LEP and HEP. The resolved PSII decay components for Δ*flv4* were considerably longer than those obtained for the WT and OE, both in LEP and HEP measurements (Paper III, Table 2). This indicates a significant build-up of RCs with reduced Q_A in Δ*flv4* already occurring in LEP conditions, when the probability of a PSII being excited is almost negligible due to low photon density. Thus, the PSII lifetimes of Δ*flv4* in LEP are affected by decreased charge separation, while the longer PSII lifetimes in HEP are caused by Q_A reduction as well as by the concomitant reduction of the PQ pool. Also, the *flv4-2* operon affects neither the PSI fluorescence lifetimes nor the PSII/PSI ratio, as deduced from amplitudes and lifetimes of the first, PSI-related, component in the strains. Thus, the deficiency of *flv4-2* operon-encoded proteins strongly slows down PSII fluorescence kinetics by reducing Q_A, even when the measuring conditions minimize the chance of PSII being excited. This indicates a strong decrease of charge separation with concomitant increase of backward charge recombination.

O_2 evolution measurements with a number of electron acceptors allowed for further illustration of the Flv2/Flv4 electron transfer route (Paper II, Table I). In agreement with the results of Zhang et al. (2012), the rate of Δ*flv4* O_2 evolution from water to the DCBQ electron acceptor (mainly accepting electrons at the Q_B pocket of PSII (Graan and Ort, 1986)) was higher than the rates obtained in the presence of DMBQ (accepting electrons from the PQ pool). Whereas in the WT, the O_2 evolution rates with DMBQ were higher than those with DCBQ (Table I in Paper II). Interestingly, the overexpression of the *flv4-2* operon resulted in elevated rates of O_2 evolution in the presence of DMBQ compared to the WT, whereas the rates with DCBQ were lower. These data revealed that, in the presence of DMBQ, electron transport to Flv2/Flv4 takes place, whereas DCBQ inhibits this electron transfer route. Therefore, Flv2 and Flv4 constitute an alternative electron transport mechanism that sequesters electrons at the Q_B pocket of PSII (suggested by Zhang et al., 2012), thus maintaining a more oxidized PQ pool in LC. O_2 evolution measurements, which were performed in the presence of low concentrations of DBMIB, which partially inhibits electron transfer to Cyt b_6f, showed about 30% decreased rates in Δ*flv4* compared to the WT, while the OE mutant had around 10% higher rates than the control strains.

The reason for pronounced differences in the reduction state of Q_A between different *flv4-2* operon mutants remained unclear. To solve this question, thermoluminescence (TL) measurements of *flv4-2* operon mutants were executed (Paper III and Paper IV). Interestingly, the peak temperatures for the Q band were similar in the mutants and

the WT (Paper III, Fig. 9B; Paper IV, Supplemental Fig. S2), demonstrating a lack of shift in the redox potential of Q_A. Conversely, a change in the B band position in the mutants (compared with control strains) suggests that the presence of Flv2 and Flv4 proteins (WT, OE and Δ*sll0218*) involves an increase of the redox potential of Q_B, thus expanding the redox gap between Q_A and Q_B and supporting forward electron transfer. When Flv2 and Flv4 proteins are not present (Δ*flv2*, Δ*flv4,* Δ*sll0218-flv2*), the downshift of the B band might correlate with a reduced redox potential of Q_B (Paper IV, Supplemental Figure S2), thus favoring backward electron transfer to Q_A, as observed in TCSPC measurements for Δ*flv4*.

4.2.2 Relative carotenoid content, production of singlet oxygen and photodamage are influenced by *flv4-2* operon-encoded proteins

Evident differences in the color of the cell cultures exposed to HL suggested modifications of the pigment composition in WT and the various *flv* mutants (Paper II, IV). At 500-HL, the OE strain showed a darker green color than the WT strain, whereas the Δ*flv2,* Δ*sll0218-flv2,* Δ*sll0218 and* Δ*flv4* mutants had an obvious yellow color (Paper II, Fig. 2C; Paper IV, Fig. 1B). Further, the OE mutant remained unbleached when grown at 1500-HL, in contrast to the other strains, including the WT. Growth experiments clearly showed that the OE mutant tolerated HL intensities better than all other strains. When cells were grown in GL and 500-HL, the Δ*flv4* strain showed the highest carotenoid/Chl *a* ratio (Car/Chl *a*), whereas the OE mutant had the lowest ratio among all of the strains (Paper II, Fig. 3). In fact, the OE mutant had ~22% lower Car/Chl *a*, whereas Δ*flv4* had ~10% higher Car/Chl *a* compared with respective control strains (Paper II, Fig. 3). Thus, the HL-tolerant phenotype of the OE mutant is based on a specific function of the *flv4-2* operon but not on the accumulation of carotenoids.

To further study the HL sensitivity of the mutants, PSII photodamage was assessed in the presence of lincomycin, an inhibitor of *de novo* protein synthesis which excludes the contribution of PSII repair. O_2-evolving activity was recorded in the presence of DMBQ as an artificial electron acceptor. Compared with the control strains, the OE mutant experienced less PSII photodamage during exposure to HL, which was demonstrated by higher PSII activity (Paper II, Fig. 5). Photoinhibition curves in the absence and/or presence of lincomycin (Paper IV, Fig. 3) might indicate that the protection afforded PSII by Flv2/Flv4 mainly occurs in the beginning of the shift to HL.

Singlet oxygen ($^1O_2$) formation was tested by measuring His-mediated O_2 uptake (Rehman et al., 2013). In the Δ*flv4* strain, $^1O_2$ production increased compared with the WT, despite an elevated level of carotenoids (Paper II, Fig. 4). A large decrease in $^1O_2$ formation in the OE mutant compared with all other strains was observed (40%

decrease compared to the WT strain), even though the OE strain had a lower carotenoid content than the WT. These data correlated with light sensitivities of the strains and indicated that the *flv4-2* operon plays an important role in photoprotection by decreasing the formation of $^1O_2$, an important contributor to PSII photodamage (Vass et al., 1992a).

4.2.3 Sll0218 stabilizes the PSII dimer and PSII repair

PSII activity in the Δ*sll0218* mutant was only slightly inferior (~10%) to the WT (Paper IV, Fig. 2B). Thus, Sll0218 does not play a significant role in PSII functionality. However, the Δ*flv2* mutant, which still encodes Sll0218, had higher O_2 evolution rates in the presence of DMBQ than did the Δ*flv4* mutant.

Even in GL conditions, the Chl content was lower (~25%) in all of the *flv4-2* operon deletion mutants than in the WT, while it increased in the OE strain. In 500-HL conditions the mutants lacking all three proteins of the operon, or only Sll0218, demonstrated an approximate 50% decrease in Chl content. When Sll0218 was present (Δ*flv2*), the decrease was less (~25%). The overexpression of the entire operon induced higher Chl content than in the WT under both GL and 500-HL (Paper IV, Fig. 1C). When the D1 content was investigated by immunoblot analysis of protein extracts from cells grown in GL, a striking feature was observed: the lowest levels of D1 accumulation (50% decrease) were found in mutants lacking all three proteins of the operon, but also in the Δ*sll0218* mutant (Paper IV, Fig. 2A). The D1 protein accumulation appeared to be impaired in the Δ*sll0218* mutant despite almost WT-levels of PSII activity. The mutants which lacked Sll0218 showed a higher sensitivity to photodamage after 90 min of exposure to 1000 µmol photons m^{-2} s^{-1}. When lincomycin was added, photoinhibition curves showed differences between the Sll0218-lacking mutants and WT in the beginning of the measurements. However, these differences disappeared after 60 min of exposure to 1000 µmol photons m^{-2} s^{-1} (Paper IV, Fig. 3). Even in the absence of lincomycin, the Sll0218 lacking mutants suffered from chronic photoinhibition, indicating that PSII repair was unable to compete with the rate of damage. These results were supported by immunoblot analysis where the degradation of D1 protein was shown not to be affected in the mutants (Paper IV, Supplemental Fig. S3). Instead, an accumulation of PSII assembly intermediates was observed in the Sll0218-lacking mutant strains. The assembly intermediate complexes contained D1 and YCF48 protein (Paper IV, Fig. 4), and could represent forms of RCa complex identified by Komenda et al. (2008). YCF48, a PSII assembly factor, accumulated to a higher extent in mutants lacking Sll0218 than in the WT (Paper IV, Fig. 5A). Further, a Δ*ycf48* mutant failed to accumulate the Sll0218 protein, whereas Flv2 and Flv4 were present (Paper IV,

Fig. 5C). Other PSII assembly factors accumulated in a similar manner as in the WT. However, a protein of the stomatin family called Phb3 (Slr1128), was present at very low levels in the Sll0218-lacking mutants (Paper IV, Supplemental Fig. S5).

Fusion of YFP with Sll0218 revealed its localization at the peripheral external side of TMs, at an average of two puncta per cell (Paper IV, Fig. 6A-C). Furthermore, the Sll0218 protein was selectively found in the PDM fractions (Paper IV, Fig. 6D), which represent specific areas of the thylakoid biogenesis centers where the first steps of PSII assembly occurs (Rengtsl et al., 2011). It was also shown that the PSII dimer/monomer ratios were lower in Δ*flv4* while the OE mutant showed the same ratio as the WT. Notably, the OE strain showed a lesser amount of CP47-RC (Paper III, Table 1).

4.3 The *flv4-2* operon-encoded photoprotective mechanism and the light harvesting process reciprocally influence each other

When the *flv4-2* operon was deleted, a consistent uncoupling of PBS antenna was observed through a variety of methods (Papers II, III, and IV). In order to further examine this relationship, the expression of the *flv4-2* operon was investigated in mutants with disturbed light-harvesting.

4.3.1 Deletion of the *flv4-2* operon causes PSII dimer instability resulting in antenna detachment

In the Δ*flv4* mutant, the 77K and RT fluorescence emission spectra using an excitation light of 580 nm showed higher peaks at 685 nm and 660 nm respectively, when compared to WT spectra (Paper II, Fig. 10; Paper III, Fig. 1A). The increase at 660 nm in the RT spectra for Δ*flv4* indicates lower energy transfer from the PBSs to the RCs, in agreement with the 77 K spectra observed by Zhang et al. (2012). Distinctively different 77K and RT fluorescence spectra were observed for the OE mutant: compared to the control strains, lower peaks of 685 nm and 660 nm respectively were detected, suggesting an increased efficiency of energy transfer from PBSs to the PSII RCs (Paper II, Fig. 10; Paper III, Fig 1A, C). Importantly, no significant differences were observed in the 77K fluorescence spectra when Chl was excited with 440 nm light (Paper II, Supplemental Fig. S5). Furthermore, Δ*flv4*, OE, and control strains showed no differences in PC and APC-D contents (Paper II, Fig. 8A) and there were no significant differences observed in phycobilin/Chl a ratios (Paper II, Supplemental Fig. S6; Paper III, Supplemental Fig. S6). Thus, the increased F_0 level detected in Chl fluorescence curves in the Δ*flv4* mutant (Paper II, Fig. 6) was not influenced by phycobilin amounts, but was probably caused by a reduced energy transfer from PBSs to PSII RCs, again in agreement with 77K fluorescence results.

The effect of the deletion or overexpression of *flv4-2* operon-encoded proteins on EET from light harvesting antenna to PSII RCs was specifically investigated using time-resolved fluorescence spectroscopy. First, the possibility that the OE strain has an improved efficiency of EET from PBSs toward PSII RCs at RT was investigated. This line of investigation arose from the steady-state 77K fluorescence emission spectra (Paper II and III). The obtained OE and WT datasets, as well as the resolved decay associated spectra (DAS, Paper III, Fig. 3-4), did not show considerable differences between the two strains, demonstrating that EET from PBS to RCs does not differ between the OE strain and the WT.

However, streak-camera data showed that the Δ*flv4* fluorescence decay was slower in the OE strain than in the WT (Paper III, Fig. 4). Consequently, the WT and Δ*flv4* datasets were subject to a linked analysis whereby lifetimes were equalized, while amplitudes were allowed to vary. The first two components represented EET within PBSs. The amplitudes of the WT and Δ*flv4* were comparable, confirming that EET stages within PBSs are not influenced by the *flv4-2* operon-encoded proteins. The DAS of the 159 ps component was mostly assigned to PBSs because of the spectral contour. Importantly, the amplitude of the 159 ps component decreased by ~16% in Δ*flv4*. This reduction corresponded to a similar increment of the amplitude of the fourth (654 ps) DAS in Δ*flv4* compared to the WT. The maximum of the fourth DAS for Δ*flv4* was at ~665 nm, while for the WT it was 680 nm. A difference spectrum for the WT and Δ*flv4* mutant was calculated by subtracting the fluorescence emission spectrum of the fourth DAS of the WT from that of Δ*flv4* (Paper III, Fig. 6 insert). The difference spectrum revealed a characteristic PBS peak at 660 nm. Therefore, in Δ*flv4* the fluorescence increase in the spectra represents the contribution of uncoupled PBSs and does not represent a higher influence of closed RCs. The decoupling of ~16% of the PBSs, as calculated from the change in amplitude of the third component, is responsible for the changes in spectral shape and the lengthening of the fourth fluorescence decay component of Δ*flv4*.

Next, to investigate the accumulation of PSII complexes, TM extracts of the WT and *flv4-2* operon mutants were examined using BN-PAGE gels (Paper III, Fig. 7). The PSII dimer, the PSII monomer, and the CP47-RC monomer complexes were identified after immunoblotting with anti-D1 antibodies. The PSII RC protein D1 was then quantified, in order to estimate the accumulation of the different PSII complexes (Paper III, Table 1). The PSII total content and the PSII dimer to monomer ratio (~1) in the WT and OE strains were similar (Paper III, Fig. 7 and Table 1). The Δ*flv4* mutant had lower amounts of PSII than the WT, as was reported earlier by Zhang et al. (2012). A consistent decrease of PSII dimer and a minor decrease of PSII monomer complexes were observed in the

Δ*flv4* strain, causing a decreased PSII dimer-to-monomer ratio (~0.6). The relative decrease of PSII dimer content in relation to the WT was about 20% (Paper III, Table 1). An increase of EET efficiency toward PSII in the OE mutant was not detected, but almost 20% of PBSs were uncoupled from the RCs in Δ*flv4*. The phycobilin/Chl *a* ratio was not considerably altered in the three strains (Paper III, Supplemental Fig. 6), suggesting that the quantity of PBS is proportional to the Chl *a*-comprising complexes in the strains. These results suggest a correlation between the drop of the PSII dimer to monomer ratio and PBS detachment, which was revealed by a major increase of PBS fluorescence in Δ*flv4*. Zhang et al. (2012) proposed that the PSII dimer to monomer ratio was regulated by the Sll0218 protein. To clarify the role of Sll0218 in PBS uncoupling, 77K fluorescence emission spectra were recorded with other *flv4-2* operon mutants. Importantly, only the mutants lacking Sll0218 showed a higher peak at 685nm, corresponding to PBS detachment from RCs. Conversely, the spectra of a mutant expressing Sll0218 (Δ*flv2*) was similar to the WT. Therefore, it is possible that a regular coupling of PBS to PSII RCs is enabled by the effect of Sll0218 on PSII assembly and on PSII dimer stabilization.

4.3.2 Interplay between the *flv4-2* operon related photoprotective mechanism with OCP mediated NPQ for excess energy dissipation

Photochemistry, fluorescence, and NPQ are in competition to dissipate the energy absorbed by Chls (see review by Bailey and Grossman 2008). Therefore, the enhanced photochemistry of PSII observed in the OE strain was examined for its influence on the NPQ process. This was achieved by assessing OCP-related NPQ (Wilson et al., 2006). The OE strain demonstrated about 20% lower amplitude in the quenching of maximal fluorescence than did the control strains (Paper II, Fig. 7). However, the amount of OCP protein did not change significantly between the WT and the OE mutant (Paper II, Fig. 8A). Remarkably, in the ΔOCP mutant the transcription of the *flv4-2* operon was increased and a very high content of Flv4, Sll0218 and Flv2 proteins were produced as compared to the WT (Paper II, Fig. 8B). These findings again confirmed the crucial role of the *flv4-2* operon-encoded proteins in photoprotection of PSII, especially when the OCP photoprotective mechanism is absent (Paper II, Fig. 8B-C).

4.3.3 PBSs are required for the photoprotective mechanisms encoded by the *flv4-2* operon

The expression levels of Flv4, Sll0218, and Flv2 proteins in LC conditions were determined in different PBS mutants to characterize the role of antennae on the *flv4-2* operon-mediated photoprotective mechanism (Paper II, Fig. 8B). In the absence of PBSs (PAL mutant, Ajlani and Vernotte, 1998), the *flv4-2* operon-encoded proteins

could not be detected. When PBSs lacked PC rods and consisted of only the APC core (CK mutant, described in Thomas et al., 2006), reductions of approximately 75% of Flv4, Sll0218, and Flv2 proteins were observed compared with WT levels. In the Δ*ApcDF* mutant which, due to a lack of ApcD and F terminal emitters, displays a severely impaired energy transfer from PBSs to PSII RCs (Ashby and Mullineaux, 1999; Jallet et al., 2012) the Flv4, Flv2, and Sll0218 proteins were nearly absent compared with the WT (Paper II, Fig. 8B). Conversely, the ΔOCP mutant, impaired in the quenching of excess excitation energy collected by the PBS (Wilson et al., 2006), revealed a clear upregulation of Flv2, Flv4, and Sll0218 protein content compared with the WT. It was thus of interest whether decreased expression of the *flv4-2* operon in PBS mutants arose at the transcript or protein level. RT-PCR results correlated with immunoblotting experiments (Paper II, Fig. 8B-C), indicating a regulation of the *flv4-2* operon at the transcriptional level, dependent on the presence of functional PBSs.

4.4 Occurrence of genes related to different photoprotective mechanisms in different phototrophic organisms

Through literature mining and BLAST analysis, it was determined that the *flv4-2* operon is conserved in nearly all genomes of β-cyanobacteria, with a few exceptions (*Synechococcus sp.* PCC 7002*, Synechococcus elongatus* PCC 7942, *T. elongatus* BP-1*, Trychodesmium* IMS 101, Table 3). Intriguingly, the cyanobacteria that do not possess the *flv4-2* operon in their genome have a further D1 copy, called D1:2, involved in HL resistance (Table 3). The single D1 protein present in algae and plants shares more common residues with the D1:2 cyanobacterial D1 copy, including the 130E residue (Svensson et al., 1991; Winhauer et al. 1991; Campbell et al., 1998; Takishita and Uchida, 1999). This suggests that the Q130E D1 copy was a favorable strategy for survival in photosynthetic organisms, eventually becoming ubiquitous among them.

OCP genes were found in all cyanobacteria containing PBS, with only two exceptions in *Synechococcus elongatus* and *T. elongatus* BP-1 (Table 3; Boulay et al., 2008).

Many β-cyanobacteria species contain *flv4-2* operon homologues, but do not possess homologues of the *PTOX* gene. PTOX is involved in an AET route that mediates electron flow from PQH_2 to O_2 (for a review, see McDonald et al., 2011). Other cyanobacteria, especially those inhabiting the iron-poor marine environment, do not contain *flv4-2* operon homologues but instead possess a *PTOX* gene (Table 3). *PTOX* gene homologues are also found in algae and plants (McDonald et al. 2011).

	Strains	Type	Ecological niche	Antenna system	OCP	*flv4-2* operon	D1:2 copy (Q130E)	PTOX
Cyanobacteria	*Synechocystis* sp. PCC 6803	β	freshwater	PBS	+	+	-	-
	Microcystis aeruginosa sp. PCC 7806	β	freshwater	PBS	+	+	-	-
	Microcystis aeruginosa NIES-843	β	marine	PBS	+	+	-	-
	Cyanothece sp. PCC 8801	β	freshwater	PBS	+	+	-	-
	Cyanothece sp. ATCC 51142	β	marine	PBS	+	+	+	-
	Trychodesmium IMS 101	β	marine	PBS	+	-	+	-
	Synechococcus sp. PCC 7002	β	marine	PBS	+	-	+	-
	Anabaena sp. PCC 7120	β	freshwater	PBS	+	+	+	+
	Synechococcus elongatus PCC 7942	β	freshwater	PBS	-	-	+	-
	Thermosynechococcus elongatus BP-1	β	freshwater thermophile	PBS	-	-	+	-
	Synechococcus sp. WH7803	α	marine	PBS	+	-	+	-
	Synechococcus sp. WH8102	α	marine	PBS	+	-	+	+
	Prochlorococcus marinus str. MIT9211	α	marine (LL)	Pcb	-	-	-	-
	Prochlorococcus marinus str. MED4	α	marine (HL)	Pcb	-	-	-	+
Viridiplantae	*Chlamydomonas reinhardtii*		freshwater	LHCII/I	-	-	+	+
	Arabidopsis thaliana		land	LHCII/I	-	-	+	+

Table 3. A brief overview of photoprotection mechanisms found in different cyanobacterial species and photosynthetic eukaryotes. Homology analysis of the D1:2 copy was performed with BLASTP at http://blast.ncbi.nlm.nih.gov. Some data were obtained from Boulay et al., (2008), McDonald et al., (2011) and Zhang et al., (2012). Pcb, chlorophyll a/b binding light harvesting protein; LHCII/I, Light-harvesting complex II/I; HL, high light ecotype; LL, low light ecotype.

5. DISCUSSION

5.1 The novel NdhS subunit of NDH-1M and NDH-1L complexes: a bridge for electrons from Ferredoxin

A novel subunit of the NDH-1 complexes, NdhS, was identified in Paper I. NdhS has hydrophilic properties but associates to the TM, as do NdhM, NdhN, and NdhO (Battchikova et al., 2005).

The NdhS subunit plays a role in the acclimation of *Synechocystis* to LC since the expression of the Ssl0352 protein, as well as NDH-1 complexes, significantly increased in LC (Paper I, Battchikova et al., 2010). NdhS is present in the NDH-1L complex but also in NDH-1M, which together with NDH-1S forms NDH-1MS involved in inducible CO_2 uptake (Zhang et al., 2004). However, the NdhS subunit was not detected in the NDH-1S complex, which is predicted to possess carbonic anhydrase activity (Kaplan and Reynold, 1999). Therefore, we assume that it does not directly participate in CO_2 uptake.

The deletion of NdhS impaired the NDH-CET levels and delayed the growth of cells under HL conditions (Paper I). Such impairment does not result in the reduction of total NDH-1 proteins or the disassociation of the NDH-1 complexes. It was therefore concluded that the cyanobacterial NdhS subunit is either directly or indirectly involved in PSI-dependent CET. For this reason, NdhS could also be important in energizing CO_2 uptake through NDH-1MS mediated CET around PSI. NdhS is an SH3-like domain protein, conserved in cyanobacteria and green plants. In *Arabidopsis thaliana*, an NdhS homologue CRR31 was found in the plastidial NDH complex (Yamamoto et al. 2011). Like NdhS, CRR31 has been shown to be important for efficient NDH activity. The global structural similarity of NdhS and the PsaE subunit of the PSI complex prompted Yamamoto et al. (2011) to propose that the SH3 domain in CRR31 forms a Fd docking site. They indeed showed that plastidial NDH receives electrons from Fd rather than from NAD(P)H (Yamamoto et al., 2011; Yamamoto and Shikanai 2013). The SH3 domain-like fold of NdhS contains a pocket with positive surface charges which are essential for electrostatic interaction with Fd. In particular, the arginine 193 of NdhS is required for the formation of the positively-charged pocket (Yamamoto and Shikanai 2013). Recently, an affinity purified NDH-1L complex of *T. elongatus* was obtained. The purified complex contained 14 NDH-1 subunits including NdhS, and protein interaction between NdhS and Fd was confirmed by surface plasmon resonance analysis (He et al., 2015). In addition, He et al. (2015) employed a yeast-two-hybrid assay to show that NdhS interacts with NdhH, NdhI, and Fd, suggesting that NdhS might be located beside NdhH and NdhI, accepting electrons from Fd (Fig. 9). Thus it is evident

that Fd is the electron donor to the cyanobacterial NDH-1 complex, or at least the NDH-1L complex. This is, despite pioneering studies reporting an NAD(P)H oxidizing activity of NDH-1 (Matsuo et al., 1998, Deng et al., 2003 a-b; Ma et al., 2006). It is possible that contaminating enzyme activities might have caused the detection of NAD(P)H dehydrogenase activity of the NDH-1 complex reported in early works. The FNR_S isoform which is an NADPH oxidase accumulating mainly under heterotrophic conditions (Thomas et al., 2006; Korn 2010), could be involved in donation of electrons from reduced Fd to NDH-1 complexes for respiratory function.

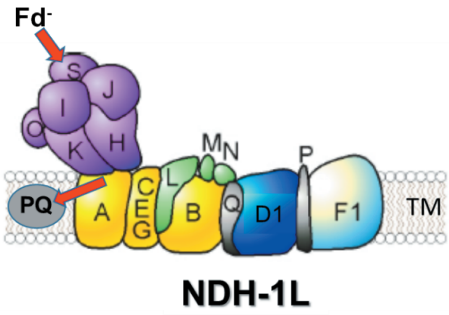

Figure 9. Model of cyanobacterial NDH-1L complex. According to recent literature NdhS is located in the vicinity of NdhI and NdhH, providing the docking site for Fd. Red arrows indicate electron transfer from Fd to the NDH-1L complex and from the complex to PQ pool. Figure modified from Peltier et al. (2015).

Although relatively rare, the loss of a number of *ndh* genes has occurred across diverse lineages of photoautotrophic seed plants. Interestingly, the nuclear gene encoding NdhS is retained across the majority of taxa which have lost *ndh* genes, except gnetophytes (Ruhlman et al., 2015). Moreover, NdhS has been found to accumulate in the TM of mutants that do not express NDH (Yamamoto et al., 2011). The hypothesis of an additional role of NdhS in plants requires further investigation.

5.2 Flv2/Flv4 and Sll0218 entwine their functions to ensure optimal PSII activity in LC and HL, in cooperation with PBSs

5.2.1 Protection of PSII activity by the Flv2/Flv4 heterodimer

In HC conditions, which mimic atmospheric CO_2 concentrations at the evolution of oxygenic photosynthesis (Kaufman and Xiao 2003), photosynthetic processes in cyanobacteria are optimal: the high amount of CO_2 offers an unlimited sink for electrons obtained from the water oxidation activity of PSII and cells grow faster (Marco et al., 1993; MacKenzie et al., 2004). In these conditions, the *flv4-2* operon is not expressed and it does not provide benefit for the cells (Paper II, Supplemental Fig. S7, Zhang et al., 2012). Indeed, tight control over the expression of the *flv4-2* operon is needed to avoid energy waste for unstressed cells in HC conditions. Conversely, expression of the *flv4-2* operon is required for the provision of photoprotection in LC

and HL conditions. Notably, the antisense RNA As1_flv4 prevents expression of the *flv4-2* operon in the initial phase after a shift from HC to LC conditions (Eisenhut et al., 2012). In LC conditions, where the *flv4-2* operon is strongly expressed, there is a limitation of the electron acceptor CO_2. In cyanobacteria, this invokes a strong expression of CCMs in order to concentrate as much CO_2 as possible around Rubisco whilst inducing CET to contribute to ATP production (for reviews, see Kaplan and Reinhold 1999; Badger and Price, 2003; Price et al., 2008). In this manner, photosynthetic efficiency is gained. However, electron acceptors are more reduced than in HC conditions (Melis et al., 1999, Asada et al., 1999), causing ROS accumulation and a higher risk of photoinhibition (Kaplan 1981; Miller and Canvin 1989).

In LC conditions, a number of constitutively expressed electron sinks are further induced in order to dissipate excess excitation energy. Examples include Flv3 (Zhang et al., 2009; Allahverdiyeva et al., 2011) and NDH-1 complexes routes (Battchikova et al., 2010). The former dissipates electrons at the PSI acceptor side and the latter performs CET around PSI to adjust the ATP/NADPH ratio under stressful conditions. Remarkably, the induction of these sinks is not sufficient to avoid an over-accumulation of electrons in the photosynthetic chain. Thus, the risk of affecting the first steps of light energy absorption and conversion increases, affecting PSII and its ability to utilize energy collected by the antennae. The sensitivity of PSII to such conditions required the evolution of a safeguarding electron dissipation mechanism in the first steps of photosynthesis.

The experiments conducted with mutant strains of *Synechocystis* clearly demonstrated that the expression of the *flv4-2* operon provide a more photoprotected phenotype in LC and HL conditions. This was coupled with an improved photochemistry of PSII. Importantly, strains expressing the *flv4-2* operon showed an oxidized PQ pool, allowing PSII to function efficiently with a reduced risk of photoinhibition (Paper II and IV). The oxidized state of the PQ pool correlated with a decrease in the production of $^1O_2$ (Paper II, Fig. 4) and less photodamage of PSII centers (Paper II, Fig. 5). Both outcomes indicated that expression of the *flv4-2* operon resulted in a greater tolerance to photoinhibition. Furthermore, this protection from photoinhibition was not associated with increased carotenoid production (Paper II). The *flv4-2* operon-encoded proteins and carotenoids contribute to protection against $^1O_2$-mediated damage in a complementary manner: when the *flv4-2* operon-encoded proteins provide adequate photoprotection, the content of carotenoids remains at a low level.

PSII activity and Q_A^- reoxidation were specifically protected by the action of the Flv2/Flv4 heterodimer (Paper II, III, and IV). Moreover, the effect of the Flv2/Flv4 heterodimer on PSII activity was not wholly dependent on the presence of the Sll0218

protein (Paper IV). When Flv2/Flv4 was not present (Δ*flv2* strain), the D1 protein content decreased by approximately 30%, demonstrating an effect of Flv2/Flv4 on PSII accumulation in the presence of Sll0218. These data, together with the results of Zhang et al. (2012), provide clear evidence for the participation of Flv2 and Flv4 in an AET process that intercepts electrons at the Q_B pocket of PSII, thus maintaining the PQ pool in an oxidized state under LC and HL conditions.

The lifetime analysis of TCSPC data indicated that, in the presence of *flv4-2* operon-encoded proteins, charge separation rates increased whereas backward charge recombination rates decreased; thus supporting the decreased production of $^1O_2$ reported in Paper II. On the other hand, the TL data in Papers III and IV suggest that the presence of the Flv2/Flv4 heterodimer induces an increase in the redox potential of Q_B, thus stabilizing forward electron transfer.

It is conceivable that docking of the Flv2/Flv4 heterodimer in the surroundings of the Q_B pocket improves charge separation in PSII by increasing the redox potential of Q_B. This could enhance electron transfer to Q_B and the Flv2/Flv4-related AET route could remove electrons from reduced Q_B, thus keeping the PQ pool in a more oxidized state, resulting in shorter PSII fluorescence lifetimes in HEP (Paper III, Fig. 7). The effect on the redox potential of Q_B could represent a "turn on" switch for the Flv2/Flv4 AET mechanism.

Finally, the electron acceptor of the Flv2/Flv4 heterodimer is still under debate: on the basis of *in vitro* experiments, Shimakawa et al., (2014) proposed O_2 as the ultimate electron acceptor, similarly to Flv1/Flv3. However, this cannot be the case *in vivo*, since it has previously been shown that the Flv1/3 heterodimer is solely responsible for light-induced O_2 uptake (Allahverdiyeva et al., 2011; Ermakova et al., submitted). Moreover, under low O_2 conditions, the expression of the *flv4-2* operon is strongly induced (Summerfield et al., 2008, 2011), suggesting that Flv2/Flv4 could act as a safety valve in micro-oxic conditions when terminal oxidases and Flv1/Flv3 do not work. The role of NO as an electron acceptor for Flv2/Flv4 needs further investigation, considering that this molecule destabilizes HCO_3^- binding to the non-heme iron at the acceptor side of PSII, thus slowing down Q_A to Q_B electron transfer (Diner and Petrouleas 1990; Petrouleas and Diner 1990). In fact, there is evidence that increasing CO_2 concentration influences the charge accumulation process around PSII as a consequence of an increasing bicarbonate effect (Cao and Govindjee 1988; Garab et al., 1988). Thus it is possible that the differences observed in TL data between strains could relate to the stabilization of the HCO_3^- binding site on the acceptor side of PSII by Flv2/Flv4 in LC conditions (for reviews about the bicarbonate effect, see McConnell et al., 2012; Shevela et al., 2012).

5.2.2 The contribution of Sll0218 to PSII stabilization and subsequent optimization of light harvesting

It has been suggested that CO_2 limitation might inhibit the repair of PSII rather than accelerating photodamage to PSII (reviewed in Nishiyama and Murata 2014). Several lines of evidence have shown that an interruption of CO_2 fixation enhances the production of ROS (Radmer and Kok 1976; Radmer and Ollinger 1980; Asada and Badger 1984; Allakhverdiev et al., 2005), which then inhibits the synthesis of proteins and, in particular, synthesis of the D1 protein (for details, see Takahashi and Murata 2008). In fact, the regulation and function of Sll0218 in PSII stabilization differs from that of Flv2 and Flv4. The first indication of this came from the accumulation of the *flv4-2* operon-encoded proteins in the Δ*flv2* mutant. When Flv2 was deleted, the amount of Flv4 protein was significantly decreased, a first indication of the function of Flv2 in association with Flv4. However, the amount of Sll0218 protein remained similar to that in the WT. Further, in mutants lacking YCF48, Flv2 and Flv4 could be detected at the protein level, unlike Sll0218. According to data presented in Paper IV, the Sll0218 protein has a stabilizing role in PSII assembly and repair processes. In its absence, a PSII assembly intermediate containing at least D1 and YCF48 accumulated significantly and photoinhibition was accelerated compared to strains expressing Sll0218 in the absence, but not in the presence, of lincomycin. The accumulation of YCF48, an assembly factor of PSII (Komenda et al., 2008), increased in the absence of Sll0218 and decreased when the *flv4-2* operon was overexpressed. Sll0218 localized to PDM membranes, where the initial steps of PSII assembly occur (Rengstl et al., 2011). In addition, the content of a Phb3 protein in the family of Stomatins strongly decreased when Sll0218 was not present. Proteins of the stomatin family might have a scaffold function in the organization of the membrane (Browman et al., 2007) and consequently have extensive effects on membrane structure and function. In plants, stomatin-like proteins are considered to be scaffolds for respiratory chain assembly (Gehl and Sweetlove 2014). In *Synechocystis*, Phb3 forms a ring-like assembly with a diameter of ~16 nm (Boehm et al., 2009) and it was shown to be localized in PSII repair zones of the membrane (Sacharz et al., 2015).

The lower relative content of the CP47-RC complex in the OE strain (Paper III, Fig. 7) seems to indicate that the steps to PSII monomer and PSII dimer formation are stabilized when the *flv4-2* operon-encoded proteins (including Sll0218) are overexpressed. Further, PBS detachment was first observed in Δ*flv4*, where almost 20% of PBSs were uncoupled from the RCs. The decrease of 20% of relative PSII dimer content in relation to the WT correlated with the amount of detached PBSs. The decrease of PSII dimers was already related to Sll0218 by Zhang et al. (2012) but

stronger evidence was needed. In Paper IV, using several other *flv4-2* operon mutants, it was shown by fluorescence emission measurements that the absence of Sll0218 is linked to the F685 effect related to antenna uncoupling. It has previously been shown that several mutations triggering a lower PSII dimer to monomer ratio distorted EET from PBSs to RCs, resulting in increased F685 in the 77 K fluorescence spectra (Sakurai et al., 2007; Wilson et al., 2007; Bentley et al., 2008; Young 2010). PBSs associate with PSII dimers, but not with monomers (Mörschel and Mühlethaler 1983; Mörschel and Schatz 1987; Bald et al., 1996; Barber et al., 2003). Thus, the energy harvested by PBSs flows preferentially to PSII dimers, and not to PSII monomers, explaining the distorted energy transfer in Δ*flv4* and other mutants with comparatively decreased PSII dimer content. It has been shown that PBS detachment is a typical response when photoprotective processes are congested and light harvesting and energy transfer are both unnecessary and harmful (Tamary et al., 2012).

Sll0218 predominantly forms a high molecular mass complex comparable with PSII dimer, but with a slightly lower mass (Zhang et al., 2012). Interestingly, a weak band detected with the D2 antibody overlapping with the Sll0218 band, indicated a possible association of Sll0218 with an intermediate step of PSII assembly (Zhang et al., 2012). Unfortunately, it has not been possible to determine other partners of this complex yet. It is plausible that Sll0218 could coordinate the assembly steps from PSII monomer to PSII dimer. Indeed, its absence results in the considerable accumulation of the relative content of PSII monomers and other intermediates, including the D1-YCF48-containing complexes (Fig. 10).

Using the Δ*sll0218* mutant, it was observed that the function of Flv2/Flv4 in electron transfer is not alone sufficient to rescue PSII accumulation, but requires the presence of Sll0218.

According to these results, I propose that Sll0218 and Flv2/Flv4 cooperate in LC conditions to protect and boost PSII activity. Sll0218 stabilizes PSII assembly/repair ensuring an increased number of active PSII centers which could efficiently receive energy from antennae; and the higher electron sink capacity provided by the Flv2/Flv4 heterodimer ensures a safer and enhanced activity of PSII (Fig. 10).

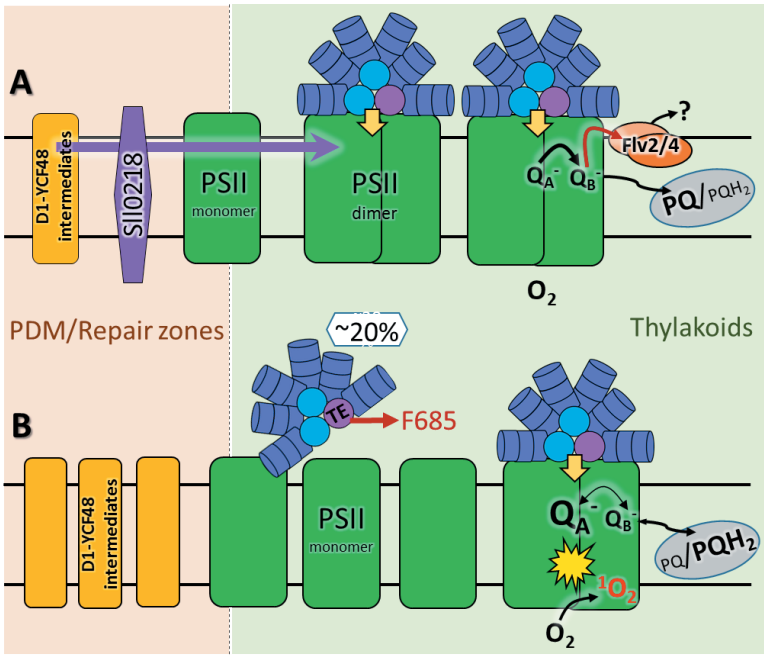

Figure 10. Schematic model of the *flv4-2* operon-encoded photoprotective mechanism. (**A**) In LC conditions, Sll0218 supports PSII assembly/repair upon transition from smaller complexes (D1-YCF48-containing intermediates) to PSII dimers (purple arrow). The stabilization of PSII dimers by the Sll0218 protein results in efficient EET from PBSs toward PSII RCs (yellow arrows). The docking of the Flv2/Flv4 heterodimer to the vicinity of PSII increases the Q_B redox potential, thus stabilizing the forward electron transfer and accelerating the charge separation rates in PSII. The activity of the Flv2/Flv4 heterodimer provides a more oxidized state of the PQ pool. (**B**) The lack of Sll0218 protein destabilizes PSII dimers, resulting in the detachment of ~20% of the antenna indicated by the increase of fluorescence of terminal emitters at 685 nm at 77K (F685). An accumulation of PSII monomers and D1-YCF48-containing intermediates have also been observed. When Flv2/Flv4 is missing, the PQ pool is more reduced, leading to an increased probability of backward electron transfer from reduced Q_B, and keeping Q_A more reduced. Consequently, the accumulation of excited states result in a higher production of $^1O_2$, which intensifies the probability of photodamage to PSII (yellow spark). TE, terminal emitters.

5.2.2 An efficient EET from PBSs to PSII regulates the expression of the *flv4-2* operon

My results (Papers II, III, IV) and earlier published reports on Flv2, Flv4, and Sll0218 (Zhang et al., 2012) together demonstrate the crucial role that these proteins play in ensuring an efficient distribution of the energy collected by PBS to PSII in LC conditions. The expression of the *flv4-2* operon at both the transcript and protein levels is dependent on the presence of PBSs and on the efficiency of energy transfer from PBSs to RCs. These conditions also impart a certain level of excitation pressure on PSII, reflected in the redox state of the PQ pool, which could be required for optimal transcription of the *flv4-2* operon. Indeed, the *flv4-2* operon is most efficiently

transcribed under combined HL and LC conditions, when the PQ pool is over-reduced (Zhang et al., 2009). Whereas when the PQ pool is more oxidized (e.g. in the presence of DCMU, Schuurmans et al., 2014), the transcription of the *flv4-2* operon is diminished (Hihara et al., 2003). Thus, the expression of the *flv4-2* operon could be redox-regulated by the PQ pool, in addition to the strict control by the NdhR transcription factor and several noncoding RNAs (Eisenhut et al., 2012).

Upon overexpression of the *flv4-2* operon, photochemical processes are enhanced and the amplitude of OCP-mediated NPQ of maximal fluorescence is reduced by approximately 20% compared to the control strain (Paper II, Fig. 7). The Flv2/Flv4-related electron transport mechanism and the OCP-mediated NPQ could be in competition for energy dissipation. However, they are more likely to be active in different circumstances. OCP-mediated NPQ is more active in HL conditions (El Bissati et al., 2000), while the Flv2/Flv4-AET is active in LC conditions, even at GL. Moreover, at higher light intensities (350 µmol photons m^{-2} s^{-1}), only about 29% of PBSs were quenched by the OCP *in vivo* (Tian et al., 2011). Therefore, the Flv2/Flv4 heterodimer could play a role as an electron sink at the acceptor side of those PSII complexes that received energy from PBSs. Additionally, high amounts of Flv4, Sll0218, and Flv2 proteins in the ΔOCP mutant compared with the WT, confirming the important share in photoprotection of the *flv4-2* operon-encoded proteins, especially in the absence of the OCP photoprotective mechanism.

5.3 Evolutionary trends of cyanobacterial PSII photoprotective mechanisms

In this work, the importance of the *flv4-2* operon for PSII photoprotection in LC and HL conditions has been clearly demonstrated. It is conceivable that the *flv4-2* operon-encoded photoprotective mechanism, essential for the survival of *Synechocystis*, was lost relatively early in the course of the evolution of cyanobacteria. The appearance of the D1:2 copy might have contributed to the elimination of the *flv4-2* operon (Results, Table 3; Paper II, Table II). It is noteworthy that *flv4-2* operon mRNA levels have been shown to be drastically reduced in iron-limited conditions (Singh et al., 2003; Hernandez-Prieto et al., 2012), suggesting that Flv2 and Flv4 are a metabolic burden for the cells in this specific situation. Iron is a limiting factor for cyanobacterial growth and can be limiting especially in marine environments (Behrenfeld et al., 1996). The selection pressure by iron limitation in seawater might have favored the loss of the *flv4-2* operon in those marine cyanobacteria that could rely on the evolutionarily more recent D1:2 form. The absence of the *flv4-2* operon is indeed mostly characteristic of marine species, including two β-cyanobacteria, *Trychodesmium* IMS 101 and

Synechococcus sp. PCC 7002 (Table 3). Conversely, the supply of C_i, which regulates the accumulation of *flv4-2* operon transcripts and influences PSII activity/stability, is expected to be quite steady in open marine environments, whilst it is often a limiting factor in freshwater (Badger et al., 2006). Since the *flv4-2* operon-encoded proteins play a key role in cell survival under conditions of strong over-reduction of the PQ pool induced by C_i limitation, I suggest a positive selection of the *flv4-2* operon-encoded photoprotective mechanism in conditions of adequate iron availability but fluctuating C_i supply. These considerations might collectively explain why the *flv4-2* operon is present in the genomes of freshwater β-cyanobacteria, while it is less common in marine species (Table 3 in Results).

In contrast to the *flv4-2* operon, OCP genes are present in almost all cyanobacteria containing PBSs, with the exception of *Synechococcus elongatus* and *T. elongatus* BP-1 (Table 3; Boulay et al., 2008). This observation suggests that the OCP mechanism has been the more successful of the two photoprotective mechanisms, due to its high efficiency combined with a low metabolic cost, which is particularly important under stressful conditions. In fact, two important functions are condensed in the OCP protein: NPQ (Wilson et al., 2006) and singlet oxygen quenching (Sedoud et al., 2014).

Almost all β-cyanobacteria have *flv4-2* operon homologues, but do not contain *PTOX* gene homologues. In other cyanobacteria, especially those growing in the iron-poor open marine environment, the *flv4-2* operon homologues are not present, but a *PTOX* gene can be found (Table 3). *PTOX* gene homologues are also found in marine *Synechococcus* species (Bailey et al., 2008). Since PTOX alleviates excessive PSII excitation pressure and increases the ΔpH, this mechanism represents a potential adaptation to a low iron environment in the oligotrophic oceans (Bailey et al., 2008).

Prochlorococcus species lack most of the photoprotection mechanisms found in other cyanobacteria. This genus lacks PBSs and possesses Pcb (Chl *a*/*b*-Binding light-harvesting Protein) antenna embedded in the membrane, which contains Chl *a* and *b*. HL ecotypes of *Prochlorococcus* strains, such as *Prochlorococcus marinus* MED4 (Table 3) possess a *PTOX* gene homologue, while it is not found in low light ecotypes (McDonald et al., 2005). *Prochlorococcus marinus sp*. PCC 9511 tolerates HL by temporarily down-regulating some of the main metabolic processes and by enhancing a minimal set of protection mechanisms, for example by overexpressing the *PTOX* and *psbA* genes (Mella-Flores et al. 2012).

In plants grown under stressful conditions, PTOX can utilize around 30% of electrons originating from PSII (Stepien and Johnson 2009; Savitch et al., 2010; Ivanov et al., 2012). A similar value was obtained in this work for the deviation of electrons from PSII

by the Flv2/Flv4 heterodimer for *Synechocystis* (Paper II). It is conceivable that PTOX is analogous in function to the Flv2/Flv4 heterodimer but is evolutionarily younger. In heterocystous cyanobacteria where *PTOX* gene homologues are found (*Anabaena sp.* PCC 7120 and *Anabaena variabilis* ATCC 29413, see McDonald et al., 2011), PTOX might contribute to maintain an O_2-free environment in the heterocysts, in cooperation with the Flv3B form identified by Ermakova et al. (2014), thus allowing N_2 fixation to work. While the PTOX final electron acceptor is O_2, the electron acceptor of the Flv2/Flv4 heterodimer is still unknown.

The *flv4-2* operon might have played a crucial role in the maintenance of oxygenic photosynthesis in the first steps of its evolution; nevertheless, it was successively lost because of its apparently high metabolic cost for a cell, compared with other efficient and less expensive photoprotective tools. Of these, the Q130E D1 form was a successful strategy, diffused among several photosynthetic organisms. Further, *PTOX* genes are widely present in algae and plants (McDonald et al. 2011). McDonald and Vanlerberghe (2006) suggested that PTOX arose in phototrophic eukaryotes through the primary endosymbiotic event that gave rise to chloroplasts. Afterwards, these proteins were distributed through eukaryotic organisms by vertical inheritance and, in other cases, via secondary and tertiary endosymbiotic events. The need for mechanisms which dissipate high excitation pressure at the PSII acceptor side (Flv2/Flv4 and PTOX) is evidenced by their occurrence in different and evolutionarily distinct groups of organisms, such as cyanobacteria, algae and plants (Table 3).

6. CONCLUSIONS AND FUTURE PERSPECTIVES

My thesis deals with the identification of a novel subunit of NDH-1 complexes involved in electron transfer, and in establishing the physiological role for the *flv4-2* operon in photoprotection. Electron transfer mediated by these pathways is currently a hot topic of photosynthetic research in cyanobacteria.

In addition to providing consistent information on the physiology of cyanobacteria, this research is important in paving the way towards direct solar fuel production by photosynthetic microorganisms; the aim is to eliminate "superfluous" electron transfer routes and to make photosynthetic electron transfer from water to target biofuel molecules more efficient and direct.

The NdhS subunit was identified as an essential link for CET around PSI, and recently NdhS was shown to interact with Fd (Yamamoto et al., 2011; He et al., 2015), thus providing a bridge for electrons from PSI. In this way FNR_L and NDH-1 might compete for electrons from Fd, avoiding a delay in the adjustment of NADPH/ATP ratios and an overreduction of the PSI acceptor side in stress conditions. However, the diversity of the NDH-1 complexes in cyanobacteria does not totally exclude the involvement of NADPH and FNR as electron donors in as yet uncharacterized conditions. Curiously, NdhS might play an additional role in plants, since it still accumulates when NDH complexes are absent, and it is also retained in plant lineages lacking most or all of the *ndh* genes. Yet another question is whether the NDH-1L complex forms a supercomplex with PSI as it has been reported in plant TMs (Peng et al., 2008).

The majority of my thesis work has been directed toward characterizing the photoprotective mechanism enabled by the *flv4-2* operon. Molecular, biochemical and different biophysical approaches were used to differentiate the functions of the three proteins encoded by the operon (Flv2, Sll0218 and Flv4) and it was shown that their functions are highly intertwined to guarantee an optimal PSII activity in LC and HL conditions. The functional characterization of Flv2 and Flv4, together with other works conducted in our laboratory focusing on the role of Flv1 and Flv3, confirmed the importance of these diversified groups of proteins in the evolution and maintenance of oxygenic photosynthesis in different environmental conditions (Allahverdiyeva et al., 2015b). Flv2/Flv4 provides an electron sink from the Q_B pocket of the acceptor side of PSII, triggered by a shift in the redox potential of Q_B. This reaction safeguards PSII activity, prevents singlet oxygen formation, and keeps the PQ pool more oxidized in LC conditions. However, the electron acceptor of Flv2/Flv4 is still unclear. To clarify whether it is NO, or a protein, requires further in-depth studies. The interplay of

Flv2/Flv4 with terminal oxidases and Flv1/Flv3 is currently under investigation. Further, a direct interaction of Flv2/Flv4 with PSII has not been demonstrated as yet.

The Sll0218 protein stabilizes PSII assembly/repair, in particular the formation of the PSII dimer, and optimizes energy transfer from PBSs to stabilized PSII dimers. Its function is required to ensure a photoprotective role of Flv2/Flv4. Many details, however, still need to be clarified such as i) the identification of the Sll0218 interacting partners; and ii) the elucidation of the effects on PSII assembly/repair, and whether they are direct or indirect. The characterization of the role of Sll0218 in the PSII assembly/repair process presents a major challenge: the expression of the *flv4-2* operon proteins seems to be dependent on an efficient LET activity/high excitation pressure of PSII. The approach utilized by many laboratories, applying the deletion of some PSII subunits in order to clearly visualize PSII assembly intermediates in native gels and western blots, will not be effective in studying Sll0218, because the methodology results in the disruption of LET/excitation pressure on PSII. On the other hand, work without the deletion of PSII subunits brings with it the strong accumulation of bulky PSII complexes which hides the less abundant PSII intermediates in native gels and western blots.

The expression of the *flv4-2* operon is controlled by a plethora of regulatory mechanisms and it is likely that some of them remain to be discovered. Here, I have identified a novel mechanism. The presence of PBSs and a correct energy transfer from PBSs to the reaction centers were shown to be essential for the transcription of the *flv4-2* operon, suggesting the involvement of a novel regulatory mechanism triggered by changes in the excitation pressure of PSII. Furthermore, the *flv4-2* operon-encoded proteins operate in photoprotection in a complementary manner to the orange carotenoid protein related nonphotochemical quenching.

Finally, in this thesis I present an overview on the occurrence of different PSII photoprotective mechanisms in cyanobacteria. I suggest that the *flv4-2* operon-based photoprotective mechanism was outcompeted in the course of evolution by the appearance of a HL-tolerant form of the D1 protein, the D1:2 copy. The redundancy of these two photoprotective mechanisms still needs to be confirmed experimentally.

7. ACKNOWLEDGEMENTS

The Laboratory of Molecular Plant Biology of University of Turku is a truly unique environment where it is possible to perform excellent research. I am deeply grateful to Academy Prof. Eva-Mari Aro for the opportunity to work in her laboratory, for providing a thriving environment and for supporting my research with a caring and thoughtful guidance and great encouragement. I am thankful to Dr. Natalia Battchikova for guiding me through Molecular Biology and Biochemistry techniques and for her concise and synthetic approach which I often lack of. Dr. Yagut Allahverdiyeva taught me how to handle biophysical techniques and provided great help and support, especially in the last phase of my PhD, for all this I am very thankful. Prof. Eevi Rintamäki is acknowledged for guiding me through the formalities of my studies and the bureaucratical steps of the PhD thesis. I would like to thank the collaborators Prof. Imre Vass, Prof. Herbert van Amerongen and Prof. Jörg Nickelsen for contributing importantly to the research outcomes of this work. In particular, I am thankful to Dr. Volha Chukhutsina for bringing me in the world of time-resolved fluorescence spectroscopy and for her friendship. Our collaboration was also possible thanks to the financial support from the Marie Curie Initial Training Network Harvest: this network gave me the possibility to grow as a researcher, learning different techniques and improving my presentation skills and meeting other PhD students around Europe with whom to share knowledge and friendship. Other financial sources are gratefully acknowledged: UTUGS, DPMLS, FDPPS, Alfred Kordelin foundation, Academy of Finland, the Finnish Centers of Excellence "Integrative Photosynthesis and Bioactive Compound Research at Systems Biology Level" and "Molecular Biology of Primary Producers". An amazing help and support in the lab (and not only) was provided by Essi Ruohisto and Maija Lespinasse, for this I am deeply grateful. The Flv group and Cyanobacterial groups, from which I would like to mention especially Gayathri, Hariharan, Henna, Heta, Julia, Linda, Martina A, Martina J, Masha, Pasi, Tuomas, Veronica are acknowledged for their scientific contributions, support and friendly (and crazy) moments. The technical staff (Anniina, Eve, Kurt, Janne, Mika, Ulla-Maija and Vipu), as well as the administrative staff have been extremely helpful in many different circumstances.

I would like to thank Dr. Marc Nowaczyk and Prof. Ondřej Prášil for reviewing the thesis and providing useful comments. Many thanks to Fiona for the language correction of the thesis. I would like to thank especially Martina Angeleri for being extremely patient with me and supporting me in many challenging moments, especially during the writing of the thesis, and for providing rivers of sweets and chocolates. Further, I thank Ninni and Masha for helping me during the last phases of the thesis preparation and Anita for supporting me and sharing funny moments while working continuously in Pharmacity. I would like to thank some of the guests which visited our laboratory in Turku for sharing knowledge and friendship, thank you Dr. Alessia Antonacci, Dr. Lorenzo Ferroni, Dr. Martina Giovanardi and Félix Ramos-León. Further all the principal investigators and Prof. Marjatta Raudaskoski are acknowledged for fruitful discussions and suggestions. I would like to thank all the former and actual PhD students and Postdocs of the lab for sharing joyful and depressing moments and for their help.

I cannot finish this thesis without acknowledging my family, in particular my parents and my sister for their endless support and care. Further my friends have been very important during these years. I already mentioned many of them above (yes, you know who you are!) and now it is time to mention the others in random order: Aisling, Kostas, Heidi, Joel, Natalia, Hannele, Bogdan, Jenni, Robert, Leea, Meri, Olga, Julian, Denise, Julien, Outi, Pinja, Minna, Susa, Ida, Jarmo and the Italians, Andrea, Vincenza, Matilde and Michele, and also all my friends in Italy and friends around the world. Thank you!!!

8. REFERENCES

Acuña AM, Snellenburg JJ, Gwizdala M, Kirilovsky D, van Grondelle R, van Stokkum IH (2015) Resolving the contribution of the uncoupled phycobilisomes to cyanobacterial pulse-amplitude modulated (PAM) fluorometry signals. Photosynthesis Res: 1-12.

Ajlani G, Vernotte C (1998) Construction and characterization of a phycobiliprotein-less mutant of *Synechocystis* sp. PCC 6803. Plant Mol Biol 37: 577-580.

Allakhverdiev SI, Nishiyama Y, Takahashi S, Miyairi S, Suzuki I, Murata N (2005) Systematic analysis of the relation of electron transport and ATP synthesis to the photodamage and repair of photosystem II in *Synechocystis*. Plant Physiol 137: 263-273**.**

Allahverdiyeva Y, Ermakova M, Eisenhut M, Zhang P, Richaud P, Hagemann M, Cournac L, Aro EM (2011) Interplay between flavodiiron proteins and photorespiration in *Synechocystis* sp. PCC 6803. J Biol Chem 286: 24007-24014.

Allahverdiyeva Y, Mustila H, Ermakova M, Bersanini L, Richaud P, Ajlani G, Battchikova N, Cournac L, Aro EM (2013) Flavodiiron proteins Flv1 and Flv3 enable cyanobacterial growth and photosynthesis under fluctuating light. Proc Natl Acad Sci USA 110: 4111-4116.

Allahverdiyeva Y, Suorsa M, Tikkanen M, Aro EM (2015a) Photoprotection of photosystems in fluctuating light intensities. J Exp Bot 66: 2427-2436.

Allahverdiyeva Y, Isojärvi J, Zhang P, Aro EM (2015b) Cyanobacterial oxygenic photosynthesis is protected by flavodiiron proteins. Life 5: 716-743.

Allen MM (1968) Simple conditions for growth of unicellular blue-green algae on plates. J Phycol 4: 1-4.

Allen JF, Santabarbara S, Allen CA, Puthiyaveetil S (2011) Discrete redox signaling pathways regulate photosynthetic light-harvesting and chloroplast gene transcription. PLoS ONE 6: e26372.

Anbudurai PR, Mor TS,Ohad I, Shestakov SV, Pakrasi HB (1994) The *ctpA* gene encodes the C-terminal processing protease for the D1 protein of the photosystem II reaction center complex. Proc Natl Acad Sci USA 91: 8082-86.

Anderson SL, McIntosh L (1991) Light activated heterotrophic growth of the cyanobacterium *Synechocystis* sp. strain PCC 6803: a blue-light requiring process. J Bacteriol 173: 2761-2767.

Aoki M, Katoh S (1983) Size of the plastoquinone pool functioning in photosynthetic and respiratory electron transport of *Synechococcus* sp. Plant Cell Physiol 24: 1379-1386.

Appel J, Phunpruch S, Steinmüller K, Schulz R (2000) The bidirectional hydrogenase of *Synechocystis* sp. PCC 6803 works as an electron valve during photosynthesis. Arch Microbiol 173: 333-338.

Armbruster U, Zühlke J, Rengstl B, Kreller R, Makarenko E, Rühle T, Schünemann D, Jahns P, Weisshaar B, Nickelsen J, Leister D (2010) The *Arabidopsis* thylakoid protein PAM68 is required for efficient D1 biogenesis and photosystem II assembly. Plant Cell 22: 3439-3460.

Arteni AA, Zhang P, Battchikova N, Ogawa T, Aro EM, Boekema EJ (2006) Structural characterization of NDH-1 complexes of *Thermosynechococcus elongatus* by single particle electron microscopy. Biochim Biophys Acta 1757: 1469-1475**.**

Aro EM, Virgin I, Andersson B (1993) Photoinhibition of photosystem II. Inactivation, protein damage and turnover. Biochim Biophys Acta 1143: 113-134.

Aro EM, Suorsa M, Rokka A, Allahverdiyeva Y, Paakkarinen V, Saleem A, Battchikova N, Rintamäki E (2005) Dynamics of photosystem II: a proteomic approach to thylakoid protein complexes. J Exp Bot 56: 347-356.

Asada K (1999) The water-water cycle in chloroplasts: scavenging of active oxygens and dissipation of excess photons. Annu Rev Plant Physiol Plant Mol Biol 50: 601-639.

Asada K, Badger MR (1984) Photoreduction of $^{18}O_2$ and $H_2{}^{18}O$ with concomitant evolution of $^{16}O_2$ in intact spinach chloroplasts: evidence for scavenging of hydrogen peroxide by peroxidase. Plant Cell Physiol 25: 1169-1179.

Ashby MK, Mullineaux CW (1999) The role of ApcD and ApcF in energy transfer from phycobilisomes to PSI and PSII in a cyanobacterium. Photosynth Res 61(2): 169-179.

Badger MR, Hanson DT, Price GD (2002) Evolution and diversity of CO_2 concentrating mechanisms in cyanobacteria. Functional Plant Biology 29: 161-173

Badger MR, Price GD (2003) CO_2 concentrating mechanisms in cyanobacteria: molecular components, their diversity and evolution. Journal of Experimental Botany 54: 609-622.

Badger MR, Price GD, Long BM, Woodger FJ (2006). The environmental plasticity and ecological genomics of the cyanobacterial CO_2 concentrating mechanism. J Exp Bot 57: 249-265.

Bailey S, Grossman A (2008) Photoprotection in cyanobacteria: regulation of light harvesting. Photochem Photobiol 84: 1410-1420.

Bailey S, Melis A, Mackey KR, Cardol P, Finazzi G, van Dijken G, Berg GM, Arrigo K, Shrager J, Grossman A (2008) Alternative photosynthetic electron flow to oxygen in marine *Synechococcus*. Biochim Biophys Acta 1777: 269-276.

Bald D, Kruip J, Rögner M (1996) Supramolecular architecture of cyanobacterial thylakoid membranes: how is the phycobilisome connected with the photosystems? Photosyn Res 49: 103-118.

Barbato R, Friso G, Rigoni F, Dalla Vecchia F, Giacometti GM (1992) Structural changes and lateral redistribution of photosystem II during donor side photoinhibition of thylakoids. J Cell Biol 119: 325:335.

Barber J (2003) Photosystem II: the engine of life. Q Rev Biophys 36: 71-89.

Barber J (2012) Photosystem II: The Water-Splitting Enzyme of Photosynthesis. Cold Spring Harbor Symp Quant Biol 77: 295-307.

Barber J, Morris EP, da Fonseca PCA (2003) Interaction of the allophycocyanin core complex with photosystem II. Photochem Photobiol Sci 2: 536-541.

Battchikova N, Zhang P, Rudd S, Ogawa T, Aro EM (2005) Identification of NdhL and Ssl1690 (NdhO) in NDH-1L and NDH-1M complexes of *Synechocystis* sp PCC 6803. J Biol Chem 280: 2587-2595.

Battchikova N, Vainonen JP, Vorontsova N, Keränen M, Carmel D, Aro EM (2010) Dynamic changes in the proteome of *Synechocystis* 6803 in response to CO_2 limitation revealed by quantitative proteomics. J Proteome Res 9: 5896-5912.

Battchikova N, Eisenhut M, Aro EM (2011) Cyanobacterial NDH-1 complexes: novel insights and remaining puzzles. Biochim Biophys Acta 1807: 935-944.

Behrenfeld MJ, Bale AJ, Kolber ZS, Aiken J, Falkowski PG (1996) Confirmation of iron limitation of phytoplankton photosynthesis in the equatorial pacific-ocean. Nature 383: 508-511.

Behrenfeld MJ, Halsey KH, Milligan AJ (2008) Evolved physiological responses of phytoplankton to their integrated growth environment. Philos Trans R Soc Lond B Biol Sci 363: 2687-2703.

Bentley FK, Luo H, Dilbeck P, Burnap RL, Eaton-Rye JJ (2008) Effects of inactivating psbM and psbT on photodamage and assembly of photosystem II in *Synechocystis* sp. PCC 6803. Biochemistry 47: 11637-11646.

Berger S, Ellersiek U, Steinmuller K (1991) Cyanobacteria contain a mitochondrial complex-I-homologous NADH-dehydrogenase. FEBS Lett 286: 129-132.

Bernat G, Appel J, Ogawa T, Roegner M (2011) Distinct roles of multiple NDH-1 complexes in the cyanobacterial electron transport network as revealed by kinetic analysis of P700(+) reduction in various ndh-deficient mutants of *Synechocystis* sp. strain PCC6803. J Bacteriol 193: 292-295.

Berry S, Schneider D, Vermaas WFJ, Rögner M (2002) Electron transport routes in whole cells of *Synechocystis* sp. strain PCC 6803: the role of the cytochrome bd-type oxidase. Biochemistry 41: 3422-3429.

Birungi M, Folea M, Battchikova N, Xu M, Mi H, Ogawa T, Aro EM, Boekema EJ (2010) Possibilities of subunit localization with fluorescent protein tags and electron microscopy examplified by a cyanobacterial NDH-1 study. Biochim Biophys Acta 1797: 1681-1686.

Blankenship RE (1992) Origin and early evolution of photosynthesis. Photosynth Res 33: 91-111.

Blankenship RE (2002) Molecular mechanisms of photosynthesis. Oxford: Blackwell Science.

Blum H, Beier H, Gross HJ (1987) Improved silver staining of plant proteins, RNA and DNA in polyacrylamide gels. Electrophoresis 8: 93-99.

Boehm M, Nield J, Zhang P, Aro EM, Komenda J, Nixon P.J (2009) Structural and mutational analysis of band 7 proteins in the cyanobacterium *Synechocystis* sp strain PCC 6803. J Bacteriol 191: 6425-6435.

Bonaventura C, Myers J (1969) Fluorescence and oxygen evolution from *Chlorella pyrenoidosa*, Biochim Biophys Acta 189: 366-383.

Boulay C, Abasova L, Six C, Vass I, Kirilovsky D (2008) Occurrence and function of the orange carotenoid protein in photoprotective mechanisms in various cyanobacteria. Biochim Biophys Acta 1777(10): 1344-1354.

Böthe H, Schmitz O, Yates MG, Newton WE (2010) Nitrogen fixation and hydrogen metabolism in cyanobacteria. Microbiol Mol Biol Rev 74: 529-551.

Branco dos Santos F, Du W, Hellingwerf KJ (2014) *Synechocystis*: not just a plug-bug for CO_2, but a green *E. coli*. Front Bioeng Biotechnol 2: 36.

Brandt U, Kerscher S, Drose S, Zwicker K, Zickermann V (2003) Proton pumping by NADH : ubiquinone oxidoreductase. A redox driven conformational change mechanism? FEBS Lett 545: 9-17.

Brandt U (2006) Energy converting NADH: quinone oxidoreductase (Complex I). Annu Rev Biochem 75: 69-92.

Brändén G, Gennisb RB, Brzezinskia P (2006) Transmembrane proton translocation by cytochrome c oxidase. Biochim Biophys Acta 1757: 1052-1063.

Browman DT, Hoegg MB, Robbins SM (2007) The SPFH domain-containing proteins: more than lipid raft markers. Trends Cell Biol 17: 394-402.

Bryant DA (2003) The beauty in small things revealed. Proc Nat Adac Sci USA 100: 9647-9649.

Bryant DA, Frigaard N-U (2006) Prokaryotic photosynthesis and phototrophy illuminated. Trends Microbiol 14: 488-96.

Burnap RL, Hagemann M, Kaplan A (2015) Regulation of CO_2 concentrating mechanism in cyanobacteria. Life 5: 348-371.

Burroughs NJ, Boehm M, Eckert C, Mastroianni G, Spence EM, Yu J, Nixon PJ, Appel J, Mullineaux CW, Bryan SJ (2014) Solar powered biohydrogen production requires specific localization of the hydrogenase. Energy Environ Sci 7: 3791-3800.

Campbell D, Eriksson MJ, Oquist G, Gustafsson P, Clarke AK (1998) The cyanobacterium *Synechococcus* resists UV-B by exchanging photosystem II reaction-center D1 proteins. Proc Natl Acad Sci USA 95: 364-369.

Cao J, Govindjee (1988) Bicarbonate effect on electron flow in a cyanobacterium *Synechococcus* PCC6803. Photosynth Res 19: 277-285.

Carroll J, Fearnley IM, Skehel JM, Shannon RJ, Hirst J, Walker JE (2006) Bovine complex I is a complex of 45 different subunits. J Biol Chem 281: 32724-32727.

Cassier-Chauvat C, Chauvat F (2014) Function and regulation of ferredoxins in the cyanobacterium, *Synechocystis* PCC 6803: recent advances. Life 4: 666-680.

Cavalier-Smith T (2000) Membrane heredity and early chloroplast evolution. Trends Plant Sci 5: 174-182.

Chen L, Liu MY, LeGall J, Fareleira P, Santos H, Xavier AV (1993) Rubredoxin oxidase, a new flavo-hemo-protein, is the site of oxygen reduction to water by the "strict anaerobe" *Desulfovibrio gigas*. Biochem Biophys Res Commun 193: 100-105.

Chidgey, JW, Linhartová M, Komenda J, Jackson PJ, Dickman MJ, Canniffe DP, Koník P, Pilný J, Hunter CN, Sobotka R (2014). A cyanobacterial chlorophyll synthase-HliD complex associates with the Ycf39 protein and the YidC/Alb3 insertase. Plant Cell 26(3): 1267-1279.

Chukhutsina V, Bersanini L, Aro EM, van Amerongen H (2015) Cyanobacterial light harvesting phycobilisomes uncouple from photosystem I during dark-to-light transitions. Sci Rep 5: 14193.

Clarke AK, Hurry VM, Gustafsson P, Öquist G (1993) Two functionally distinct forms of the photosystem II reaction-center protein D1 in the cyanobacterium *Synechococcus* sp. PCC 7942. Proc Natl Acad Sci USA 90: 11985-11989.

Cohen Y, Gurevitz M (2006) The Cyanobacteria-Ecology, Physiology and Molecular Genetics" in The Prokaryotes: The handbook on the biology of Bacteria, ed M. Dworking, 3rd ed, Springer, pp 1074-1098.

Cooley JW, Howitt CA, Vermaas WFJ (2000) Succinate:Quinol oxidoreductases in the cyanobacterium *Synechocystis* sp. srain PCC 6803: presence and function in metabolism and electron transport. J Bacteriol 182: 714-722.

Cooley JW, Vermaas WFJ (2001) Succinate dehydrogenase and other respiratory pathways in thylakoid membranes of *Synechocystis* sp. strain PCC 6803: capacity comparisons and physiological function. J Bacteriol 183: 4251-4258.

Cournac L, Guedeney G, Peltier G, Vignais PM (2004) Sustained photoevolution of molecular hydrogen in a mutant of *Synechocystis* sp. strain PCC 6803 deficient in the type I NADPH-dehydrogenase complex. J Bacteriol 186: 1737-1746.

Croce R, van Amerongen H (2013) Light-harvesting in photosystem I. Photosynth Res 116: 153-166.

Cser K, Vass I (2007) Radiative and non-radiative charge recombination pathways in Photosystem II studied by thermoluminescence and chlorophyll fluorescence in the cyanobacterium *Synechocystis* 6803. Biochim Biophys Acta 1767: 233-243.

Dai H, Zhang L, Zhang J, Mi H, Ogawa T, Ma W (2013) Identification of a cyanobacterial CRR6 protein, Slr1097, required for efficient assembly of NDH-1 complexes in *Synechocystis* sp PCC 6803. Plant J 75: 858-866.

Dasgupta J, Ananyev GM, Dismukes GC (2008) Photoassembly of the water-oxidizing complex in photosystem II. Coord Chem Rev 252: 347-360.

de Mendez I, Garrett MC, Adams AG, Leto TL (1994) Role of $p67^{phox}$ SH3 domains in assembly of the NADPH oxidase system. J Biol Chem 269: 16326- 16332.

Deng Y, Ye J, Mi H (2003a) Effects of low CO_2 on NAD(P)H dehydrogenase, a mediator of cyclic electron transport around photosystem I in the cyanobacterium *Synechocystis* PCC6803. Plant Cell Physiol 44: 534-540.

Deng Y, Ye J, Mi H, Shen Y (2003b) Separation of hydrophobic NAD(P)H dehydrogenase subcomplexes from cyanobacterium *Synechocystis* PCC6803. Acta Biochim Biophys 35: 723-727.

DeRuyter YA, Fromme P (2008) Molecular structure of the photosynthetic apparatus. In: The cyanobacteria molecular biology, genomics and evolution (Herrero A and Flores E ed) pp 217-269. Caister Academic Press, Norfolk UK.

Di Matteo A, Scandurra FM, Testa F, Forte E, Sarti P, Brunori M, Giuffrè A (2008). The O_2-scavenging flavodiiron protein in the human parasite *Giardia intestinalis*. J Biol Chem 283: 4061-4068.

Diner BA, Petrouleas V (1990) Formation by NO of nitrosyl adducts of redox components of the Photosystem II reaction center. II. Evidence that HCO_3^-/CO_2 binds to the acceptor side non-heme iron. Biochim Biophys Acta 1015: 141-149.

Dobáková M, Tichy M, Komenda J (2007) Role of the PsbI protein in photosystem II assembly and repair in the cyanobacterium *Synechocystis* sp. PCC 6803. Plant Physiol 145: 1681-91.

Dolganov NAM, Bhaya D, Grossman AR (1995) Cyanobacterial protein with similarity to the chlorophyll a/b binding proteins of higher plants: Evolution and regulation. Proc Natl Acad Sci USA 92: 636-640.

Eaton-Rye JJ (2004) The construction of gene knockouts in the cyanobacterium *Synechocystis* sp. PCC 6803. In: Methods in Molecular Biology vol 274: photosynthesis research protocols. (Carpentier R ed) pp 309-323. Humana Press Inc Totowa, NJ USA.

Edelman M, Mattoo AK (2008) D1-protein dynamics in photosystem II: the lingering enigma. Photosynth Res 98: 609-620**.**

Efremov RG, Baradaran R, Sazanov LA (2010) The architecture of respiratory complex I. Nature 465: 441-461.

Eisenhut M, Georg J, Klähn S, Sakurai I, Mustila H, Zhang P, Hess WR, Aro EM (2012) The antisense RNA As1_flv4 in the cyanobacterium *Synechocystis* sp. PCC 6803 prevents premature expression of the *flv4-2* operon upon shift in inorganic carbon supply. J Biol Chem 287: 33153-33162.

El Bissati K, Delphin E, Murata N, Etienne A, Kirilovsky D (2000) Photosystem II fluorescence quenching in the cyanobacterium *Synechocystis* PCC 6803: involvement of two different mechanisms. Biochim Biophys Acta 1457(3): 229-242.

Emlyn-Jones D, Ashby MK, Mullineaux CW (1999) A gene required for the regulation of photosynthetic light harvesting in the cyanobacterium *Synechocystis* 6803. Mol Microbiol 33(5): 1050-1058.

Engelken J, Brinkmann H, Adamska I (2010) Taxonomic distribution and origins of the extended LHC (light-harvesting complex) antenna protein superfamily. BMC Evol Biol 10: 233.

Ermakova M, Battchikova N, Richaud P, Leino H, Kosourov S, Isojärvi J, Peltier G, Flores E, Cournac L, Allahverdiyeva Y, Aro EM (2014) Heterocyst-specific flavodiiron protein Flv3B enables oxic diazotrophic growth of the filamentous cyanobacterium *Anabaena* sp. PCC 7120. Proc Natl Acad Sci USA 111: 11205-11210.

Fatihi A, Latimer S, Schmollinger S, Block A, Dussault PH, Vermaas WFJ, Merchant SS, Basset GJ (2015) A dedicated type II NADPH dehydrogenase performs the penultimate step in the biosynthesis of vitamin K-1 in *Synechocystis* and *Arabidopsis*. Plant Cell 27: 1730-1741.

Field CB, Behrenfeld MJ, Randerson JT, Falkowski P (1998) Primary production of the biosphere: integrating terrestrial and oceanic components. Science 281: 237-240.

Finazzi G, Johnson G, Dall'Osto L, Zito F, Bonente G, Bassi R, Wollman F (2006) Nonphotochemical quenching of chlorophyll fluorescence in *Chlamydomonas reinhardtii*. Biochemistry 45: 1490-1498.

Flores E, Frias JE, Rubio LM, Herrero A (2005) Photosynthetic nitrate assimilation in cyanobacteria, Photosynth Res 83:117-133.

Flores E, Herrero A (2010) Compartmentalized function through cell differentiation in filamentous cyanobacteria. Nat Rev Microbiol 8: 39-50.

Folea IM, Zhang P, Aro EM, Boekema EJ (2008) Domain organization of photosystem II in membranes of the cyanobacterium *Synechocystis* PCC6803 investigated by electron microscopy, FEBS Lett 582: 1749-1754.

Frankenberg N, Mukougawa K, Kohchi T, Lagarias JC (2001) Functional genomic analysis of the HY2 family of ferredoxin-dependent bilin reductases from oxygenic photosynthetic organisms. Plant Cell 13: 965-978.

Friedrich T, Steinmuller K, Weiss H (1995) The proton-pumping respiratory Complex-I of bacteria and mitochondria and its homolog in chloroplasts. FEBS Lett 367: 107-111.

Friedrich T, Scheide D (2000) The respiratory complex I of bacteria, archaea and eukarya and its module common with membrane-bound multisubunit hydrogenases. FEBS Lett 479: 1-5.

Gantt E, Conti SF (1966) Phycobiliprotein localization in algae. Brookhaven Symp Biol 19: 393-405.

Garab G, Rozs, Z, Govindjee (1988) Carbon dioxide affects charge accumulation in leaves. Naturwissenschaften 75: 517-519.

Garcia-Pichel F, Belnap J, Neuer S, Schanz F (2003) Estimates of global cyanobacterial biomass and its distribution. Arch Hydrobiol Algol Stud 109: 213-228.

Gehl B, Sweetlove LJ (2014) Mitochondrial Band-7 family proteins: scaffolds for respiratory chain assembly? Front Plant Sci 5:141.

Glazer AN (1984) Phycobilisome: a macromolecular complex optimized for light energy transfer. Biochim Biophys Acta 768: 29-51.

Gomes, CM, Giuffre A, Forte E, Vicente JB, Saraiva LM, Brunori M, Teixeira M (2002) A novel type of nitric-oxide reductase: *Escherichia coli* flavorubredoxin. J Biol Chem 277: 25273-25276.

Gonçalves VL, Saraiva LM, Teixeira M (2011) Gene expression study of the flavodi-iron proteins from the cyanobacterium *Synechocystis* sp. PCC 6803. Biochem Soc Trans 39: 216-218.

Gonçalves VL, Vicente JB, Saraiva LM, Teixeira M (2012) Flavodiiron proteins and their role in cyanobacteria. In: Bioenergetic processes of cyanobacteria - from evolutionary singularity to ecological diversity; Peschek GA, Obinger C, Renger G, Eds; Springer: Berlin/Heidelberg, Germany. pp 631-653.

Gonçalves VL, Vicente JB, Pinto L, Romão CV, Frazão C, Sarti P, Giuffrè A, Teixeira M (2014) Flavodiiron oxygen reductase from *Entamoeba histolytica*: modulation of substrate preference by tyrosine 271 and lysine 53. J Biol Chem 289: 28260-28270.

Graan T, Ort DR (1986) Detection of oxygen-evolving photosystem II centers inactive in plastoquinone reduction. Biochim Biophys Acta 852: 320-330.

Grigorieva G, Shestakov, S (1982) Transformation in the cyanobacterium *Synechocystis* sp. PCC 6803. FEMS Microbiol 13: 367-370.

Grossman AR, Schaefer MR, Chiang GG, Collier JL (1993) The phycobilisome, a light harvesting complex responsive to environmental conditions. Microbiol Reviews 57(3): 725-749.

Gutekunst K, Chen X, Schreiber K, Kaspar U, Makam S, Appel J (2014) The bidirectional NiFe-hydrogenase in *Synechocystis* sp. PCC 6803 is reduced by flavodoxin and ferredoxin and is essential under mixotrophic, nitrate-limiting conditions. J Biol Chem 289: 1930-1937.

Gwizdala M, Wilson A, Kirilovsky D (2011) In vitro reconstitution of the cyanobacterial photoprotective mechanism mediated by the orange carotenoid protein in *Synechocystis* PCC 6803. Plant Cell 23(7): 2631-2643.

Hackenberg C, Huege J, Engelhardt A, Wittink F, Laue M, Matthijs HCP, Kopka J, Bauwe H, Hagemann M (2012) Low-carbon acclimation in carboxysome-less and photorespiratory mutants of the cyanobacterium *Synechocystis* sp. strain PCC 6803. Microbiology 158: 398-413.

Hakala M, Tuominen I, Keränen M, Tyystjärvi T, Tyystjärvi E (2005) Evidence for the role of the oxygen-evolving manganese complex in photoinhibition of photosystem II. Biochim Biophys Acta 1706: 68-80.

Hakkila K, Antal T, Gunnelius L, Kurkela J, Matthijs HCP, Tyystjärvi E, Tyystjärvi T (2013). Group 2 sigma factor mutant ΔsigCDE of the cyanobacterium *Synechocystis* sp. PCC 6803 reveals functionality of both carotenoids and flavodiiron proteins in photoprotection of photosystem II. Plant Cell Physiol 54: 1780-1790.

Hankamer B, Barber J, Boekema EJ (1997) Structure and membrane organisation of PSII in green plants. Annu Rev Plant Phys Mol Biol 48: 641-671.

Hanke GT, Satomi Y, Shinmura K, Takao T, Hase T (2011) A screen for potential ferredoxin electron transfer partners uncovers new, redox dependent interactions. Biochim Biophys Acta 1814: 366-374.

He Q, Vermaas WFJ (1998) Chlorophyll *a* availability affects *psbA* translation and D1 precursor processing in vivo in *Synechocystis* sp. PCC 6803. Proc. Natl. Acad. Sci. USA 95: 5830-5835.

He Z, Zheng F, Wu Y, Li Q, Lv J, Fu P, Mi H (2015) NDH-1 L interacts with ferredoxin via the subunit NdhS in *Thermosynechococcus elongates*. Photosynth Res 126(2): 341-349.

Hedges SB, Blair JE, Venturi ML, ShoeJL (2004) A molecular timescale of eukaryote evolution and the rise of complex multicellular life. BMC Evol Biol 4: 2.

Helman Y, Tchernov D, Reinhold L, Shibata M, Ogawa T, Schwarz R, Ohad I, Kaplan A (2003) Genes encoding A-type flavoproteins are essential for photoreduction of O_2 in cyanobacteria. Curr Biol 13: 230-235.

Hernández-Prieto MA, Schön V, Georg J, Barreira L, Varela J, Hess WR, Futschik ME (2012) Iron deprivation in *Synechocystis*: inference of pathways, non-coding RNAs, and regulatory elements from comprehensive expression profiling. G3 2: 1475-1495.

Herranen M, Battchikova N, Zhang PP, Graf A, Sirpio S, Paakkaarinen V, Aro EM (2004) Towards functional proteomics of membrane protein complexes in *Synechocystis* sp PCC 6803. Plant Physiol 134: 470-481**.**

Hihara Y, Kamei A, Kanehisa M, Kaplan A, Ikeuchi M (2001) DNA microarray analysis of cyanobacterial gene expression during acclimation to high light. Plant Cell 13: 793-806.

Hihara Y, Sonoike K, Kanehisa M, Ikeuchi M (2003) DNA microarray analysis of redox-responsive genes in the genome of the cyanobacterium *Synechocystis* sp. strain PCC 6803. J Bacteriol 185: 1719-1725.

Hill R, Bendall F (1960) Function of two cytochrome components in chloroplasts: a working hypothesis. Nature 186: 136-137.

Hillman F, Fischer RJ, Caranto JD, Mot A, Kurtz DM, Bahl H (2009) Reductive dioxygen scavenging of flavodiiron proteins of *Clostridium acetobutylicum*. FEBS Lett 583: 241-245.

Hishiya S, Hatakeyama W, Mizota Y, Hosoya-Matsuda N, Motohashi K, Ikeuchi M, Hisabori T (2008) Binary reducing equivalent pathways using NADPH-thioredoxin reductase and ferredoxin-thioredoxin reductase in the cyanobacterium *Synechocystis* sp strain PCC 6803. Plant Cell Physiol 49: 11-18.

Holland SC, Kappel AD, Burnap RL (2014) Redox changes accompanying inorganic carbon limitation in *Synechocystis* sp. PCC 6803. Biochim Biophys Acta 1847(3): 355-363.

Horton P, Ruban A, Walters R (1996) Regulation of light harvesting in green plants. Ann Rev Plant Physiol Plant Mol Biol 47: 655-684.

Horton P, Ruban A (2005) Molecular design of the photosystem II light-harvesting antenna: Photosynthesis and photoprotection. J Exp Bot 56: 365-373.

Howitt CA, Vermaas WFJ (1998) Quinol and cytochrome oxidases in the cyanobacterium *Synechocystis* sp. PCC 6803. Biochemistry 37: 17944-17951.

Howitt CA, Udall PK, Vermaas WFJ (1999) Type 2 NADH dehydrogenases in the cyanobacterium *Synechocystis* sp. strain PCC 6803 are involved in regulation rather than respiration. J Bacteriol 181: 3994-4003.

Hu P, Lv J, Fu P, Mi H (2013) Enzymatic characterization of an active NDH complex from *Thermosynechococcus elongatus*. FEBS Lett 587: 2340-2345.

Hunte C, Zickermann V, Brandt U (2010) Functional modules and structural basis of conformational coupling in mitochondrial Complex I. Science 329: 448-451.

Ikeuchi M, Tabata S (2001) *Synechocystis* sp. PCC 6803 – a useful tool in the study of genetics in cyanobacteria. Photosynth Res 70: 73-83.

Inoue S, Ejima K, Iwai E, Hayashi H, Appel J, Tyystjärvi E, Murata N, Nishiyama Y (2011) Protection by α-Tocopherol of the Repair of Photosystem II During Photoinhibition in *Synechocystis* sp. PCC 6803. Biochim Biophys Acta 1807(2): 236-241.

Ivanov AG, Rosso D, Savitch LV, Stachula P, Rosembert M, Oquist G, Hurry V, Hüner NP (2012) Implications of alternative electron sinks in increased resistance of PSII and PSI photochemistry to high light stress in cold-acclimated *Arabidopsis thaliana*. Photosynth Res 113: 191-206.

Iwata S, Ostermeier C, Ludwig B, Michel H (1995) Structure at 2.8-Angstrom Resolution of Cytochrome-C-Oxidase from *Paracoccus Denitrificans*. Nature 376: 660-669.

Jallet D, Gwizdala M, Kirilovsky D (2012) ApcD, ApcF and ApcE are not required for the orange carotenoid protein related phycobilisome fluorescence quenching in the cyanobacterium *Synechocystis* PCC 6803. Biochim Biophys Acta 1817: 1418-1427.

Jokel M, Kosourov S, Battchikova N, Tsygankov AA, Aro EM, Allahverdiyeva Y (2015) *Chlamydomonas* flavodiiron proteins facilitate acclimation to anoxia during sulfur deprivation. Plant Cell Physiol 56: 1598-1607.

Jordan P, Fromme P, Witt HT, Klukas O, Saenger W, Krauss N (2001). Three-dimensional structure of cyanobacterial photosystem I at 2.5 A resolution. Nature 411: 909-917.

Joshua S, Mullineaux CW (2004) Phycobilisome diffusion is required for light-state transitions in cyanobacteria. Plant Physiol 135(4): 2112-2119**.**

Kaneko T, Sato S, Kotani H, Tanaka A, Asamizu E, Nakamura Y, Miyajima N, Hirosawa M, Sugiura M, Sasamoto S, Kimura T, Hosouchi T, Matsuno A, Muraki A, Nakazaki N, Naruo K, Okumura S, Shimpo S, Takeuchi C, Wada T, Watanabe A, Yamada M, Yasuda M, Tabata S (1996) Sequence analysis of the genome of the unicellular cyanobacterium *Synechocystis* sp. strain PCC6803. Sequence determination of the entire genome and assignment of potential protein-coding regions. DNA Res 3: 109-136.

Kaňa R, Prašil O, Komarek O, Papageorgiou GC (2009) Spectral characteristic of fluorescence induction in a model cyanobacterium, *Synechococcus* sp. (PCC 7942). Biochim Biophys Acta 1787: 1170–1178.

Kaplan A (1981) Photoinhibition in *Spirulina platensis*—response of photosynthesis and HCO_3^- uptake capability to CO_2-depleted conditions. J Exp Bot 32: 669-677.

Kaplan A, Reinhold L (1999) CO_2 concentrating mechanisms in photosynthetic microorganisms. Annu Rev Plant Physiol Plant Molec Biol 50: 539-570.

Kashino Y, Lauber WM, Carroll JA, Wang Q, Whitmarsh J, Satoh K, Pakrasi HB (2002). Proteomic analysis of a highly active photosystem II preparation from the cyanobacterium *Synechocystis* sp PCC 6803 reveals the presence of novel polypeptides. Biochemistry 41: 8004-8012.

Kaufman AJ, Xiao S (2003) High CO_2 levels in the Proterozoic atmosphere estimated from analyses of individual microfossils. Nature 425: 279-282.

Keren N, Berg A, van Kan PJM, Levanon H, Ohad I (1997) Mechanism of photosystem II photoinactivation and D1 protein degradation at low light: the role of back electron flow. Proc Natl Acad Sci USA 94: 1579-1584.

Kerfeld CA, Heinhorst S, Cannon GC (2010) Bacterial microcompartments. Annu Rev Microbiol 64: 391-408.

Kirilovsky D (2014) Modulating energy arriving at photochemical reaction centers: orange carotenoid protein-related photoprotection and state transitions. Photosynth Res doi: 10.1007/s11120-014-0031-7.

Kirilovsky D, Kaňa R, Prášil O (2013) Mechanisms modulating energy arriving at reaction centers in cyanobacteria. In: Demmig-Adams B, Adams W, Garab G, Govindjee (eds) Non-photochemical quenching and thermal energy dissipation in plants, algae and cyanobacteria. Advances in photosynthesis and respiration - including bioenergy and related processes. Springer, Dordrecht.

Kishan KVR, Agrawal V (2005) SH3-like fold proteins are structurally conserved and functionally divergent. Curr Protein Pept Sci 6: 143-150.

Klotz, A, Reinhold E, Doello S, Forchhammer K (2015) Nitrogen starvation acclimation in *Synechococcus elongatus*: redox control and the role of nitrate reduction as an electron sink. Life 5: 888-904**.**

Knoll AH (2008) Cyanobacteria and Earth history. In: The cyanobacteria: molecular biology, genomics and evolution. (Herrero A, Flores E ed.) pp 1-20. Horizon Scientific Press, Norwich, UK.

Knoppová J, Sobotka R, Tichý M, Yu J, Konik P, Halada P, Nixon PJ, Komenda J (2014) Discovery of a chlorophyll binding protein complex involved in the early steps of photosystem II assembly in *Synechocystis*. Plant Cell 26: 1200-1212.

Komenda J, Reisinger V, Müller BC, Dobáková M, Granvogl B, Eichacker LA (2004) Accumulation of the D2 protein is a key regulatory step for assembly of the photosystem II reaction center complex in *Synechocystis* PCC 6803. J Biol Chem 279: 48620-48629.

Komenda J, BarkerM, Kuvikova S, de Vries R, Mullineaux CW, Tichý M, Nixon PJ (2006) The FtsH protease slr0228 is important for quality control of photosystem II in the thylakoid membrane of *Synechocystis* sp. PCC 6803. J Biol Chem 281: 1145-1151.

Komenda J, Kuvikova S, Granvogl B, Eichacker LA, Diner BA, Nixon PJ (2007) Cleavage after residue Ala352 in the C-terminal extension is an early step in the maturation of the D1 subunit of Photosystem II in *Synechocystis* PCC 6803. Biochim Biophys Acta 1767: 829-837.

Komenda J, Nickelsen J, Tichy M, Prasil O, Eichacker LA, Nixon PJ (2008) The cyanobacterial homologue of HCF136/YCF48 is a component of an early photosystem II assembly complex and is important for both the efficient assembly and repair of photosystem II in *Synechocystis* sp. PCC 6803. J Biol Chem 283: 22390-22399.

Komenda J, Knoppová J, Krynická V, Nixon PJ, Tichý M (2010) Role of $FtsH_2$ in the repair of Photosystem II in mutants of the cyanobacterium *Synechocystis* PCC 6803 with impaired assembly or stability of the $CaMn_4$ cluster. Biochim Biophys Acta 1797: 566-575.

Komenda J, Knoppová J, Kopečná J, Sobotka R, Halada P, Yu JF, Nickelsen J, Boehm M, Nixon PJ (2012). The Psb27 assembly factor binds to the CP43 complex of photosystem II in the cyanobacterium *Synechocystis* sp. PCC 6803. Plant Physiol 158: 476-486.

Korn A (2010) Respective roles of the ferredoxin :NADP-oxidoreductase isoforms in the cyanobacterium *Synechocystis* sp. PCC 6803. Biological Physics [physics.bio-ph]. Université Paris Sud - Paris XI. English version.

Kós PB, Deák Z, Cheregi O, Vass I (2008) Differential regulation of psbA and psbD gene expression, and the role of the different D1 protein copies in the cyanobacterium *Thermosynechococcus elongatus* BP-1. Biochim Biophys Acta 1777: 74-83.

Kouril R, Dekker JP, Boekema EJ (2012) Supramolecular organization of photosystem II in green plants. Biochim Biophys Acta 1817: 2-12.

Krieger-Liszkay A (2005) Singlet oxygen production in photosynthesis. J Exp Bot 56: 337-346.

Krieger-Liszkay A, Fufezan C, Trebst A (2008) Singlet oxygen production in photosystem II and related protection mechanism. Photosynth Res 98: 551-564.

Kruk J, Trebst A (2008) Plastoquinol as a singlet oxygen scavenger in photosystem II. Biochim Biophys Acta 1777: 154-162.

Krupa Z, Oquist G, Gustafsson P (1991) Photoinhibition of photosynthesis and growth responses at different light levels in *psbA* gene mutants of the cyanobacterium *Synechococcus*. Plant Physiol 82: 1-8.

Kucho K, Okamoto K, Tsuchiya Y, Nomura S, Nango M, Kanehisa M, Ishiura M (2005) Global analysis of circadian expression in the cyanobacterium *Synechocystis* sp. strain PCC 6803. J Bacteriol 187: 2190-2199.

Kunkel DD (1982) Thylakoid centers: structures associated with the cyanobacterial photosynthetic membrane system. Arch Microbiol 133: 97-99.

Kurian, D., Jansén, T. and Mäenpää, P. (2005) Proteomic analysis of heterotrophy in *Synechocystis* sp. PCC 6803. Proteomics 6: 1483-1494.

Kyle DJ, Ohad I, Arntzen CJ (1984) Membrane protein damage and repair: Selective loss of a quinone-protein function in chloroplast membranes. Proc Natl Acad Sci USA 81: 4070-4074.

Laemmli UK (1970) Cleavage of structural proteins during the assembly of the head of bacteriophage T4. Nature 227: 680-685.

Lea-Smith DJ, Ross N, Zori M, Bendall DS, Dennis JS, Scott SA, Smith AG, Howe CJ (2013) Thylakoid terminal oxidases are essential for the cyanobacterium *Synechocystis* sp. PCC 6803 to survive rapidly changing light intensities. Plant Physiol 162: 484-495.

Lea-Smith DJ, Bombelli P, Vasudevan R, Howe CJ (2015) Photosynthetic, respiratory and extracellular electron transport pathways in cyanobacteria. Biochim Biophys Acta http://dx.doi.org/10.1016/j.bbabio.2015.10.007.

Lehmann EL, Machné R, Georg J, Benary M, Axmann I, Steuer R (2013) How cyanobacteria pose new problems to old methods: challenges in microarray time series analysis. BMC Bioinformatics 14:133.

Li D, Xie J, Zhao J, Xia A, Li D, Gong Y (2004) Light-induced excitation energy redistribution in *Spirulina platensis* cells: "spillover" or "mobile PBSs"? Biochim Biophys Acta 1608(2–3): 114-121.

Li H, Li D, Yang S, Xie J, Zhao J (2006) The state transition mechanism—simply depending on light-on and -off in *Spirulina platensis*. Biochim Biophys Acta 1757(11): 1512-1519.

Liberton, M. and Pakrasi, H. (2008) Membrane systems in cyanobacteria. In: The cyanobacteria molecular biology, genomics and evolution. (Herrero A, Flores E ed) pp 271-287. Caister Academic Press, Norfolk UK.

Liu L-N, Bryan SJ, Huang F, Yu J, Nixon PJ, Rich PR, Mullineaux WC (2012) Control of electron transport routes through redox-regulated redistribution of respiratory complexes. Proc Natl Acad Sci USA 109: 11431-11436.

Liu H, Zhang H, Niedzwiedzki DM, Prado M, He G, Gross ML, Blankenship RE (2013) Phycobilisomes supply excitations to both photosystems in a megacomplex in cyanobacteria. Science. 342: 1104-1107.

Lopez-García P, Moreira D, Douzery E, Forterre P, van Zuilen M, Claeys P, Prieur D (2006) Ancient fossil record and early evolution (ca. 3.8-0.5 Ga). Earth, Moon and Planets 98: 247-290.

Ma W, Mi H (2005) Expression and activity of type-1 NAD(P)H dehydrogenase at different growth phases of cyanobacterium, *Synechocystis* PCC 6803. Physiol Plant 125: 135-140.

Ma W, Deng Y, Ogawa T, Mi H (2006) Active NDH-1 complexes from the cyanobacterium *Synechocystis* sp strain PCC 6803, Plant Cell Physiol 47: 1432-1436.

Ma W, Mi H, Shen Y (2010) Influence of the redox state of Q_A on phycobilisome mobility in the cyanobacterium *Synechocystis* sp. strain PCC6803. J Lumin 130: 1169-1173.

Mackenzie TD, Burns RA, Campbell DA (2004) Carbon status constrains light acclimation in the cyanobacterium *Synechococcus elongatus*. Plant Physiol 136: 3301-3312.

Mao HB, Li GF, Ruan X, Wu QY, Gong YD, Zhang XF, Zhao NM (2002) The redox state of plastoquinone pool regulates state transitions via cytochrome b_6f complex in *Synechocystis* sp. PCC 6803. FEBS Lett 519(1–3): 82-86.

Marco MN, Ohad I, Schwarz R, Lieman-Hurwitz J, Gabay C, Kaplan A (1993) High CO_2 concentration alleviates the block in photosynthetic electron transport in an *ndhB*-inactivated mutant of *Synechococcus* sp. PCC7942. Plant Physiol 101: 1047-1053.

Matsuo M, Endo T, Asada K (1998) Properties of the respiratory NAD(P)H dehydrogenase isolated from the cyanobacterium *Synechocystis* PCC6803, Plant Cell Physiol 39: 263-267.

Matthijs HCP, Ludérus EME, Löffler HJM, Scholts MJC, Kraayenhof R (1984) Energy metabolism in the cyanobacterium *Plectonema boryanum*: participation of the photosynthetic electron transfer chain in the dark respiration of NADPH and NADH. Biochim Biophys Acta 766: 29-37.

Matthijs HCP, Visser PM, Reeze B, Meeuse J, Slot PC, Wijn G, Talens R, Huisman J (2012) Selective suppression of harmful cyanobacteria in an entire lake with hydrogen peroxide. Water Res 46: 1460-1472.

McConnell MD, Koop R, Vasil'ev S, Bruce D (2002) Regulation of the distribution of chlorophyll and phycobilin-absorbed excitation energy in cyanobacteria. A structure-based model for the light state transition. Plant Physiol 130(3): 1201-1212.

McConnell IL, Eaton-Rye JJ, van Rensen JJ (2012) Regulation of photosystem II electron transport by bicarbonate. In Photosynthesis, Eaton-Rye JJ, Tripathy BC, Sharkey TD, eds (The Netherlands: Springer) pp 475-500.

McCormick AJ, Bombelli P, Bradley RW, Thorne R, Wenzel T, CJ Howe (2015) Biophotovoltaics: oxygenic photosynthetic organisms in the world of bioelectrochemical systems, Energy & Environmental Science 8: 1092-1109.

McDonald AE, Vanlerberghe GC (2005) Alternative oxidase and plastoquinol terminal oxidase in marine prokaryotes of the Sargasso Sea. Gene 349: 15-24.

McDonald AE, Vanlerberghe GC (2006) Origins, evolutionary history, and taxonomic distribution of alternative oxidase and plastoquinol terminal oxidase. Comp Biochem Physiol D 1: 357-364.

McDonald AE, Ivanov AG, Bode R, Maxwell DP, Rodermel SR, Huner NP (2011) Flexibility in photosynthetic electron transport: the physiological role of plastoquinol terminal oxidase (PTOX). Biochim Biophys Acta 1807: 954-967.

Meeks JC, Castenholz RW (1971) Growth and photosynthesis in an extreme thermophile *Synechococcus lividus* (Cyanophyta). Archives fur Mikrobiologie 78: 25-41.

Melis A (1999) Photosystem-II damage and repair cycle in chloroplasts: what modulates the rate of photodamage *in vivo*? Trends Plant Sci 4: 130-135.

Mella-Flores D, Six C, Ratin M, Partensky F, Boutte C, Le Corguillé G, Marie D, Blot N, Gourvil P, Kolowrat C, Garczarek L (2012) *Prochlorococcus* and *Synechococcus* have evolved different adaptive mechanisms to cope with light and UV stress. Front Microbiol 3: 285.

Melo AM, Bandeiras TM, Teixeira M (2004) New insights into type II NAD(P)H:quinone oxidoreductases. Microbiol Mol Biol Rev 68: 603-616.

Mi H, Endo T, Ogawa T, Asada K (1995) Thylakoid membrane bound pyridine nucleotide dehydrogenase complex mediated cyclic electron transport in the cyanobacterium *Synechocystis* PCC 6803. Plant Cell Physiol 36: 661-668.

Mi H, Deng Y, Tanaka Y, Hibino T, Takabe T (2001) Photo-induction of an NADPH dehydrogenase which functions as a mediator of electron transport to the intersystem chain in the cyanobacterium *Synechocystis* PCC6803. Photosynth Res 70: 167-173.

Miller AG, Canvin DT (1989) Glycoaldehyde inhibits CO_2 fixation in the cyanobacterium *Synechococcus* UTEX 625 without inhibiting the accumulation of inorganic carbon or the associated quenching of chlorophyll a fluorescence. Plant Physiol 91: 1044-1049.

Mimuro M, Katoh T (1991) Carotenoids in photosynthesis: absorption, transfer and dissipation of light energy. Pure Appl Chem 63: 123-130.

Minagawa J, Takahashi Y (2004) Structure, function and assembly of Photosystem II and its light-harvesting proteins. Photosynth Res 82(3): 241-263.

Montoya JP, Holl CM, Zehr JP, Hansen A, Villareal TA, Capone DG (2004) High rates of N_2 fixation by unicellular diazotrophs in the oligotrophic Pacific Ocean. Nature 430: 1027-1032.

Mörschel E, Mühlethaler K (1983) On the linkage of exoplasmatic freeze-fracture particles to phycobilisomes. Planta 158: 451-457.

Mörschel E, Schatz GH (1987) Correlation of photosystem-II complexes with exoplasmatic freeze-fracture particles of thylakoids of the Cyanobacterium *Synechococcus* sp. Planta 172: 145-154.

Mullen KM, van Stokkum IH (2007) TIMP: an R package for modeling multi-way spectroscopic measurements. J Stat Softw 18: 1-46.

Mullineaux CW (1992) Excitation energy transfer from phycobilisomes to photosystem-I and photosystem-II in a cyanobacterium. Photosynth Res 34(1):114.

Mullineaux CW (2008) Phycobilisome-reaction centre interaction in cyanobacteria. Photosynth Res 95: 175-182.

Mullineaux CW (2014) Electron transport and light-harvesting switches in cyanobacteria. Front Plant Sci 5:7. doi:10.3389/fpls.2014.00007.

Mullineaux CW, Allen JF (1990) State 1-state 2 transitions in the Cyanobacterium *Synechococcus* 6301 are controlled by the redox state of electron carriers between photosystem I and Photosystem II. Photosynth Res 23(3): 297-311.

Mullineaux CW, Emlyn-Jones D (2005) State transitions: an example of acclimation to low-light stress. J Exp Bot 56(411): 389-393.

Mulo P, Sicora C, Aro EM (2009) Cyanobacterial *psbA* gene family: optimization of oxygenic photosynthesis. Cell Mol Life Sci 66: 3697-3710.

Murata N (1969) Control of excitation transfer in photosynthesis. I. Light induced change of chlorophyll a fluorescence in *Porphyridium cruentum*, Biochim Biophys Acta 172: 242-251.

Müller P, Li X, Niyogi K (2001) Non-photochemical quenching. A response to excess light energy. Plant Physiol 125: 1558-1566.

Navarro F, Martin-Figueroa E, Candau P, Florencio FJ (2000) Ferredoxin-dependent iron–sulfur flavoprotein glutamate synthase (GlsF) from the cyanobacterium *Synechocystis* sp PCC 6803: expression and assembly in *Escherichia coli*. Arch Biochem Biophys 379: 267-276.

Nelson N, Yocum CF (2006) Structure and function of photosystems I and II. Annu Rev Plant Biol 57: 521-565.

Nelson N (2009) Plant photosystem I: the most efficient nanophotochemical machine. J Nanosci Nanotechnol 9(3): 1709-1713.

Nevo R, Charuvi D, Shimoni, E, Schwarz R, Kaplan A, Ohad I, Reich Z (2007) Thylakoid membrane perforations and connectivity enable intracellular traffic in cyanobacteria. EMBO J 26: 1467-1473.

Nicholls P, Obinger C, Niederhauser H, Peschek GA (1992) Cytochrome oxidase in *Anacystis nidulans*: stoichiometries and possible functions in the cytoplasmic and thylakoid membranes. Biochim Biophys Acta 1098: 184-190.

Nickelsen J, Rengstl B (2013) Assembly of photosystem II: from cyanobacteria to plants. Annu Rev Plant Biol 64: 609-635.

Nishiyama Y, Murata N (2014) Revised scheme for the mechanism of photoinhibition and its application to enhance the abiotic stress tolerance of the photosynthetic machinery. Appl Microbiol Biotechnol 98: 8777-8796.

Nixon PJ, Mullineaux CW (2001**)** Regulation of photosynthetic electron transport, in: EM Aro, B Andersson (Eds.), Regulation of photosynthesis. Advances in Photosynthesis and Respiration, Kluwer Academic Publishers, Dordrecht, pp 533–555.

Nixon PJ, Michoux F, Yu J, Boehm M, Komenda J (2010) Recent advances in understanding the assembly and repair of photosystem II. Ann Bot 106: 1-16.

Niyogi K (2000) Safety valves for photosynthesis. Curr Opin Plant Biol 3: 455-460.

Nowaczyk MM, Hebeler R, Schlodder E, Meyer HE, Warscheid B, Rögner M (2006) Psb27, a cyanobacterial lipoprotein, is involved in the repair cycle of photosystem II. Plant Cell 18: 3121-3131.

Nowaczyk MM, Wulfhorst H, Ryan CM, Souda P, Zhang H, Cramer WA, Whitelegge JP (2011) NdhP and NdhQ: two novel small subunits of the cyanobacterial NDH-1 complex. Biochemistry 50: 1121-1124.

Nozzi NE, Oliver JW, Atsumi S (2013) Cyanobacteria as a platform for biofuel production. Front Bioeng Biotechnol 1: 7.

Ogawa T (1991) A gene homologous to the subunit-2 gene of NADH dehydrogenase is essential to inorganic carbon transport of *Synechocystis* PCC6803. Proc Natl Acad Sci USA 88: 4275-4279.

Ogawa T, Mi H (2007) Cyanobacterial NADPH dehydrogenase complexes. Photosyn Res 93: 69-77.

Ohad I, Kyle DJ, Arntzen CJ (1984) Membrane protein damage and repair: removal and replacement of inactivated 32-kilodalton polypeptides in chloroplast membranes. J Cell Biol 99: 481-485.

Ohkawa H, Pakrasi HB, Ogawa T (2000) Two types of functionally distinct NAD(P)H dehydrogenases in *Synechocystis* sp strain PCC6803. J Biol Chem 275: 31630–31634.

Ohkawa H, Sonoda M, Shibata M, Ogawa T (2001) Localization of NAD(P)H dehydrogenase in the cyanobacterium *Synechocystis* sp strain PCC 6803. J Bacteriol 183: 4938-4939.

Ohkawa H, Sonoda M, Hagino N, Shibata M, Pakrasi HB, Ogawa T (2002) Functionally distinct NAD(P)H dehydrogenases and their membrane localization in *Synechocystis* sp PCC6803. Funct Plant Biol 29: 195-200.

Ohnishi N, Allakhverdiev SI, Takahashi S, Higashi S, Watanabe M, Nishiyama Y, Murata N (2005) Two-step mechanism of photodamage to photosystem II: step 1 occurs at the oxygen-evolving complex and step 2 occurs at the photochemical reaction center. Biochemistry 44: 8494-8499.

Olive J, Mbina I, Vernotte C, Astier C, Wollman FA (1986) Randomization of the Ef particles in thylakoid membranes of *Synechocystis* 6714 upon transition from State-I to State-II. FEBS Lett 208(2): 308-312.

Olive J, Ajlani G, Astier C, Recouvreur M, Vernotte C (1997) Ultrastructure and light adaptation of phycobilisome mutants of *Synechocystis* PCC 6803. Biochim Biophys Acta 1319: 275-282

Ossenbühl F, Göhre V, Meurer J, Krieger-Liszkay A, Rochaix JD, Eichacker LA (2004) Efficient assembly of photosystem II in *Chlamydomonas reinhardtii* requires Alb3.1p, a homolog of *Arabidopsis* ALBINO3. Plant Cell 16: 1790-1800.

Ossenbühl F, Inaba-Sulpice M, Meurer J, Soll J, Eichacker LA (2006) The *Synechocystis* sp PCC 6803 Oxa1 homolog is essential for membrane integration of reaction center precursor protein pD1. Plant Cell 18: 2236-2246.

Peden EA, Boehm M, Mulder DW, Davis R, Old WM, King PW, Ghirardi ML, Dubini A (2013) Identification of global ferredoxin interaction networks in *Chlamydomonas reinhardtii*. J Biol Chem 288: 35192-35209.

Peltier G, Cournac L (2002) Chlororespiration. Ann Rev Plant Physiol Plant Mol Biol 53: 523-550.

Peltier G, Tolleter D, Billon E, Cournac L (2010) Auxiliary electron transport pathways in chloroplasts of microalgae. Photosyn. Res. 106: 19-31.

Peltier G, Aro EM, Shikanai T (2015) NDH-1 and NDH-2 Plastoquinone Reductases in Oxygenic Photosynthesis: Involvement in Cyclic Electron Flow, (Chloro)respiration, and Acclimation to the Environment. Annu Rev Plant Biol Manuscript in press.

Peng L, Shimizu H, Shikanai T (2008) The chloroplast NAD(P)H dehydrogenase complex interacts with photosystem I in *Arabidopsis*. J Biol Chem 283: 34873-34879.

Petoukhov MV, Vicente JB, Crowley PB, Carrondo MA, Teixeira M, Svergun DI (2008) Quaternary structure of flavorubredoxin as revealed by synchrotron radiation small-angle X-ray scattering. Structure 16: 1428-1436.

Petrouleas V, Diner BA (1990) Formation by NO of nitrosyl adducts of redox components of the Photosystem II reaction center. I. NO binds to the acceptor-side non-heme iron. Biochim Biophys Acta 1015: 131-140.

Pils D, Schmetterer G (2001) Characterization of three bioenergetically active respiratory terminal oxidases in the cyanobacterium *Synechocystis* sp. strain PCC 6803. FEMS Microbiol Lett 203: 217-222.

Prasil O, Adir N, Ohad I (1992) Dynamics of Photosystem II: mechanism of photoinhibition and recovery processes. In: Barber J (ed) The Photosystems: Structure, Function and Molecular Biology, pp 295-348. Elsevier Publishers, Amsterdam.

Price GD, Badger MR, Woodger FJ, Long BM (2008) Advances in understanding the cyanobacterial CO_2-concentrating-mechanism (CCM): functional components, C_i transporters, diversity, genetic regulation and prospects for engineering into plants. J Exp Bot 59: 1441-1461.

Quintana N, Van der Kooy F, Van de Rhee MD, Voshol GP, Verpoorte R (2011) Renewable energy from cyanobacteria: energy production optimization by metabolic pathway engineering. Appl Microbiol Biotechnol 91: 471-490.

Radmer RJ, Kok B (1976) Photoreduction of O_2 primes and replaces CO_2 assimilation. Plant Physiol 58: 336-340.

Radmer R, Ollinger O (1980) Light-driven uptake of oxygen, carbon dioxide, and bicarbonate by the green alga *Scenedesmus*. Plant Physiol 65: 723-729.

Raines CA (2003) The Calvin Cycle revisited. Photosynth Res 75: 1-10.

Redlinger T, Gantt E (1982) A M(r) 95,000 polypeptide in Porphyridium cruentum phycobilisomes and thylakoids: possible function in linkage of phycobilisomes to thylakoids and in energy transfer. Proc Natl Acad Sci USA 79(18): 5542-5546.

Rehman AU, Cser K, Sass L, Vass I (2013) Characterization of singlet oxygen production and its involvement in photodamage of photosystem II in the cyanobacterium *Synechocystis* PCC 6803 by histidine-mediated chemical trapping. Biochim Biophys Acta 1827: 689-698.

Rengstl B, Oster U, Stengel A, Nickelsen J (2011) An intermediate membrane subfraction in cyanobacteria is involved in an assembly network for photosystem II biogenesis. J Biol Chem 286: 21944–21951.

Rengstl B, Knoppová J, Komenda J, Nickelsen J (2013) Characterization of a *Synechocystis* double mutant lacking the photosystem II assembly factors YCF48 and Sll0933. Planta 237: 471-480.

Rippka R (1972) Photoheterotrophy and chemoheterotrophy among unicellular blue-green algae. Arch Microbiol 87: 93-97.

Rippka R, Deruelles J, Waterbury JB, Herdman M, Stanier RY (1979) Generic assignments, strain histories and properties of pure cultures of cyanobacteria. J Gen Microbiol 111: 1-61.

Rippka R (1988) Isolation and purification of cyanobacteria. Methods Enzymol 167: 3-27.

Rodrigues R, Vicente JB, Felix R, Oliveira S, Teixeira M, Rodrigues-Pousada C (2006) *Desulfovibrio gigas* flavodiiron protein affords protection against nitrosative stress *in vivo*. J Bacteriol 188: 2745-2751.

Rodriguez-Ezpeleta N, Brinkmann H, Roure SC, Burger G, Loffelhardt W, Bohnert HJ, Philippe H Lang BF (2005) Monophyly of primary photosynthetic eukaryotes: green plants, red algae, and glaucophytes. Curr Biol 15: 1325-1330.

Ruhlman TA, Chang WJ, Chen JJW, Huang YT, Chan MT, Zhang J, Liao DC, Blazier JC, Jin X, Shih MC, Jansen RK, Lin CS (2015) NDH expression marks major transitions in plant evolution and reveals coordinate intracellular gene loss. BMC Plant Biol 15:100 doi: 10.1186/s12870-015-0484-7.

Rumeau D, Peltier G, Cournac L (2007) Chlororespiration and cyclic electron flow around PSI during photosynthesis and plant stress response. Plant Cell Environ 30: 1041-1051.

Sacharz J, Bryan SJ, Yu J, Burroughs NJ, Spence EM, Nixon PJ, Mullineaux CW (2015) Sub-cellular location of FtsH proteases in the cyanobacterium *Synechocystis* sp. PCC 6803 suggests localised PSII repair zones in the thylakoid membranes, Mol Microbiol 96: 448-462.

Sakurai I, Mizusawa N, Ohashi S, Kobayashi M, Wada H (2007) Effects of the lack of phosphatidylglycerol on the donor side of photosystem II. Plant Physiol 144: 1336-1346.

Sander J, Nowaczyk M, Buchta J, Dau H, Vass I, Deák Z, Dorogi M, Iwai M, Rögner M (2010) Functional characterization and quantification of the alternative PsbA copies in *Thermosynechococcus elongatus* and their role in photoprotection. J Biol Chem 285: 29851-29856.

Saraiva LM, Vicente JB, Teixeira M (2004) The role of the flavodiiron proteins in microbial nitric oxide detoxification. Adv Microb Physiol 49: 77-129.

Savitch LV, Ivanov AG, Krol M, Sprott DP, Öquist G, Huner NPA (2010) Regulation of energy partitioning during cold acclimation of Lodgepole pine is oxygen-dependent. Plant Cell Physiol 51: 1553-1570.

Sazanov LA (2007) Respiratory complex I: mechanistic and structural insights provided by the crystal structure of the hydrophilic domain. Biochemistry 46: 2275-2288.

Schatz GH, Brock H, Holzwarth AR (1988) Kinetic and energetic model for the primary processes in photosystem II. Biophys J 54: 397-405.

Scherer S (1990) Do photosynthetic and respiratory electron transport chains share redox proteins? Trends Biochem Sci 15: 458-462.

Schopf JW (1996) Microfossils of the early archaean apex chert: new evidence of the antiquity of life. Science 260: 640-646.

Schottkowski M, Gkalympoudis S, Tzekova N, Stelljes C, Schünemann D, Ankele E, Nickelsen J (2009a) Interaction of the periplasmic PratA factor and the PsbA (D1) protein during biogenesis of photosystem II in *Synechocystis* sp. PCC 6803. J Biol Chem 284: 1813-1819.

Schottkowski M, Ratke J, Oster U, Nowaczyk M, Nickelsen J (2009b) Pitt, a novel tetratricopeptide repeat protein involved in light-dependent chlorophyll biosynthesis and thylakoid membrane biogenesis in *Synechocystis* sp. PCC 6803. Mol Plant 2: 1289-1297.

Schuurmans RM, Schuurmans JM, Bekker M, Kromkamp JC, Matthijs HCP, Hellingwerf KJ (2014) The redox potential of the plastoquinone pool of the cyanobacterium *Synechocystis* species strain PCC 6803 is under strict homeostatic control. Plant Physiol 165: 463-475.

Schuurmans RM, van Alphen P, Schuurmans JM, Matthijs HCP, Hellingwerf KJ (2015) Comparison of the Photosynthetic Yield of Cyanobacteria and Green Algae: Different Methods Give Different Answers. PLoS ONE 10(9): e0139061 doi:10.1371/journal.pone.0139061.

Schwarz D, Schubert H, Georg J, Hess WR, Hagemann M (2013) The gene sml0013 of *Synechocystis* species strain PCC 6803 encodes for a novel subunit of the NAD(P)H oxidoreductase or Complex I that is ubiquitously distributed among cyanobacteria. Plant Physiol 163: 1191-1202.

Sedoud A., Lopez-Igual R, Ur Rehman A, Wilson A, Perreau F, Boulay C, Vass I, Krieger-Liszkay A, Kirilovsky D (2014) The cyanobacterial photoactive orange carotenoid protein is an excellent singlet oxygen quencher. Plant Cell 26: 1781-1791.

Seedorf H, Hagemeier CH, Shima S, Thauer, RK, Warketin E, Ermler U (2007) Structure of coenzyme $F_{420}H_2$ oxidase (FprA): A di-iron flavoprotein from methanogenic Archaea catalyzing the reduction of O_2 to H_2O. FEBS J 274: 1588-1599.

Shen JR (2015) The structure of Photosystem II and the mechanism of water oxidation in photosynthesis. Annu Rev Biochem 66: 23-48.

Shevchenko A, Wilm M, Vorm O, Mann M (1996) Mass spectrometric sequencing of proteins from silver-stained polyacrylamide gels. Anal Chem 68: 850-858.

Shevela D, Eaton-Rye JJ, Shen JR, Govindjee (2012) Photosystem II and the unique role of bicarbonate: a historical perspective. Biochim Biophys Acta 1817: 1134-1151.

Shi LX, Hall M, Funk C, Schroder WP (2012) Photosystem II, a growing complex: updates on newly discovered components and low molecular mass proteins. Biochim Biophys Acta 1817: 13-25.

Shimakawa G, Shaku K, Nishi A, Hayashi R, Yamamoto H, Sakamoto K, Makino A, Miyake C (2015) FLAVODIIRON2 and FLAVODIIRON4 proteins mediate an oxygen-dependent alternative electron flow in *Synechocystis* sp. PCC 6803 under CO_2-limited conditions. Plant Physiol 167: 472-480.

Shimizu T, Ohtani K, Hirakawa H, Ohshima K, Yamashita A, Shiba T, Ogasawara N, Hattori M, Kuhara S, Hayashi H (2002) Complete genome sequence of *Clostridium perfringens,* an anaerobic flesh-eater. Proc Natl Acad Sci U S A 99 (2): 996-1001.

Sicora CI, Appleton SE, Brown CM, Chung J, Chandler J, Cockshutt AM, Vass I, Campbell DA (2006) Cyanobacterial *psbA* families in *Anabaena* and *Synechocystis* encode trace, constitutive and UVB-induced D1 isoforms. Biochim Biophys Acta 1757: 47-56.

Silaghi-Dumitrescu R, Kurtz DM, Ljungdahl LG, Lanzilotta WN (2005) X-ray crystal structures of *Moorella thermoacetica* FprA: Novel diiron site structure and mechanistic insights into a scavenging nitric oxide reductase. Biochem 44: 6492-6501.

Silva P, Thompson E, Bailey S, Kruse O, Mullineaux CW, Robinson C, Mann NH, Nixon PJ (2003) FtsH is involved in the early stages of repair of photosystem II in *Synechocystis* sp. PCC 6803. Plant Cell 15: 2152-2164.

Singh A K, McIntyre LM, Sherman LA (2003) Microarray analysis of the genome-wide response to iron deficiency and iron reconstitution in the cyanobacterium *Synechocystis* sp. PCC 6803. Plant Physiol 132: 1825-1839.

Singh SP, Montgomery BL (2011) Determining cell shape: adaptive regulation of cyanobacterial cellular differentiation and morphology. Trends in Microbiology 19(6): 278-285.

Sippola K, Aro EM (2000) Expression of *psbA* genes is regulated at multiple levels in the cyanobacterium *Synechococcus* sp. PCC 7942. Photochem Photobiol 71: 706-714.

Snellenburg JJ, Laptenok SP, Seger R, Mullen KM, van Stokkum IHM (2012) Glotaran: a Java-based graphical user interface for the R package TIMP. J Stat Softw 49: 1-22**.**

Soitamo AJ, Zhou G, Clarke AK, Öquist G, Gustafsson P, Aro EM (1996) Over-production of the D1:2 protein makes *Synechococcus* cells more tolerant to photoinhibition of photosystem II. Plant Mol Biol 30: 467-478.

Somsen OJ, Keukens LB, de Keijzer MN, van Hoek A, van Amerongen H (2005) Structural heterogeneity in DNA: temperature dependence of 2-aminopurine fluorescence in dinucleotides. ChemPhysChem 6: 1622-1627.

Staleva H, Komenda J, Shukla MK, Slouf V, Kana R, Polivka T, Sobotka R (2015) Mechanism of photoprotection in the

cyanobacterial ancestor of plant antenna proteins. Nat Chem Biol 11: 287-291.

Stanier RY, Kunisawa R, Mandel M, Cohen-Bazire G (1971) Purification and properties of unicellular blue-green alga (order Choorococcales). Bacteriol Rev 35: 171-205.

Stanier RY, Cohen-Bazire G (1977) Phototrophic prokaryotes: the cyanobacteria. Ann Rev Microbiol 31: 225-274.

Stengel A, Gügel IL, Hilger D, Rengstl B, Jung H, Nickelsen J (2012) Initial steps of photosystem II de novo assembly and preloading with manganese take place in biogenesis centers in *Synechocystis*. Plant Cell 24: 660-675.

Stepien P, Johnson GN (2009) Contrasting responses of photosynthesis to salt stress in the glycophyte *Arabidopsis* and the halophyte *Thellungiella*: role of the plastid terminal oxidase as an alternative electron sink. Plant Physiol 149: 1154-1165.

Stewart DH, Brudvig GW (1998) Cytochrome b_{559} of photosystemII. Biochim Biophys Acta 1367: 63-87.

Stoitchkova K, Zsiros O, Javorfi T, Pali T, Andreeva A, Gombos Z, Garab G (2007) Heat- and light-induced reorganizations in the phycobilisome antenna of *Synechocystis* sp. PCC 6803. Thermo-optic effect, Biochim. Biophys. Acta 1767: 750-756.

Sugiura M, Kato Y, Takahashi R, Suzuki H, Watanabe T, Noguchi T, Rappaport F, Boussac A (2010) Energetics in photosystem II from *Thermosynechococcus elongatus* with a D1 protein encoded by either the *psbA1* or *psbA3* gene. Biochim Biophys Acta 1797: 1491-1499.

Sumimoto H, Kage Y, Nunoi H, Sasaki H, Nose T, Fukumaki Y, Ohno M, Minakami S, Takeshige K (1994) Role of Src homology 3 domains in assembly and activation of the phagocyte NADPH oxidase. Proc Natl Acad Sci USA 91: 5345-5349.

Summerfield TC, Toepel J, Sherman LA (2008) Low-oxygen induction of normally cryptic *psbA* genes in cyanobacteria. Biochemistry 47: 12939-12941.

Summerfield TC, Nagarajan S, Sherman LA (2011) Gene expression under low-oxygen conditions in the cyanobacterium *Synechocystis* sp. PCC 6803 demonstrates Hik31-dependent and -independent responses. Microbiology 157: 301-312.

Svensson B, Vass I, Styring S (1991) Sequence analysis of the D1 and D2 reaction center proteins of photosystem II. Z Naturforsch 46: 765-776.

Szczepaniak M, Sander J, Nowaczyk M, Muller MG, Rögner M, Holzwarth AR (2009) Charge separation, stabilization, and protein relaxation in photosystem II core particles with closed reaction center. Biophys J 96: 621-631.

Szilárd A, Sass L, Hideg É, Vass I (2005) Photoinactivation of photosystem II by flashing light. Photosynth Res 84: 15-20.

Takahashi S, Murata N (2008) How do environmental stresses accelerate photoinhibition? Trends in Plant Science 13: 178-182.

Takishita K, Uchida A (1999) Molecular cloning and nucleotide sequence analysis of *psbA* from the dinoflagellates: Origin of the dinoflagellate plastid. Phycol Res 47: 207–216.

Tamary E, Kiss V, Nevo R, Adam Z, Bernat G, Rexroth S, Rögner M, Reich Z (2012). Structural and functional alterations of cyanobacterial phycobilisomes induced by high-light stress. Biochim Biophys Acta 1817: 319-327.

Telfer A, Bishop SM, Phillips D, Barber J (1994) Isolated photosynthetic reaction center of photosystem II as a sensitizer for the formation of singlet oxygen. Detection and quantum yield determination using a chemical trapping technique. J Biol Chem 269: 13244-13253.

Thomas JC, Ughy B, Lagoutte B, Ajlani G (2006) A second isoform of the ferredoxin:NADP oxidoreductase generated by an in-frame initiation of translation. Proc Natl Acad Sci U S A 103: 18368-18373.

Thompson JD, Higgins DG, Gibson TJ (1994) CLUSTAL W: weighting, positions-specific gap penalties and weight matrix choice. Nucleic Acids Res 22: 4673-4680.

Tian L, van Stokkum IH, Koehorst RB, Jongerius A, Kirilovsky D, van Amerongen H (2011) Site, rate, and mechanism of photoprotective quenching in cyanobacteria. J Am Chem Soc133: 18304-18311.

Tian L, Farooq S, van Amerongen H (2013) Probing the picosecond kinetics of the photosystem II core complex *in vivo*. Phys Chem Chem Phys 15: 3146-3154.

Tichý M, Lupínková L, Sicora C, Vass I, Kuviková S, Prásil O, Komenda J (2003) *Synechocystis* 6803 mutants expressing distinct forms of the photosystem II D1 protein from *Synechococcus* 7942: relationship between the *psbA* coding region and sensitivity to visible and UV-B radiation. Biochim Biophys Acta 1605: 55-66.

Tomo T, Akimoto S, Tsuchiya T, Fukuya M, Tanaka K, Mimuro M (2008) Isolation and spectral characterization of photosystem II reaction center from *Synechocystis* sp. PCC6803. Photosynth Res 98: 293-302.

Trebst A (1980) Inhibitors in electron flow: tools for the functional and structural localization of carriers and energy conservation sites. Methods Enzymol 69: 675-715.

Trebst A, Depka B, Holländer-Czytko H (2002) A specific role for tocopherol and of chemical singlet oxygen quenchers in the maintenance of Photosystem II structure and function in *Chlamydomonas reinhardtii*. FEBS Lett 516: 156-160.

Triantaphylides C, Krischke M, Hoeberichts FA, Ksas B, Gresser G, Havaux M, Van Breusegem F, Mueller MJ (2008) Singlet oxygen is the major reactive oxygen species involved in photooxidative damage to plants. Plant Physiol 148: 960-968.

Triantaphylides C, Havaux M (2009) Singlet oxygen in plants: production, detoxification and signaling. Trends Plant Sci 14: 219-228.

Tyler SA, Barghoorn ES (1954) Occurrence of structurally preserved plants in Precambrian rocks of the Canadian shield. Science 119: 606-608.

Tyystjärvi E (2008) Photoinhibition of photosystem II and photodamage of the oxygen evolving manganese cluster. Coord Chem Rev 252: 361-376.

Tyystjärvi E, Rantamäki S, Tyystjärvi J (2009) Connectivity of photosystem II is the physical basis of retrapping in photosynthetic thermoluminescence. Biophys J 96: 3735-3743.

Umena Y, Kawakami K, Shen JR, Kamiya N (2011) Crystal structure of oxygen-evolving photosystem II at a resolution of 1.9 angstrom. Nature 473: 55-65.

van de Meene A, Hohmann-Marriott M, Vermaas WFJ, Roberson R (2006) The three-dimensional structure of the cyanobacterium *Synechocystis* sp. PCC 6803. Arch Microbiol 184: 259-70.

van Oort, B., Murali, S., Wientjes, E., Koehorst, R.B.M., Spruijt, R.B., van Hoek, A., Croce, R., and van Amerongen, H. (2009). Ultrafast resonance energy transfer from a site-specifically attached fluorescent chromophore reveals the folding of the N-terminal domain of CP29. Chem Phys 357: 113-119.

van Oort B, Alberts M, de Bianchi S, Dall'Osto L, Bassi R, Trinkunas G, Croce R, van Amerongen H (2010). Effect of antenna-depletion in photosystem II on excitation energy transfer in *Arabidopsis thaliana*. Biophys J 98: 922-931.

van Stokkum IHM, Gobets B, Gensch T, van Mourik F, Hellingwerf KJ, van Grondelle R, Kennis JTM (2006) (Sub)-picosecond spectral evolution of fluorescence in photoactive proteins studied with a synchroscan streak camera system. Photochem Photobiol 82: 380-388.

van Thor JJ, Gruters OW, Matthijs HCP, Hellingwerf KJ (1999) Localization and function of ferredoxin:$NADP^+$ reductase bound to the phycobilisomes of *Synechocystis*. Embo J 18: 4128-4136.

van Thor JJ, Jeanjean R, Havaux M, Sjollema KA, Joset F, Hellingwerf KJ, Matthijs HCP (2000) Salt shock-inducible photosystem I cyclic electron transfer in *Synechocystis* PCC6803 relies on binding of ferredoxin: NADP1 reductase to the thylakoid membranes via its CpcD phycobilisome-linker homologous N-terminal domain. Biochim Biophys Acta 1457: 129-144.

Vass I, Styring S, Hundal T, Koivuniemi A, Aro EM, Andersson B (1992a) Reversible and irreversible intermediates during photoinhibition of photosystem II: stable reduced Q_A species promote chlorophyll triplet formation. Proc Natl Acad Sci USA 89: 1408-1412.

Vass I, Cook KM, Deák Z, Mayes SR, Barber J (1992b) Thermoluminescence and flash-oxygen characterization of the IC2 deletion mutant of *Synechocystis* sp. PCC 6803 lacking the photosystem II 33 kDa protein. Biochim Biophys Acta 1102: 195-201.

Vass I (2011) Role of charge recombination processes in photodamage and photoprotection of the photosystem II complex. Physiol Plant 142: 1-11.

Vass I (2012) Molecular mechanisms of photodamage in the photosystem II complex. Biochim Biophys Acta, 1817: 209-217.

Vass I, Kirilovsky D, Etienne A-L (1999) UV-B radiation-induced donorand acceptor-side modifications of photosystem II in the cyanobacterium *Synechocystis* sp. PCC 6803. Biochemistry 38: 12786-12794.

Vass I, Cser K (2009) Janus-faced charge recombinations in photosystem II photoinhibition. Trends Plant Sci 14: 200-205.

Vavilin D, Yao D, Vermaas WFJ (2007) Small Cab-like proteins retard degradation of photosystem II-associated chlorophyll in *Synechocystis* sp. PCC 6803: Kinetic analysis of pigment labeling with 15N and 13C. J Biol Chem 282: 37660-37668.

Vicente J B, Gomes C M, Wasserfallen A, Teixeira M (2002) Module fusion in an A-type flavoprotein from the cyanobacterium *Synechocystis* condenses a multiple component pathway in a single polypeptide chain. Biochem Biophys Res Commun 294: 82-87.

Vicente JB, Scandurra FM, Rodrigues JV, Brunori M, Sarti P, Teixeira M, Giuffre A (2007) Kinetics of electron transfer from NADH to the *Escherichia coli* nitric oxide reductase flavorubredoxin. FEBS J 274: 677-686.

Vicente JB, Carrondo MA, Teixeira M, Frazão C (2008a) Structural studies on flavodiiron proteins. Methods Enzymol 437: 3-19.

Vicente JB, Justino MC, Gonçalves VL, Saraiva LM, Teixeira M (2008b) Biochemical, spectroscopic, and thermodynamic properties of flavodiiron proteins. Methods Enzymol 437: 21-45.

Vicente JB, Testa F, Mastronicola D, Forte E, Sarti P, Teixeira M, Giuffrè A (2009) Redox properties of the oxygen-detoxifying flavodiiron protein from the human parasite *Giardia intestinalis*. Arch Biochem Biophys 488: 9-13.

Wang HL, Postier BL, Burnap RL (2004) Alterations in global patterns of gene expression in *Synechocystis* sp. PCC 6803 in response to inorganic carbon limitation and the inactivation of *ndhR*, a LysR family regulator. J Biol Chem 279: 5739-5751.

Wasserfallen A, Ragettli S, Jouanneau Y, Leisinger T (1998) A family of flavoproteins in the domains Archaea and Bacteria. Eur J Biochem 254: 325-332.

Weidner U, Geier S, Ptock A, Friedrich T, Leif H, Weiss H (1993) The gene locus of proton-translocating NADH-ubiquinone oxidoreductase in *Escherichia coli*— organization of the 14 genes and relationship between the derived proteins and subunits of mitochondrial Complex I. J Mol Biol 233: 109-122.

Westall F (2005) Life on the early Earth: a sedimentary view. Science 308: 366-367.

Whitelegge JP, Zhang H, Aguilera R, Taylor RM, Cramer WA (2002) Full subunit coverage liquid chromatography electrospray ionization mass spectrometry (LCMS1) of an oligomeric membrane protein: Cytochrome $b_{(6)}$f complex from spinach and the cyanobacterium *Mastigocladus laminosus*. Mol Cell Proteomics 1: 816-827.

Williams JGK (1988) Construction of specific mutations in photosystem II photosynthetic reaction center by genetic engineering methods in *Synechocystis* 6803. Methods Enzymol 167: 766-778.

Wilson A, Ajlani G, Verbavatz JM, Vass I, Kerfeld CA, Kirilovsky D (2006) A soluble carotenoid protein involved in phycobilisomerelated energy dissipation in cyanobacteria. Plant Cell 18(4): 992-1007.

Wilson A, Boulay C, Wilde A, Kerfeld CA, Kirilovsky D (2007) Light-induced energy dissipation in iron-starved cyanobacteria: roles of OCP and IsiA proteins. Plant Cell 19(2): 656-672.

Winhauer T, Jäger S, Valentin K, Zetsche K (1991) Structural similarities between *psbA* genes from red and brown algae. Curr Genet 20: 177-180.

Wulfhorst H, Franken LE, Wessinghage T, Boekema EJ, Nowaczyk MM (2014) The 5 kDa protein NdhP is essential for stable NDH-1L assembly in *Thermosynechococcus elongatus*. PLoS One 9(8): e103584. doi:10.1371/journal.pone.0103584**.**

Xu M, Ogawa T, Pakrasi HB, Mi H (2008) Identification and localization of the CupB protein involved in constitutive CO_2 uptake in the cyanobacterium, *Synechocystis* sp strain PCC 6803. Plant Cell Physiol 49: 994-997.

Yadav DK, Kruk J, Sinha RK, Pospísil P (2010) Singlet oxygen scavenging activity of plastoquinol in photosystem II of higher plants: electron paramagnetic resonance spin-trapping study. Biochim Biophys Acta 1797: 1807-1811.

Yagi T, Yano T, Di Bernardo S, Matsuno-Yagi A (1998) Procaryotic complex I (NDH-1), an overview, Biochim Biophys Acta 1364: 125-133.

Yamamoto H, Peng L, Fukao Y, Shikanai T (2011) An Src homology 3 domain-like fold protein forms a ferredoxin binding site for the chloroplast NADH dehydrogenaselike complex in Arabidopsis. Plant Cell 23: 1480-1493.

Yamamoto H, Shikanai T. (2013) In planta mutagenesis of Src homology 3 domain-like fold of NdhS, a ferredoxin-binding subunit of the chloroplast NADH dehydrogenaselike complex in Arabidopsis: a conserved Arg-193 plays a critical role in ferredoxin binding. J Biol Chem 288: 36328-36337.

Yao D, Kieselbach T, Komenda J, Promnares K, Prieto MA H, Tichý M, Vermaas WFJ, Funk C (2007) Localization of the small CAB-like proteins in photosystem II. J Biol Chem 282: 267-276.

Yeremenko N, Jeanjean R, Prommeenate P, Krasikov V, Nixon PJ, Vermaas WFJ, Havaux M, Matthijs HCP (2005) Open reading frame *ssr2016* is required for antimycin A-sensitive photosystem I-driven cyclic electron flow in the cyanobacterium *Synechocystis* sp. PCC 6803. Plant Cell Physiol 46: 1433-1436.

Yoon HS, Hackett JD, Ciniglia C, Pinto G, Bhattachraya D (2004) A molecular timeline for the origin of photosynthetic eukaryotes. Mol Biol Evol 21: 809-818.

Young RD (2010) Characterisation of the Role of the PsbT Subunit of Photosystem II in *Synechocystis* sp. PCC 6803: a Thesis Submitted for the Degree of Master of Science at the University of Otago (Dunedin: University of Otago).

Zak E, Norling B, Maitra R, Huang F, Andersson B, Pakrasi HB (2001) The initial steps of biogenesis of cyanobacterial photosystems occur in plasma membranes. Proc Natl Acad Sci USA 98: 13443-13448.

Zhang P, Battchikova N, Jansen T, Appel J, Ogawa T, Aro EM (2004) Expression and functional roles of the two distinct NDH-1 complexes and the carbon acquisition complex NdhD3/NdhF3/CupA/Sll1735 in *Synechocystis* sp PCC 6803. Plant Cell 16: 3326-3340.

Zhang P, Battchikova N, Paakkarinen V, Katoh H, Iwai M, Ikeuchi M, Pakrasi HB, Ogawa T, Aro EM (2005) Isolation, subunit composition and interaction of the NDH-1 complexes from *Thermosynechococcus elongatus* BP-1. Biochem J 390: 513-520.

Zhang P, Allahverdiyeva Y, Eisenhut M, Aro EM (2009) Flavodiiron proteins in oxygenic photosynthetic organisms: Photoprotection of photosystem II by Flv2 and Flv4 in *Synechocystis* sp. PCC 6803. PLoS ONE 4:e5331.

Zhang P, Eisenhut M, Brandt AM, Carmel D, Silén HM, Vass I, Allahverdiyeva Y, Salminen TA, Aro EM (2012) Operon *flv4-flv2* provides cyanobacterial photosystem II with flexibility of electron transfer. Plant Cell 24: 1952-1971.

Zhao J, Gao F, Zhang J, Ogawa T, Ma W (2014) NdhO, a subunit of NADPH dehydrogenase, destabilizes medium size complex of the enzyme in *Synechocystis* sp strain PCC 6803. J Biol Chem 289: 26669-26676.